ni

NASA CR-134915

NASA

QUIET CLEAN SHORT-HAUL EXPERIMENTAL ENGINE (QCSEE)

The Aerodynamic and Mechanical Design of The QCSEE Over-the-Wing Fan

April 1976

by

Advanced Engineering & Technology Programs Department

General Electric Company

Prepared For

National Aeronautics and Space Administration

(NASA-CR-134915) QUIET CLEAN SHORT-HAUL EXPERIMENTAL ENGINE (QCSEE). THE AERODYNAMIC AND MECHANICAL DESIGN OF THE QCSEE OVER-THE-WING FAN (General Electric Co.) 98 p HC A05/MF A01 CSCL 21E G3/07

N80-15089

Unclas 33466

NASA Lewis Research Center

Contract NAS3-18021

TABLE OF CONTENTS

LIST OF ILLUSTRATIONS

LIST OF ILLUSTRATIONS (Concluded)

LIST OF TABLES

SECTION 1.0

OTW FAN DESIGN

1.1 SUMMARY

An Under-the Wing and an Over-the Wing fan rotor will be built and tested as part of the NASA QCSEE program.

The aerodynamic design of both the fixed-pitch OTW and variable-pitch UTW geared fans was completed during the Preliminary Design Phase.

At the major operating conditions of takeoff and maximum cruise, a corrected flow of 405.5 kg/sec (894 lbm/sec) was selected for both fans which enables common inlet hardware to yield the desired 0.79 average throat Mach number at the critical takeoff noise measurement condition. The aerodynamic design bypass pressure ratio is 1.36 for the OTW and 1.34 for the UTW which is intermediate between the takeoff and maximum cruise power settings. The takeoff pressure ratios are 1.34 for the OTW and 1.27 for the UTW. the takeoff corrected tip speeds are 354 m/sec (1162 ft/sec) for the OTW and 289 m/sec (950 ft/sec) for the UTW. These pressure ratios and speeds were selected on the basis of minimum noise within the constraints of adequate stall margin and core engine supercharging.

The OTW fan employs 28 fixed-pitch fan blades. A flight version of the design would use composite fan blades, but titanium fan blades will be used in the experimental fan as a cost saving measure. The conceptual design with composite blades was used to establish the number of fan blades, and in conjunction with the aerodynamic design, the blade airfoil shape. The metal blades require a larger fan disk rim than would be required for composite blades. The fan disk support cone and the remaining fan components on the experimental engine will be of flight design.

SECTION 2.0

OTW FAN AERODYNAMIC DESIGN

2.1 OPERATING REQUIREMENTS

The major operating requirements for the over-the-wing (OTW) fan, Figure 1, are takeoff, where noise and thrust are of primary importance, and maximum cruise, where economy and thrust are of primary importance. A secondary requirement was to utilize hardware common to the UTW fan when no significant performance penalty was involved. At takeoff, a low fan pressure ratio of 1.34 was selected to minimize the velocity of the bypass stream at nozzle exit. A corrected flow of 405.5 kg/sec (894 lb/sec), the same as for the UTW, at this pressure ratio yields the required engine thrust. The inlet throat is sized at this condition for an average Mach number of 0.79 to minimize forward propagation of fan noise. This sizing of the inlet throat prohibits higher corrected flow at altitude cruise. The required maximum cruise thrust is obtained by raising the fan pressure ratio to 1.38. The aerodynamic design point was selected at an intermediate condition, which is a pressure ratio of 1.36 and a corrected flow of 408 kg/sec (900 lb/sec). Table I summarizes the key parameters for these three conditions.

Table I. QCSEE OTW Fan.

Parameter	Design Point	Takeoff	Maximum Cruise
Total fan flow	408 kg/sec (900 lb/sec)	405.5 kg/sec (894 lb/sec)	405.5 kg/sec (894 lb/sec)
Pressure ratio - bypass flow	1.36	1.34	1.38
Pressure ratio - core flow	1.43	1.43	1.44
Bypass ratio	9.9	10.1	9.8
Corrected tip speed	358 m/sec (1175 ft/sec)	354 m/sec (1162 ft/sec)	359 m/sec (1178 ft/sec)

2.2 BASIC DESIGN FEATURES

A cross section of the selected OTW fan configuration is shown in Figure 2. The fan outer flowpath, vane-frame including outer and inner flowpath, and transition duct including the six frame struts are all common to the UTW fan configuration. Thus the integrated nacelle vane-frame assembly is common to both propulsion systems. There are 28 fixed-pitch rotor blades. The overall proportions for the rotor blades, blade number, and radial distributions of thickness and chord were selected to provide a satisfactory aeromechanical flight-type composite configuration. However, to minimize overall program costs, titanium was substituted for the actual blade construction. The stall

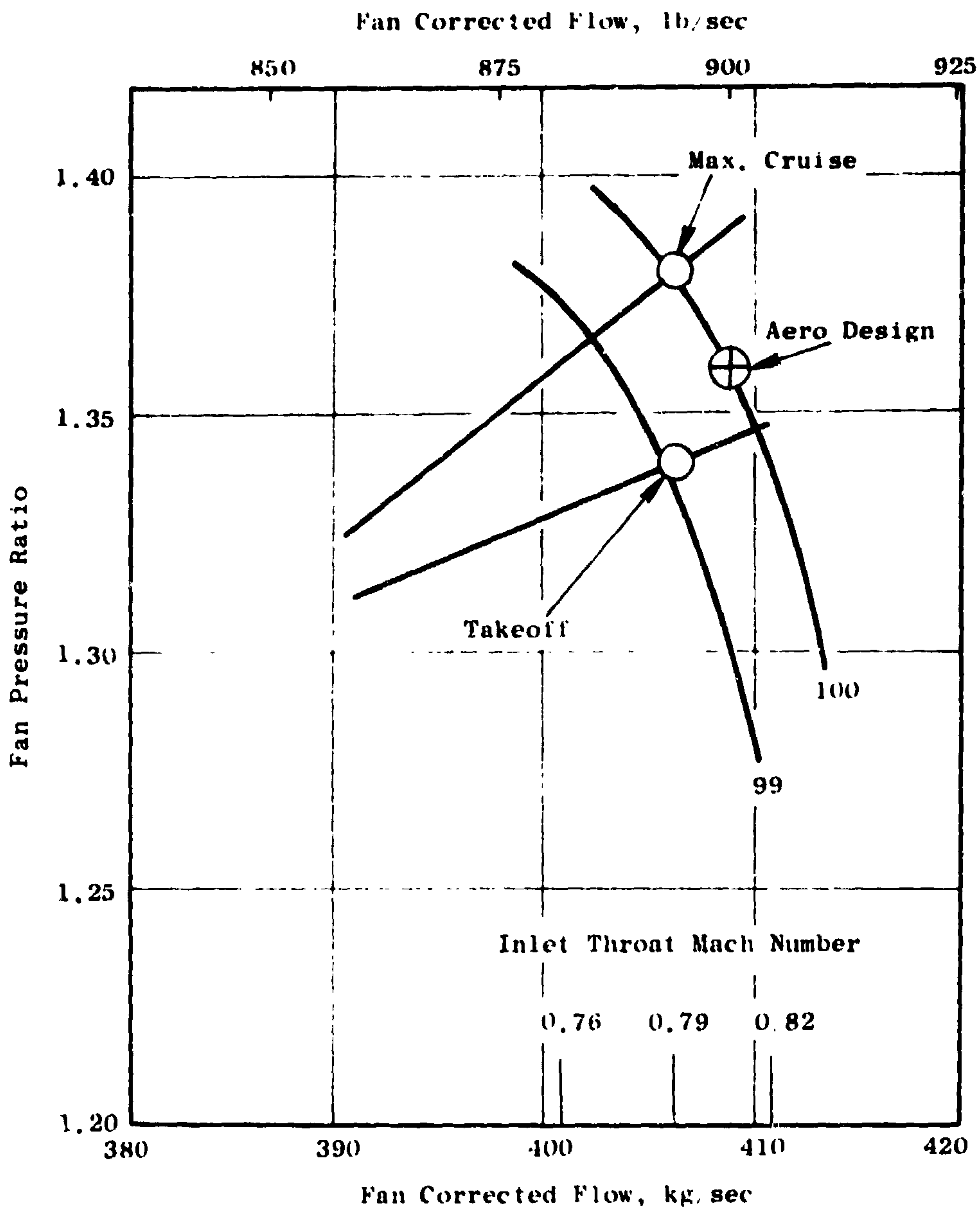

Figure 1. Major Operating Requirements for OTW Fan.

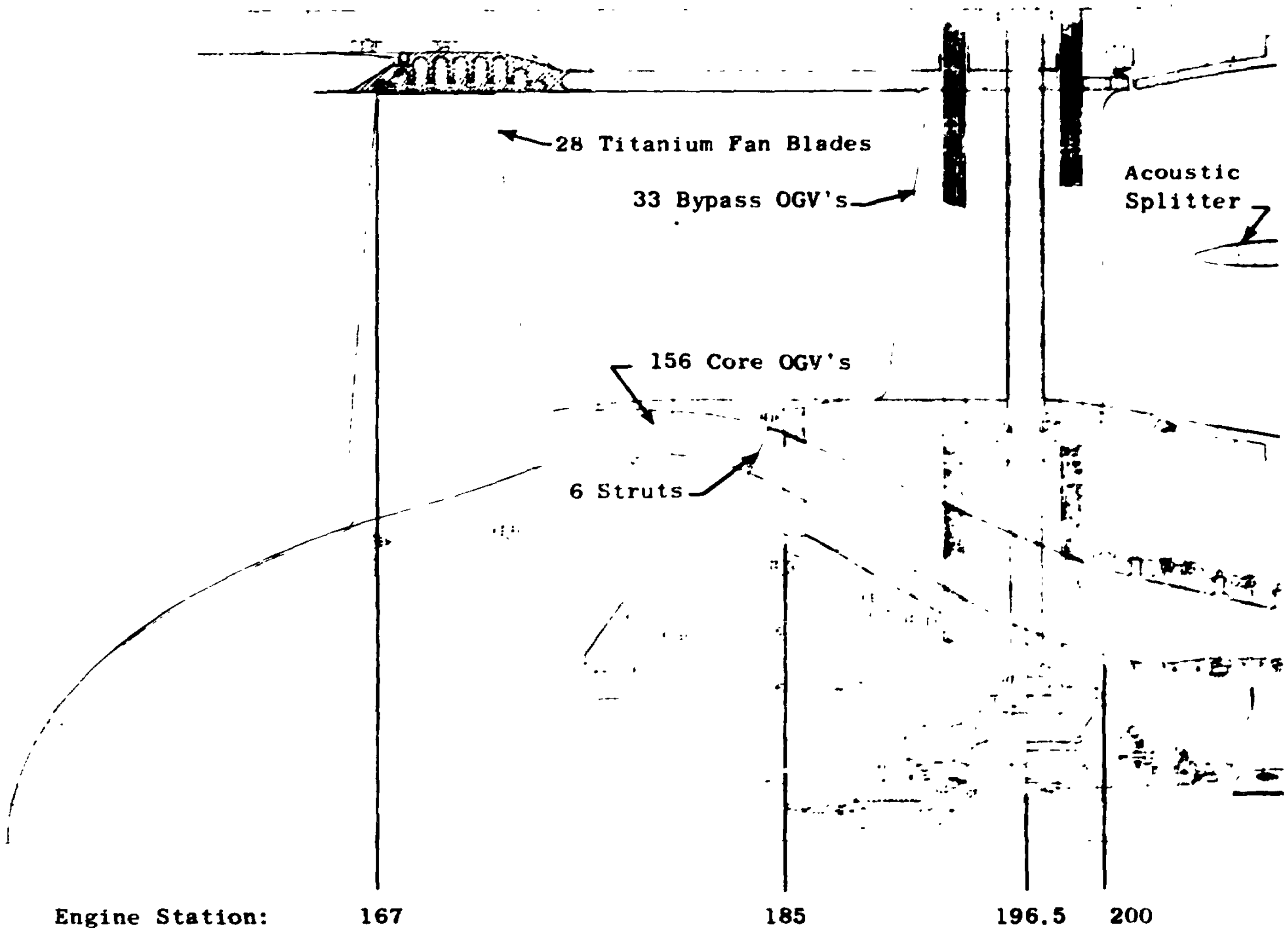

Figure 2. Cross Section of OTW Fan.

margin for the OTW fan is projected to be adequate. The circumferential grooved casing treatment, however, can be retained from the UTW fan to provide added protection against stall. The rotor was positioned axially such that the trailing edge hub intersects the hub flowpath at the same axial station as the UTW which puts the aft face of the fan disk at approximately the same engine station. A tip axial spacing between rotor trailing edge and vane-frame leading edge equal to 1.9 true rotor tip chords results. The vane-blade ratio is 1.18. Immediately following the rotor, in the hub region, is a splitter which divides the flow into the bypass portion and core portion. The proximity of the splitter leading edge to the rotor blade is to enable additional design control on the streamlines in the hub region to provide improved surface velocity and loading distributions. The 156 OGV's for the fan hub, or core portion, flow are in the annular space under the splitter. There are six struts in the gooseneck which guides the fan hub flow into the core compressor.

In the vane-frame, which is common with the UTW Fan, the vanes are non-axisymmetric in that five vane geometries, each with a different camber and stagger, are employed around the annulus. This nonaxisymmetric geometry is required to conform the vane-frame downstream flow field to the geometry of the pylon, which protrudes forward into the vane-frame, and simultaneously maintains a condition of minimum circumferential static pressure distortion upstream of the vane-frame. There are 33 vanes in the vane-frame which yield a vane-blade ratio of 1.18.

2.3 DETAILED CONFIGURATION DESIGN

The corrected tip speed at the aerodynamic design point was selected at 358 m/sec (1175 ft/sec). This was selected for design purposes, as a compromise between the takeoff and cruise tip speed requirements. The objective design point adiabatic efficiency is 88% for the bypass portion and 78% for the core portion. Requirements include 16% stall margin at takeoff and high fan hub pressure ratio to provide good core engine supercharging. An inlet radius ratio of 0.42 was selected, compared to 0.44 for the UTW fan, to provide additional annulus area convergence at rotor hub which reduces the hub aerodynamic loading. Discharge radius ratios are approximately the same for the two fans. For the 1.803 m (71.0 in.) tip diameter, a flow per annulus area of 194 kg/sec-m^2 (39.8 lb/sec-ft^2) results.

The standard General Electric axisymmetric flow computation procedure was employed in calculating the velocity diagrams. Several calculation stations were included internal to the rotor blade to improve the overall accuracy of the solution in this region. The physical splitter geometry is represented in the calculations. Forward of the splitter calculation stations span the radial distance from OD to ID. Aft of the splitter, calculation stations span the radial distance between the OD and the topside of the splitter and between the underside of the splitter and the hub contour. At each calculation station effective area coefficients consistent with established design practice were assumed.

The design radial distribution of rotor total pressure ratio is shown in Figure 3. This distribution is consistent with a stage average pressure ratio of 1.36 in the bypass region. The higher than average pressure ratio

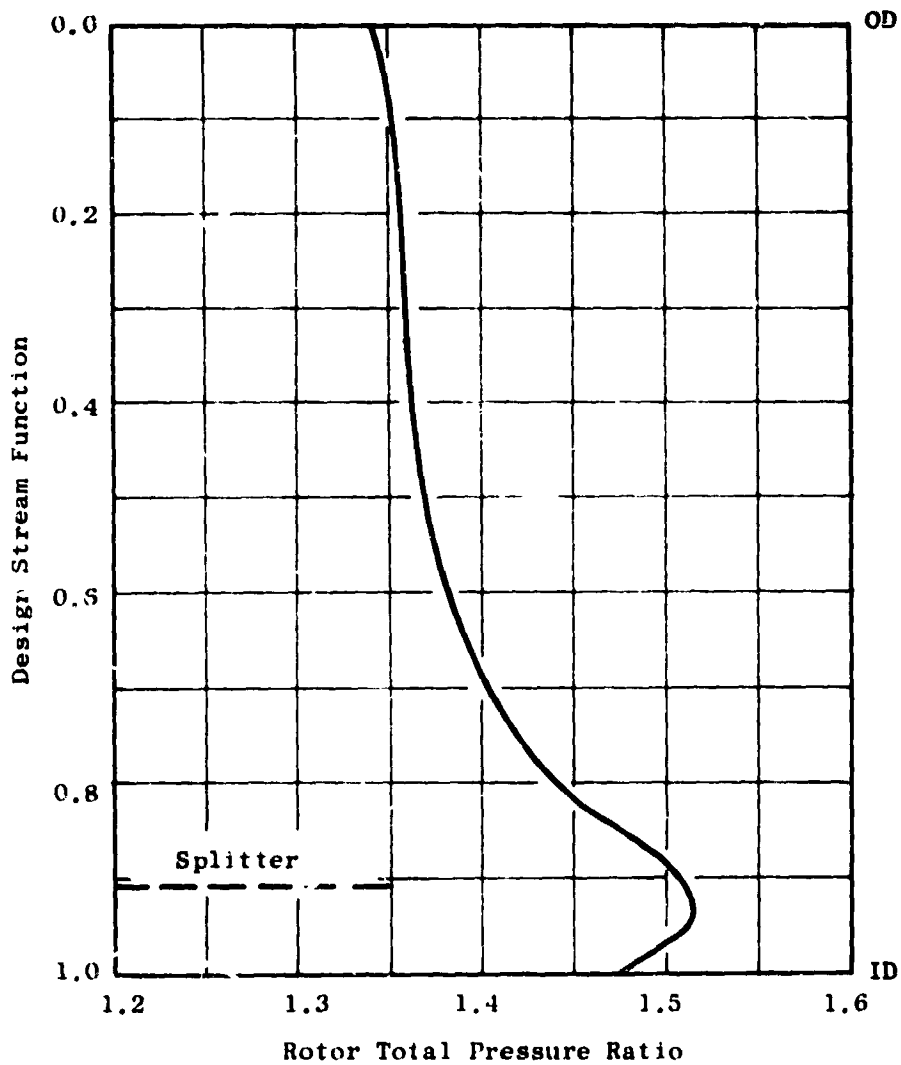

Figure 3. OTW Radial Distribution of Rotor Total Pressure Ratio.

in the hub region provides maximum core engine supercharging subject to a balance between the constraints of acceptable rotor diffusion factors, stator inlet absolute Mach numbers, and stator diffusion factors. A stage average pressure ratio of 1.43 results at the core OGV exit. The assumed radial distribution of rotor efficiency for the design is shown in Figure 4 which was based on measured results from similar configurations (Quiet Engine, Fan B). The assumption of efficiency rather than total-pressure-loss coefficient is a General Electric design practice for rotors of this type. The radial distribution of rotor diffusion factor which results from these assumptions is shown in Figure 5. Figures 6 and 7 show the radial distributions of rotor relative Mach number and air angle, respectively. At the rotor hub the flow turns 16° past axial which corresponds to a work coefficient of 2.6.

The assumed radial distribution of total-pressure-loss coefficient for the core portion OGV is shown in Figure 8. The relatively high level, particularly in the ID region, is in recognition of the very high bypass ratio of the OTW engine and, accordingly, the small relative size of the core OGV compared to the rotor. The annulus height of the core stator is approximately 70% of the rotor staggered spacing, a significant dimension when analyzing secondary flow phenomena. It is anticipated that a significant portion of the core OGV will be influenced by the rotor secondary flows. The moderately high core OGV diffusion factors, turning angles, and inlet Mach numbers, as shown in Figure 8, were contributing factors in the total-pressure-loss coefficient assumptions. An average swirl of 6° is retained in the fluid at exit from the core OGV, like the UTW configuration. This was done to lower its aerodynamic loading. The transition duct struts designed for the UTW configuration were cambered to accept this swirl.

A tabulation of significant blade element parameters for the OTW design is presented in Table II.

2.4 ROTOR BLADE DESIGN

The rotor blade tip solidity was selected as 1.3. With a rotor tip inlet relative Mach number of 1.22, a reduction in tip solidity would lower the overall performance potential of the configuration. The rotor hub solidity was selected as 2.2. The primary factors in this selection were the rotor hub loading and sufficient passage length to do the required 56° turning. The radial chord distribution is linear with radius. Mechanical input was provided to ensure that this chord distribution and the selected thickness distribution, as shown in Figures 9 and 10, produced a satisfactory aeromechanical configuration.

The detailed layout procedure employed in the design of the fan blade geometry generally parallels established design procedures. In the tip region of the blade where the inlet relative flow is supersonic, the uncovered portion of the suction surface was set to ensure that the maximum flow passing capacity is consistent with the design flow requirement. The incidence angles in the tip region were selected according to transonic blade design practice which has

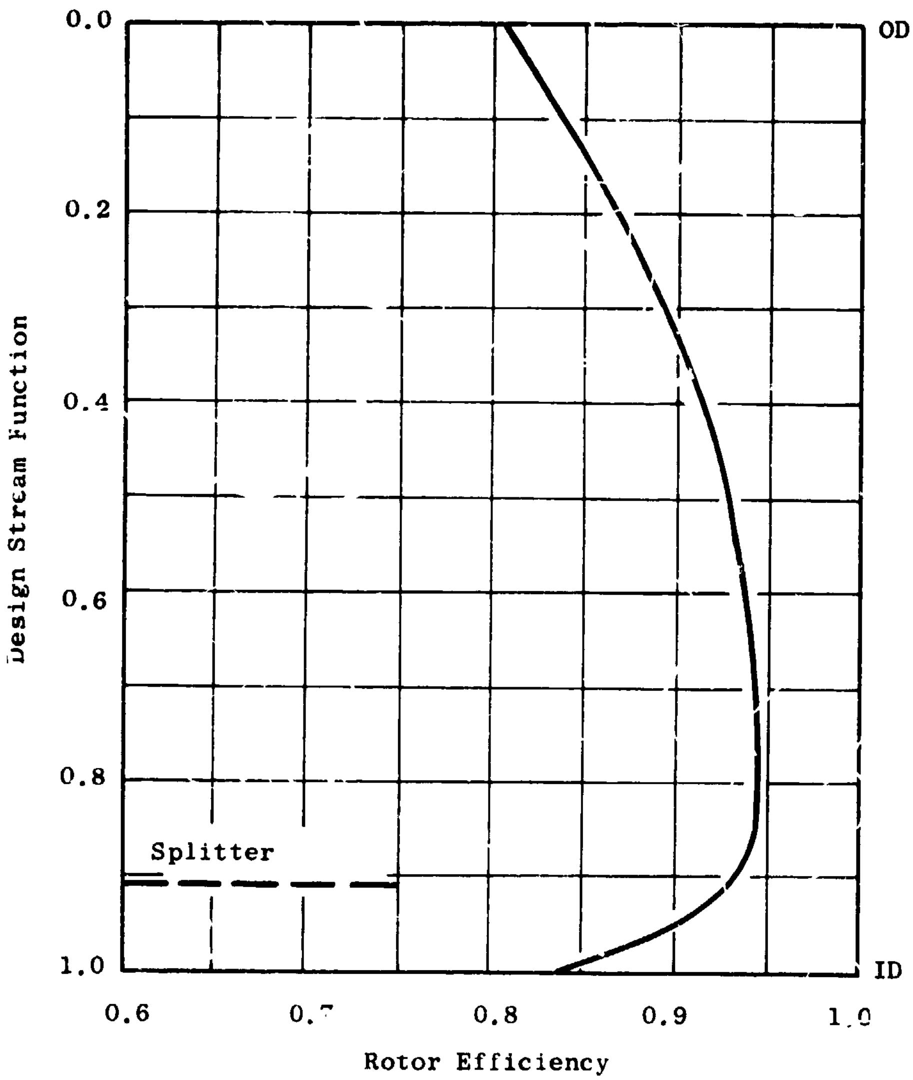

Figure 4. OTW Radial Distribution of Rotor Efficiency.

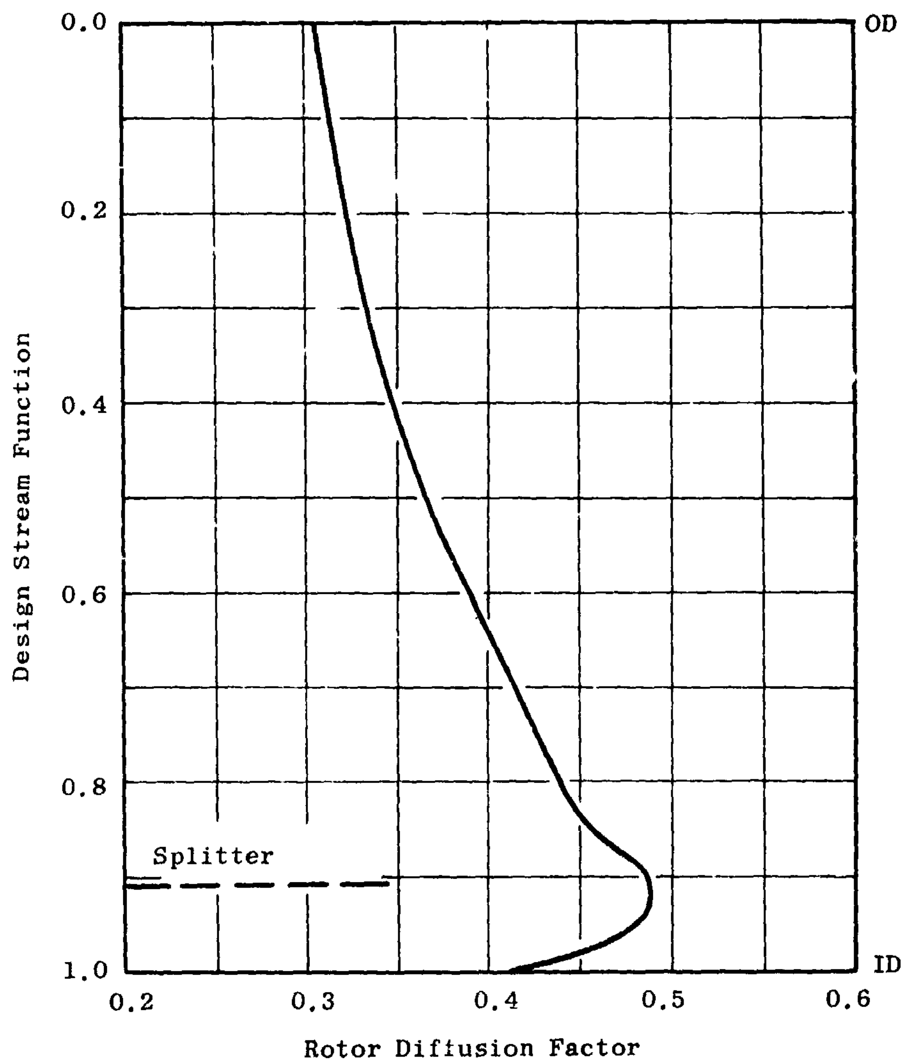

Figure 5. OTW Radial Distribution of Rotor Diffusion Factor.

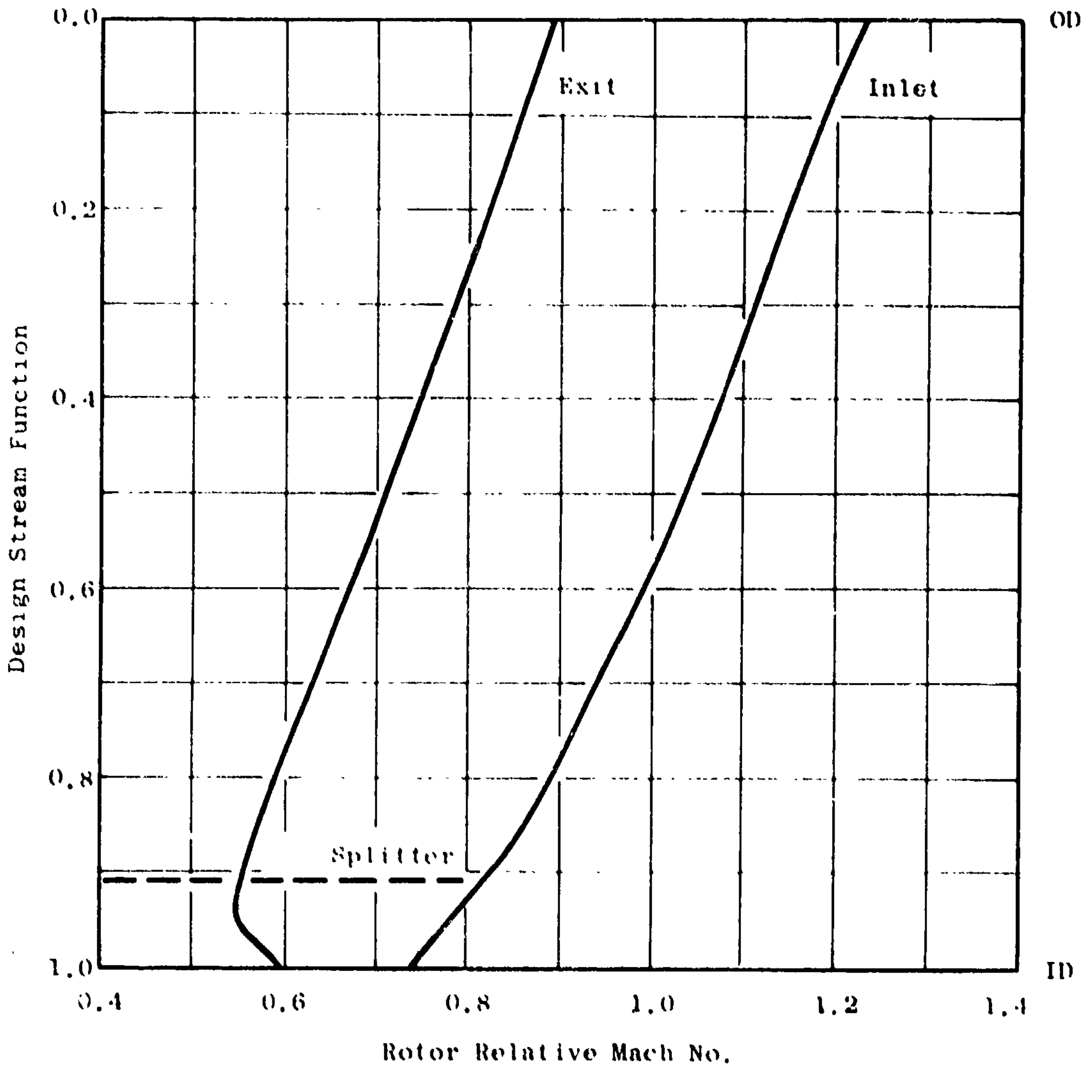

Figure 6. OTW Radial Distribution of Rotor Relative Mach Number.

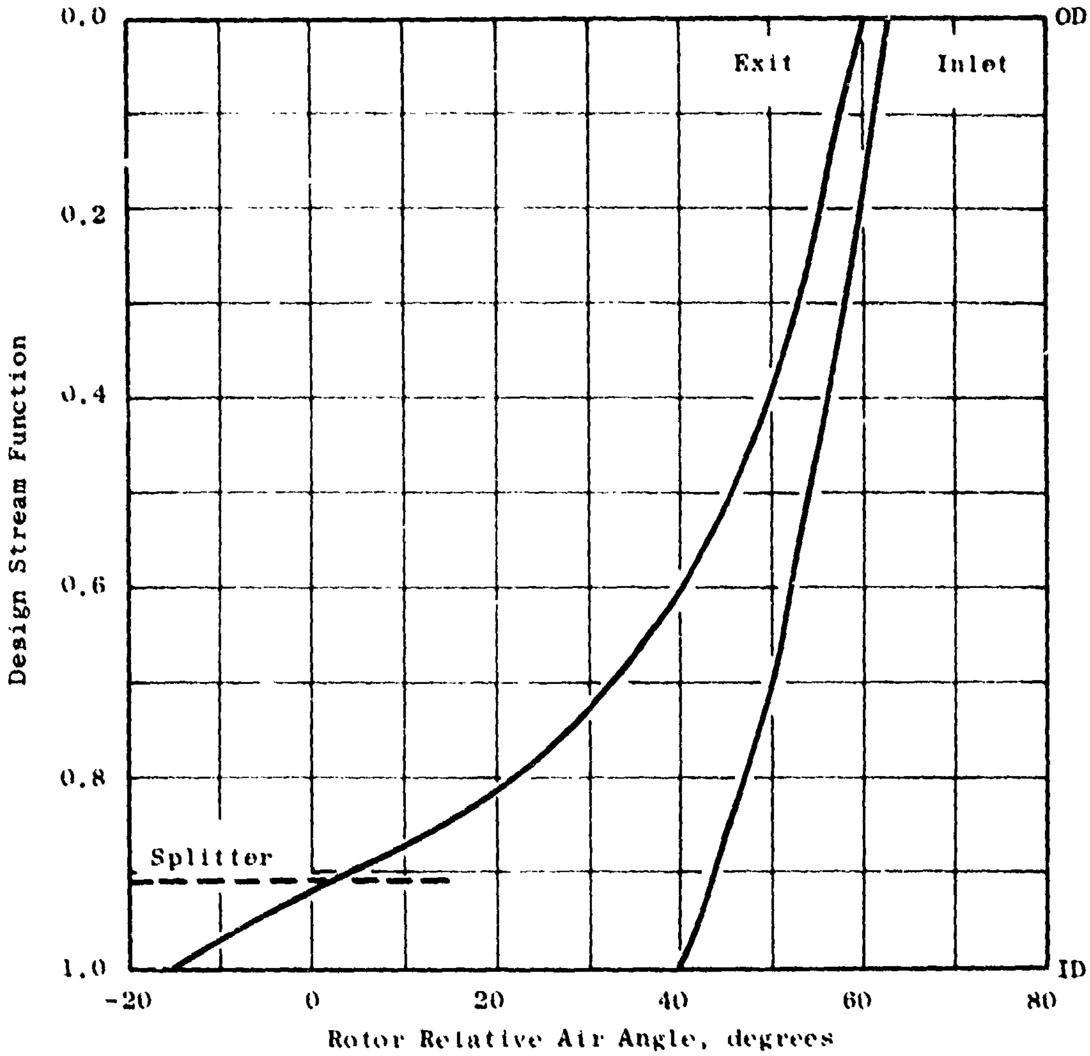

Figure 7. OTW Radial Distribution of Rotor Relative Air Angle.

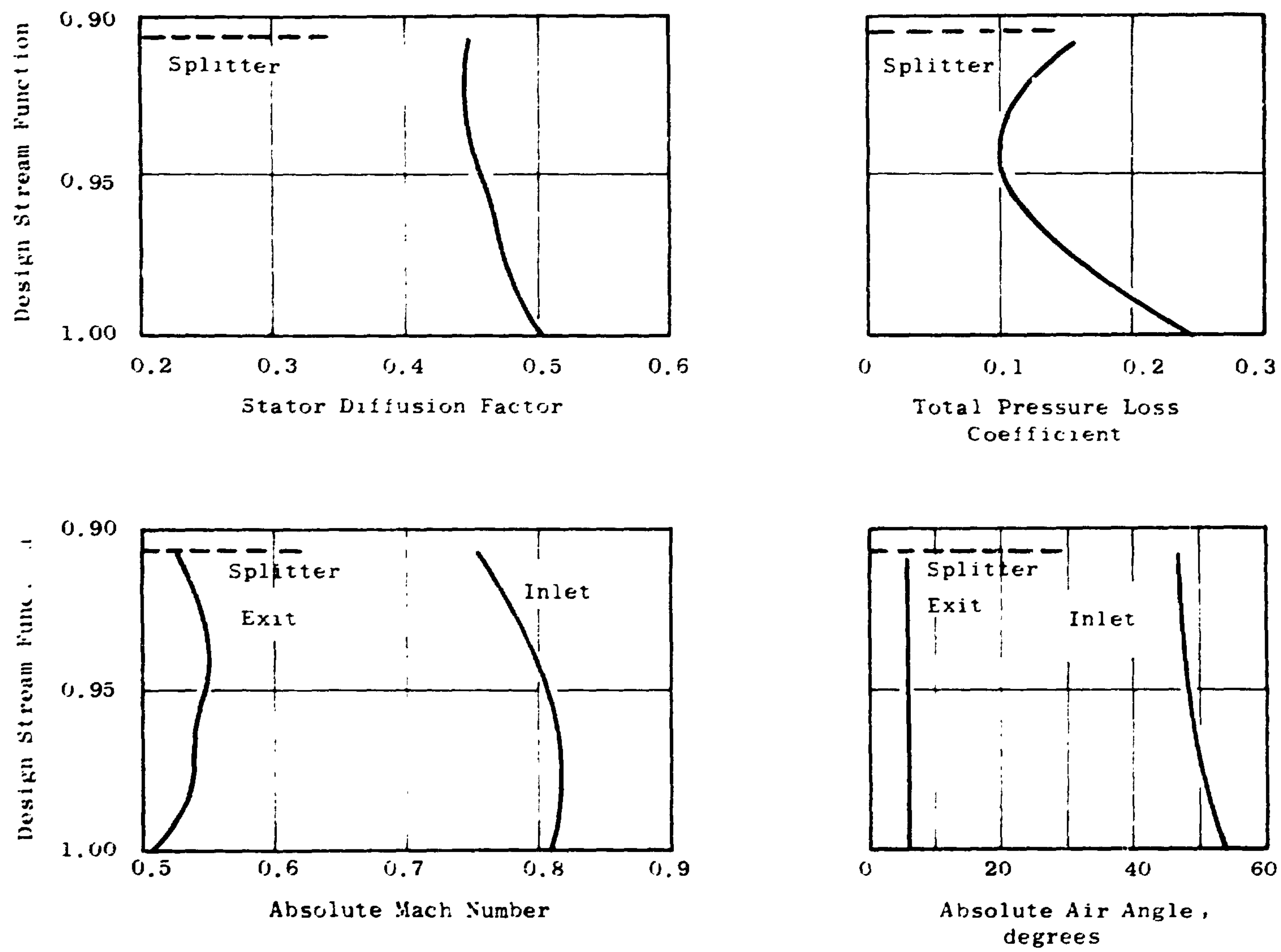

Figure 8. OTW Radial Distribution for Core OGV.

Table II. Design Blade Element Parameters for QCSEE OTW Fan.

NOMENCLATURE FOR TABULATION

HEADING	IDENTIFICATION	METRIC UNITS
GENERAL		
SL	STREAMLINE NUMBER	-
PSI	STREAM FUNCTION	-
RADIUS	STREAMLINE RADIUS	CM.
% IMM	PERCENT IMMERSION FROM OUTER WALL	%
Z	AXIAL DIMENSION	CM.
BLKAGF	ANNULUS BLOCKAGE FACTOR	-
FLOW	WEIGHT FLOW	KG/SEC
ANGLES AND MACH NUMBERS		
PHI	MERIDIONAL FLOW ANGLE	DEG.
ALPHA	ABSOLUTE FLOW ANGLE =ARCTAN (CU/CZ)	DEG.
BETA	RELATIVE FLOW ANGLE =ARCTAN (-WU/CZ)	DEG.
M-ABS	ABSOLUTE MACH NUMBER	-
M-REL	RELATIVE MACH NUMBER	-
VELOCITIES		
C	ABSOLUTE VELOCITY	M/SEC
W	RELATIVE VELOCITY	M/SEC
CZ	AXIAL VELOCITY	M/SEC
U	BLADE SPEED	M/SEC
CU	TANGENTIAL COMPONENT OF C	M/SEC
WU	TANGENTIAL COMPONENT OF W	M/SEC
FLUID PROPERTIES		
PT	ABSOLUTE TOTAL PRESSURE	N/SQ.CM.
TT	ABSOLUTE TOTAL TEMPERATURE	DEG-K
TT-REL	RELATIVE TOTAL TEMPERATURE	DEG-K
PS	STATIC PRESSURE	N/SQ.CM.
TS	STATIC TEMPERATURE	DEG-K
RHO	STATIC DENSITY	KG/CU.METER
EFF	CUMULATIVE ADIABATIC EFFICIENCY REFERENCED TO PTI, TTI	-
PTI	INLET ABSOLUTE TOTAL PRESSURE	N/SQ.CM.
TTI	INLET ABSOLUTE TOTAL TEMPERATURE	DEG-K
AERODYNAMIC BLADING PARAMETERS		
TPLC	TOTAL PRESSURE LOSS COEFFICIENT	-
PR-ROW	TOTAL PRESSURE RATIO ACROSS BLADE ROW	-
DEL-T	TOTAL TEMPERATURE RISE ACROSS ROTOR	DEG-K
D	DIFFUSION FACTOR	-
DP/Q	STATIC PRESSURE RISE COEFFICIENT	-
CZ/CZ	AXIAL VELOCITY RATIO ACROSS BLADE ROW	-
SOLDTY	SOLIDITY	-
R-AVG	AVERAGE STREAMLINE RADIUS ACROSS BLADE ROW	CM.
F-TAN	TANGENTIAL BLADE FORCE PER UNIT BLADE LENGTH	N/CM
F-AXL	AXIAL BLADE FORCE PER UNIT BLADE LENGTH	N/CM
F-COEF	FLOW COEFFICIENT =CZ1/U1	-
T-COEF	WORK COEFFICIENT =(2*G*J*CP*DEL-T)/(U2*U2)	-

Table II. Design Blade Element Parameters for QCSEE OTW Fan (Continued).

STATION 1.00000 Z 419.608826 ROTOR 1 INLET METRIC UNITS

SL	PSI	RADIUS	% IMM	PHI	ALPHA	BETA	M-ABS	M-REL	C	W	CZ	U	CU	RU	SL
1	0.	90.1702	0.	0.	0.	62.85	0.556	1.219	183.7	402.5	183.7	358.1	0.	-358.1	1
2	0.1000	86.2924	7.4	1.01	0.	61.72	0.559	1.179	184.4	389.2	184.4	342.7	0.	-342.7	2
3	0.2500	80.1662	19.1	2.46	0.	59.51	0.569	1.121	187.7	369.6	187.5	318.4	0.	-318.4	3
4	0.4500	73.6279	31.6	4.27	0.	56.72	0.585	1.063	192.5	350.1	191.9	292.4	0.	-292.4	4
5	0.5400	67.0438	44.1	6.57	0.	53.76	0.598	1.007	196.5	330.9	195.2	266.3	0.	-266.3	5
6	0.6900	59.2300	59.0	9.61	0.	50.12	0.607	0.959	199.3	308.3	196.5	235.3	0.	-235.3	6
7	0.8000	52.7467	71.4	12.57	0.	46.98	0.610	0.883	200.3	289.9	195.5	209.5	0.	-209.5	7
8	0.8800	47.4202	81.5	15.46	0.	44.46	0.606	0.834	199.0	274.5	191.8	188.3	0.	-188.3	8
9	0.9420	42.7395	90.5	17.70	0.	42.30	0.596	0.788	195.9	259.2	186.6	169.8	0.	-169.8	9
10	0.9610	41.1753	93.5	18.17	0.	41.47	0.592	0.773	194.7	254.3	185.0	163.5	0.	-163.5	10
11	0.9810	39.4530	96.7	18.39	0.	40.56	0.591	0.759	194.3	249.6	184.4	156.7	0.	-156.7	11
12	1.0000	37.7470	100.0	18.35	0.	38.77	0.598	0.752	196.7	247.3	186.7	149.9	0.	-149.9	12

SL	PSI	RADIUS	PT	TT	TT-REL	PS	TS	RHO	PT/PTI	TT/TTI	EFF	BLKAGE	SL
1	0.	90.1702	10.132	288.16	352.00	8.212	271.37	1.05422	1.0000	1.00000		0.98000	1
2	0.1000	86.2924	10.132	288.16	346.62	8.198	271.24	1.05297	1.0000	1.00000		0.98000	2
3	0.2500	80.1662	10.132	288.16	338.62	8.134	270.65	1.04708	1.0000	1.00000		0.98000	3
4	0.4500	73.6279	10.132	288.16	330.72	8.040	269.73	1.03837	1.0000	1.00000		0.98000	4
5	0.5400	67.0438	10.132	288.16	323.45	7.959	268.95	1.03089	1.0000	1.00000		0.98000	5
6	0.6900	59.2300	10.132	288.16	315.70	7.900	268.39	1.02550	1.0000	1.00000		0.98000	6
7	0.8000	52.7467	10.132	288.16	310.01	7.880	268.19	1.02364	1.0000	1.00000		0.98000	7
8	0.8800	47.4202	10.132	288.16	305.82	7.908	268.46	1.02619	1.0000	1.00000		0.98000	8
9	0.9420	42.7395	10.132	288.16	302.50	7.971	269.07	1.03204	1.0000	1.00000		0.98000	9
10	0.9610	41.1753	10.132	288.16	301.47	7.994	269.29	1.03416	1.0000	1.00000		0.98000	10
11	0.9810	39.4530	10.132	288.16	300.36	8.002	269.37	1.03488	1.0000	1.00000		0.98000	11
12	1.0000	37.7470	10.132	288.16	299.35	7.955	268.91	1.03055	1.0000	1.00000		0.98000	12

MASS AVERAGED VALUES

PT/PTI 1.0000 EFF PT 10.132 TT 288.16 TT/TTI 1.00000 CZ 190.80

CORR. FLOW 408.233 CORR. RPM 3792.8 CORR. U-TIP 358.1

PTI 10.132
TTI 288.161
GAMMA 1.4000

ORIGINAL PAGE IS
OF POOR QUALITY

Table II. Design Blade Element Parameters for QCSEE OTW Fan (Continued).

STATION 1.50000 Z 441.452866 ROTOR 1 EXIT METRIC UNITS

SL	PSI	RADIUS	% IMM	PHI	ALPHA	BETA	M-ABS	M-REL	C	W	CZ	U	CU	WU	SL
1	0,	90,1702	0,	0,	29,08	59,79	0,516	0,897	180,3	313,1	157,5	358,1	87,6	-270,5	1
2	0,1000	86,4904	8,1	0,61	29,13	57,30	0,534	0,863	186,0	300,7	162,4	343,5	90,5	-253,0	2
3	0,2500	80,8166	20,6	1,49	29,28	53,87	0,549	0,812	190,7	282,0	166,3	321,0	93,2	-227,8	3
4	0,4000	74,8402	33,7	2,62	29,98	49,54	0,567	0,757	196,3	261,9	169,9	297,3	98,0	-199,2	4
5	0,5400	68,9141	46,8	4,03	31,56	43,61	0,595	0,700	205,4	241,6	174,7	273,7	107,3	-166,4	5
6	0,6900	62,1238	61,7	6,18	34,61	33,47	0,648	0,639	222,8	219,8	182,6	246,7	126,0	-120,7	6
7	0,8000	56,7578	73,6	9,21	38,29	22,02	0,708	0,601	242,5	206,0	188,9	225,4	149,1	-76,4	7
8	0,8800	52,5054	82,9	13,34	44,29	8,37	0,769	0,564	263,2	192,9	185,8	208,5	181,2	-27,3	8
9	0,9420	48,7355	91,2	13,71	48,87	-4,44	0,819	0,549	279,2	187,2	181,4	193,6	207,6	14,1	9
10	0,9610	47,4842	94,0	14,07	49,66	-8,03	0,837	0,557	284,8	189,4	182,0	188,6	214,3	25,7	10
11	0,9610	46,1091	97,0	15,10	50,21	-11,77	0,863	0,575	292,7	195,0	184,6	183,1	221,6	38,5	11
12	1,0000	44,7422	100,0	16,96	50,63	-15,20	0,893	0,600	301,3	202,7	187,6	177,7	228,7	51,0	12

SL	PSI	RADIUS	PT	TT	TT-REL	PS	TS	RHO	PT/PT1	TT/TT1	EFF	BLKAGE	SL
1	0,	90,1702	13,587	319,39	352,00	11,328	303,22	1,30151	1,3410	1,10857	0,8069	0,96000	1
2	0,1000	86,4904	13,699	319,11	346,89	11,283	301,90	1,30195	1,3520	1,10741	0,8378	0,96000	2
3	0,2500	80,8166	13,749	317,94	339,44	11,200	299,85	1,30125	1,3570	1,10336	0,8817	0,96000	3
4	0,4000	74,8402	13,800	317,17	332,14	11,094	297,99	1,29695	1,3620	1,10066	0,9168	0,96000	4
5	0,5400	68,9141	13,912	317,39	325,45	10,949	296,40	1,28694	1,3730	1,10143	0,9347	0,96000	5
6	0,6900	62,1238	14,206	319,11	318,46	10,716	294,41	1,26798	1,4020	1,10741	0,9437	0,96000	6
7	0,8000	56,7578	14,591	321,61	313,45	10,447	292,34	1,24497	1,4400	1,11608	0,9459	0,96000	7
8	0,8800	52,5054	15,188	325,78	309,81	10,267	291,29	1,22785	1,4990	1,13054	0,9392	0,96000	8
9	0,9420	48,7355	15,346	328,17	306,81	9,879	289,37	1,18939	1,5145	1,13883	0,9070	0,96000	9
10	0,9610	47,4842	15,244	328,39	305,86	9,631	288,01	1,16497	1,5045	1,13960	0,8867	0,96000	10
11	0,9810	46,1091	15,123	328,56	304,85	9,298	285,93	1,13289	1,4925	1,14018	0,8647	0,96000	11
12	1,0000	44,7422	14,955	328,61	303,86	8,913	283,44	1,09546	1,4760	1,14037	0,8382	0,96000	12

SL	PSI	TPLC	PR-ROW	DEL-T	D	DP/Q	CZ/CZ	SOLDTY	R-AVG	F-TAN	F-AXL	F-COEF	T-COEF	SL
1	0,	0,10796	1,3410	31,23	0,306	0,255	0,858	1,3000	90,1702	959,41	1479,67	0,513	0,489	1
2	0,1000	0,09393	1,3520	30,95	0,315	0,277	0,881	1,3340	86,3914	966,16	1442,01	0,538	0,527	2
3	0,2500	0,07096	1,3570	29,78	0,328	0,316	0,887	1,3941	80,4914	943,17	1338,06	0,589	0,581	3
4	0,4000	0,05247	1,3620	29,01	0,348	0,365	0,885	1,4672	74,2341	930,17	1217,82	0,656	0,600	4
5	0,5400	0,04486	1,3730	29,23	0,376	0,414	0,895	1,5533	67,9789	946,30	1098,99	0,733	0,784	5
6	0,6900	0,04512	1,4020	30,95	0,412	0,466	0,929	1,6764	60,6769	1008,48	965,77	0,835	1,021	6
7	0,8000	0,05110	1,4400	33,45	0,437	0,493	0,966	1,7995	54,7532	1081,72	839,04	0,933	1,323	7
8	0,8800	0,06956	1,4990	37,62	0,477	0,516	0,969	1,9203	49,9628	1171,49	704,75	1,016	1,738	8
9	0,9420	0,12229	1,5145	40,01	0,486	0,472	0,972	2,0461	45,7375	1180,83	519,82	1,099	2,145	9
10	0,9610	0,15387	1,5045	40,23	0,471	0,423	0,984	2,0911	44,3297	1167,11	440,43	1,131	2,272	10
11	0,9810	0,18928	1,4925	40,39	0,441	0,349	1,001	2,1490	42,7811	1154,85	349,78	1,177	2,420	11
12	1,0000	0,22906	1,4760	40,45	0,405	0,264	1,005	2,2310	41,2446	1143,29	253,13	1,205	2,574	12

MASS AVERAGED VALUES

PT/PT1 1,5948 EFF 0,9040 PT 14,132 TT 319,95 TT/TT1 1,11052 CZ 174,26 ROW PT2/PT1 1,5948

CORR, FLOW 308,411 CORR, RPM 3599,5

ORIGINAL PAGE IS OF POOR QUALITY

Table II. Design Blade Element Parameters for QCSEE OTW Fan (Continued).

STATION 1.60000 Z 453.708389 CORE OGV INLET

METRIC UNITS

SL	PSI	RADIUS	% IMM	PHI	ALPHA	BETA	M-ABS	M-REL	C	W	CZ	U	CU	WU	SL
1	0.9082	51.9304	0.	-2.05	46.70	5.70	0.755	0.520	259.1	178.7	177.7	206.3	188.5	-17.7	1
2	0.9420	49.8937	34.2	-0.66	47.93	-1.45	0.799	0.535	273.2	185.1	183.0	198.2	202.8	4.6	2
3	0.9610	48.7022	54.2	1.13	48.95	-4.87	0.811	0.535	277.1	182.6	181.9	193.4	208.9	15.5	3
4	0.9810	47.3683	[illegible]	2.94	51.01	-8.97	0.813	0.518	277.7	177.0	174.6	188.1	215.7	27.6	4
5	1.0000	45.9741	100.0	3.30	53.84	-13.80	0.807	0.491	275.8	167.8	162.7	182.6	222.6	40.0	5

SL	PSI	RADIUS	PT	TT	TT-REL	PS	TS	RHO	PT/PTI	TT/TTI	EFF	BLKAGE	SL
1	0.9082	51.9304	15.260	326.86	309.53	10.462	293.45	1.24207	1.5061	1.13431	0.9241	0.96000	1
2	0.9420	49.8937	15.346	328.17	307.71	10.078	291.02	1.20642	1.5145	1.13883	0.9070	0.96000	2
3	0.9610	48.7022	15.244	328.39	306.78	9.888	290.18	1.18706	1.5045	1.13960	0.8867	0.96000	3
4	0.9810	47.3683	15.123	328.56	305.78	9.791	290.18	1.17548	1.4925	1.14018	0.8647	0.96000	4
5	1.0000	45.9741	14.955	328.61	304.76	9.744	290.75	1.16747	1.4760	1.14037	0.8382	0.96000	5

MASS AVERAGED VALUES

PT/PTI 1.5021 EFF 0.8894 PT 15.220 TT 328.10 TT/TTI 1.13861 CZ 178.09

CORR. FLOW 26.621 CORR. RPM 3554.5

Table II. Design Blade Element Parameters for QCSEE OTW Fan (Continued).

STATION 1.90000 Z 457.645397 CORE OGV EXIT

METRIC UNITS

SL	PSI	RADIUS	% IMM	PHI	ALPHA	BETA	M-ABS	M-REL	C	W	CZ	U	CU	WU	SL
1	0.9082	51.5824	0.	-2.03	6.00	45.17	0.526	0.742	185.5	261.6	184.4	204.9	19.4	-185.5	1
2	0.9420	49.7700	35.2	-2.36	6.00	42.57	0.551	0.744	194.3	262.3	193.1	197.7	20.3	-177.4	2
3	0.9610	48.7398	55.2	-1.21	6.00	42.25	0.544	0.731	192.1	258.1	191.0	193.6	20.1	-173.5	3
4	0.9810	47.5964	77.4	0.33	6.00	41.84	0.538	0.718	190.0	253.6	189.0	189.0	19.9	-169.2	4
5	1.0000	46.4313	100.0	3.30	6.00	42.48	0.514	0.692	181.9	245.2	180.7	184.4	19.0	-165.4	5

SL	PSI	RADIUS	PT	TT	TT-REL	PS	TS	RHO	PT/PTI	TT/TTI	EFF	BLKAGE	SL
1	0.9082	51.5824	14.507	326.86	343.80	12.015	309.73	1.35143	1.4317	1.13431	0.8039	0.94000	1
2	0.9420	49.7700	14.828	328.17	343.62	12.063	309.37	1.35834	1.4634	1.13883	0.8279	0.94000	2
3	0.9610	48.7398	14.611	328.39	343.17	11.944	310.01	1.34218	1.4420	1.13960	0.7897	0.94000	3
4	0.9810	47.5964	14.206	328.56	342.60	11.668	310.59	1.30869	1.4020	1.14018	0.7230	0.94000	4
5	1.0000	46.4313	13.680	328.61	342.05	11.426	312.14	1.27523	1.3501	1.14037	0.6379	0.94000	5

SL	PSI	TPLC	PR-ROW	DEL-T	D	DP/Q	CZ/CZ	SOLDTY	R-AVG	F-TAN	F-AXL	F-COEF	T-COEF	SL
1	0.9082	0.15705	0.9506		0.447	0.324	1.038	2.0054	51.7564	1226.83	555.15			1
2	0.9420	0.09821	0.9663		0.450	0.377	1.055	2.0778	49.8318	1310.24	697.21			2
3	0.9610	0.11828	0.9584		0.467	0.384	1.050	2.1220	48.7210	1296.05	695.55			3
4	0.9810	0.17204	0.9393		0.478	0.352	1.082	2.1725	47.4823	1254.85	655.33			4
5	1.0000	0.24477	0.9147		0.505	0.323	1.111	2.2279	46.2027	1178.56	596.12			5

MASS AVERAGED VALUES

PT/PTI 1.4280 EFF 0.7730 PT 14.469 TT 328.10 TT/TTI 1.13861 CZ 188.62 ROW PT2/PT1 0.9506

CORR. FLOW 28.004 CORR. RPM 3554.5

ORIGINAL PAGE IS OF POOR QUALITY

Table II. Design Blade Element Parameters for QCSEE OTW Fan (Continued).

STATION 11.60000 Z 487.680958 BYPASS OGV INLET METRIC UNITS

SL	PSI	RADIUS	% IMM	PHI	ALPHA	BETA	M-ABS	M-REL	C	W	CZ	U	CU	WU	SL
1	0.	90.1702	0.	0.	27.51	58.13	0.545	0.915	189.6	318.6	168.2	356.1	87.6	-270.5	1
2	0.1000	86.6702	9.4	0.09	27.63	55.80	0.561	0.884	194.8	307.0	172.5	344.2	90.3	-253.9	2
3	0.2500	81.2596	24.0	0.11	27.86	52.68	0.573	0.835	198.4	289.3	175.4	322.7	92.7	-230.0	3
4	0.4000	75.5505	39.3	-0.05	28.62	48.75	0.587	0.782	202.7	269.9	178.0	300.1	97.1	-203.0	4
5	0.5400	69.8857	54.6	-0.32	30.20	43.39	0.610	0.726	210.3	250.1	181.7	277.6	105.8	-171.8	5
6	0.6900	63.4071	72.0	-0.65	33.10	34.13	0.658	0.666	226.1	228.8	189.4	251.8	123.5	-128.4	6
7	0.8000	58.3438	85.6	-0.76	36.30	23.71	0.715	0.630	245.0	215.6	197.4	231.7	145.[illegible]	-86.7	7
8	0.8800	54.4432	96.1	-0.35	40.66	11.52	[illegible]	0.608	268.2	207.7	203.5	216.2	174.8	-41.5	8
9	0.9082	52.9921	100.0	0.	42.47	7.27	0.802	0.596	273.6	203.4	201.8	210.5	184.7	-25.7	9

SL	PSI	RADIUS	PT	TT	TT-REL	PS	TS	RHO	PT/PT1	TT/TT1	EFF	BLKAGE	SL
1	0.	90.1702	15.587	319.59	352.00	11.104	301.49	1.28306	1.3410	1.10837	0.8069	0.96000	1
2	0.1000	86.6702	15.699	319.11	347.14	11.066	300.23	1.28407	1.3520	1.10741	0.8376	0.96000	2
3	0.2500	81.2596	15.749	317.94	340.00	11.006	298.36	1.28512	1.3570	1.10336	0.8817	0.96000	3
4	0.4000	75.5505	13.800	317.17	332.97	10.928	296.71	1.28309	1.3620	1.10066	0.9166	0.96000	4
5	0.5400	69.8857	13.912	317.59	326.51	10.818	295.38	1.27593	1.3730	1.10143	0.9347	0.96000	5
6	0.6900	63.4071	14.206	319.11	319.73	10.621	293.67	1.25995	1.4020	1.10741	0.9437	0.96000	6
7	0.8000	58.3438	14.591	321.61	314.89	10.373	291.74	1.23868	1.4400	1.11608	0.9459	0.96000	7
8	0.8800	54.4432	15.188	325.78	311.43	10.104	289.97	1.21596	1.4990	1.13054	0.9392	0.96000	8
9	0.9082	52.9921	15.260	326.86	310.21	9.991	289.61	1.20187	1.5061	1.13431	0.9241	0.96000	9

MASS AVERAGED VALUES

PT/PT1 1.5842 EFF 0.9059 PT 14.026 TT 319.13 TT/TT1 1.10746 CZ 182.45

CORR. FLOW 281.868 CORR. RPM 3604.1

Table II. Design Blade Element Parameters for QCSEE OTW Fan (Continued).

STATION 11.90000 Z 508.000899 BYPASS OGV EXIT METRIC UNITS

SL	PSI	RADIUS	% IMM	PHI	ALPHA	BETA	M-ABS	M-REL	C	W	CZ	U	CU	WU	SL
1	0.	90.1702*	0.	0.	0.	66.04	0.453	1.116	159.1	391.9	159.1	358.1	0.	-358.1	1
2	0.1000	86.5840	9.6	-0.61	0.	64.00	0.479	1.093	167.8	382.6	167.7	343.9	0.	-343.9	2
3	0.2500	81.1196	24.3	-0.84	0.	62.29	0.484	1.042	169.2	363.9	169.2	322.2	0.	-322.2	3
4	0.4000	75.3356	39.9	-0.99	0.	60.44	0.487	0.986	169.7	344.0	169.7	299.2	0.	-299.2	4
5	0.5400	69.5833	55.4	-1.06	0.	58.11	0.493	0.933	172.0	325.5	172.0	276.4	0.	-276.4	5
6	0.6900	63.0610	72.9	-0.84	0.	54.34	0.515	0.883	179.7	306.3	179.7	250.5	0.	-250.5	6
7	0.8000	58.0669	86.4	-0.34	0.	50.68	0.541	0.853	188.9	298.1	188.9	230.6	0.	-230.6	7
8	0.8800	54.3422	96.4	0.00	0.	47.24	0.569	0.838	199.6	294.0	199.6	215.8	0.	-215.8	8
9	0.9082	52.9921*	100.0	0.	0.	46.68	0.565	0.823	198.4	289.3	198.4	210.5	0.	-210.5	9

SL	PSI	RADIUS	PT	TT	TT-REL	PS	TS	RHO	PT/PT1	TT/TT1	EFF	BLKAGE	SL
1	0.	90.1702	13.359	319.39	383.22	11.566	306.79	1.31568	1.3165	1.10837	0.7542	0.95000	1
2	0.1000	86.5840	13.570	319.11	377.97	11.598	305.11	1.32422	1.3393	1.10741	0.8105	0.95000	2
3	0.2500	81.1196	13.655	317.94	369.61	11.630	303.69	1.33414	1.3477	1.10336	0.8610	0.95000	3
4	0.4000	75.3356	13.713	317.17	361.73	11.663	302.83	1.34171	1.3534	1.10066	0.8971	0.95000	4
5	0.5400	69.5833	13.817	317.39	355.40	11.701	302.66	1.34677	1.3636	1.10143	0.9136	0.95000	5
6	0.6900	63.0610	14.079	319.11	350.33	11.748	303.05	1.35061	1.3895	1.10741	0.9174	0.95000	6
7	0.8000	58.0669	14.360	321.61	348.08	11.771	303.86	1.34957	1.4172	1.11608	0.9024	0.95000	7
8	0.8800	54.3422	14.664	325.78	348.96	11.771	305.95	1.34031	1.4472	1.13054	0.8533	0.95000	8
9	0.9082	52.9921	14.614	326.86	348.91	11.770	307.26	1.33444	1.4423	1.13431	0.8212	0.95000	9

SL	PSI	TFLC	PR-RLW	DEL-T	D	DP/Q	CZ/CZ	SOLDTY	R-AVG	F-TAN	F-AXL	F-COEF	T-COEF	SL
1	0.	0.09995	0.9817		0.348	0.194	0.946	1.2320	90.1702	1007.63	169.02			1
2	0.1000	0.04891	0.9906		0.315	0.202	0.972	1.3144	86.6271	1041.62	233.84			2
3	0.2500	0.03438	0.9931		0.308	0.228	0.965	1.4525	81.1896	1018.76	250.40			3
4	0.4000	0.03046	0.9937		0.311	0.256	0.954	1.6215	75.4431	1002.49	263.69			4
5	0.5400	0.03073	0.9932		0.321	0.285	0.946	1.8177	69.7345	1025.84	291.92			5
6	0.6900	0.03546	0.9911		0.336	0.314	0.949	2.0828	63.2340	1127.54	359.47			6
7	0.8000	0.05475	0.9842		0.356	0.331	0.957	2.3292	58.2053	1264.73	436.84			7
8	0.8800	0.10312	0.9655		0.384	0.328	0.981	2.5456	54.3927	1467.21	537.56			8
9	0.9082	0.12270	0.9576		0.403	0.338	0.983	2.6340	52.9921	1489.65	565.96			9

MASS AVERAGED VALUES

PT/PT1 1.3667 EFF 0.8730 PT 13.868 TT 319.13 TT/TT1 1.10746 CZ 174.83 RCA PT2/PT1 0.9885

CORR. FLOW 285.072 CORR. RPM 3664.1

*Bypass OGV exit tip and hub radii listed in this table were changed to 90.2843 cm and 52.2986 cm, respectively, after the aero design was completed in order to improve transition of the fan flowpath into the bypass exhaust duct contours. The impact of these changes on OGV blade element parameters was estimated to be small, and the design data were not recomputed.

ORIGINAL PAGE IS
OF POOR QUALITY

Table II. Design Blade Element Parameters for QCSEE OTW Fan (Continued).

NOMENCLATURE FOR TABULATION

HEADING	IDENTIFICATION	ENGLISH UNITS
GENERAL		
SL	STREAMLINE NUMBER	-
PSI	STREAM FUNCTION	-
RADIUS	STREAMLINE RADIUS	IN.
% IMM	PERCENT IMMERSION FROM OUTER WALL	%
Z	AXIAL DIMENSION	IN.
BLKAGE	ANNULUS BLOCKAGE FACTOR	-
FLOW	WEIGHT FLOW	LBM/SEC
ANGLES AND MACH NUMBERS		
PHI	MERIDIONAL FLOW ANGLE	DEG.
ALPHA	ABSOLUTE FLOW ANGLE =ARCTAN (CU/CZ)	DEG.
BETA	RELATIVE FLOW ANGLE =ARCTAN (-WU/CZ)	DEG.
M-ABS	ABSOLUTE MACH NUMBER	-
M-REL	RELATIVE MACH NUMBER	-
VELOCITIES		
C	ABSOLUTE VELOCITY	FT/SEC
W	RELATIVE VELOCITY	FT/SEC
CZ	AXIAL VELOCITY	FT/SEC
U	BLADE SPEED	FT/SEC
CU	TANGENTIAL COMPONENT OF C	FT/SEC
WU	TANGENTIAL COMPONENT OF W	FT/SEC
FLUID PROPERTIES		
PT	ABSOLUTE TOTAL PRESSURE	LBF/SQ.IN.
TT	ABSOLUTE TOTAL TEMPERATURE	DEG-R
TT-REL	RELATIVE TOTAL TEMPERATURE	DEG-R
PS	STATIC PRESSURE	LBF/SQ.IN.
TS	STATIC TEMPERATURE	DEG-R
RHO	STATIC DENSITY	LBM/CU.FT.
EFF	CUMULATIVE ADIABATIC EFFICIENCY REFERENCED TO PTI, TTI	-
PTI	INLET ABSOLUTE TOTAL PRESSURE	LBF/SQ.IN.
TTI	INLET ABSOLUTE TOTAL TEMPERATURE	DEG-R
AERODYNAMIC BLADING PARAMETERS		
TPLC	TOTAL PRESSURE LOSS COEFFICIENT	-
PR-ROW	TOTAL PRESSURE RATIO ACROSS BLADE ROW	-
DEL-T	TOTAL TEMPERATURE RISE ACROSS ROTOR	DEG-R
D	DIFFUSION FACTOR	-
DP/Q	STATIC PRESSURE RISE COEFFICIENT	-
CZ/CZ	AXIAL VELOCITY RATIO ACROSS BLADE ROW	-
SOLDTY	SOLIDITY	-
R-AVG	AVERAGE STREAMLINE RADIUS ACROSS BLADE ROW	IN.
F-TAN	TANGENTIAL BLADE FORCE PER UNIT BLADE LENGTH	LBF/IN
F-AXL	AXIAL BLADE FORCE PER UNIT BLADE LENGTH	LBF/IN
F-COEF	FLOW COEFFICIENT =CZ1/U1	-
T-COEF	WORK COEFFICIENT =(2*G*J*CP*DEL-T)/(U2*U2)	-

Table II. Design Blade Element Parameters for QCSEE OTW Fan (Continued).

STATION 1.00000 Z 165.200001 ROTOR 1 INLET ENGLISH UNITS

SL	PSI	RADIUS	% IMM	PHI	ALPHA	BETA	M-ABS	M-REL	C	W	CZ	U	CU	WU	SL
1	0.	35.5000	0.	0.	0.	62.85	0.556	1.219	602.7	1320.5	602.7	1175.0	0.	-1175.0	1
2	0.1000	33.9733	7.4	1.01	0.	61.72	0.559	1.179	605.0	1276.9	604.9	1124.5	0.	-1124.5	2
3	0.2500	31.5615	19.1	2.46	0.	59.51	0.569	1.121	615.7	1212.6	615.2	1044.6	0.	-1044.6	3
4	0.4000	28.9873	31.6	4.22	0.	56.72	0.585	1.063	631.4	1148.6	629.7	959.4	0.	-959.4	4
5	0.5400	26.3952	44.1	6.50	0.	53.76	0.598	1.007	644.6	1085.7	640.4	873.6	0.	-873.6	5
6	0.6900	23.3169	59.0	9.61	0.	50.12	0.607	0.939	654.0	1011.6	644.8	771.6	0.	-771.6	6
7	0.8000	20.7672	71.4	12.57	0.	46.98	0.610	0.883	657.2	951.0	641.5	687.4	0.	-687.4	7
8	0.8800	18.6693	81.5	15.46	0.	44.48	0.606	0.834	652.8	898.9	629.2	617.9	0.	-617.9	8
9	0.9420	16.8265	90.5	17.70	0.	42.30	0.596	0.788	642.6	850.3	612.2	556.9	0.	-556.9	9
10	0.9610	16.2107	93.5	18.17	0.	41.47	0.592	0.773	638.9	834.3	607.0	536.6	0.	-536.6	10
11	0.9810	15.5327	96.7	18.39	0.	40.36	0.591	0.759	637.6	819.0	605.0	514.1	0.	-514.1	11
12	1.0000	14.8610	100.0	18.35	0.	38.77	0.598	0.752	645.2	811.3	612.4	491.9	0.	-491.9	12

SL	PSI	RADIUS	PT	TT	TT-REL	PS	TS	RHO	PT/PT1	TT/TT1	EFF	BLKAGE	SL
1	0.	35.5000	14.696	518.69	643.59	11.910	488.46	0.06581	1.0000	1.00000		0.98000	1
2	0.1000	33.9733	14.696	518.69	623.92	11.891	488.23	0.06574	1.0000	1.00000		0.98000	2
3	0.2500	31.5615	14.696	518.69	609.51	11.798	487.14	0.06537	1.0000	1.00000		0.98000	3
4	0.4000	28.9873	14.696	518.69	595.30	11.661	485.51	0.06483	1.0000	1.00000		0.98000	4
5	0.5400	26.3952	14.696	518.69	582.21	11.543	484.11	0.06436	1.0000	1.00000		0.98000	5
6	0.6900	23.3169	14.696	518.69	568.27	11.459	483.10	0.06402	1.0000	1.00000		0.98000	6
7	0.8000	20.7672	14.696	518.69	558.01	11.430	482.74	0.06391	1.0000	1.00000		0.98000	7
8	0.8800	18.6693	14.696	518.69	550.47	11.469	483.22	0.06406	1.0000	1.00000		0.98000	8
9	0.9420	16.8265	14.696	518.69	544.50	11.561	484.33	0.06443	1.0000	1.00000		0.98000	9
10	0.9610	16.2107	14.696	518.69	542.65	11.594	484.72	0.06456	1.0000	1.00000		0.98000	10
11	0.9810	15.5327	14.696	518.69	540.69	11.606	484.86	0.06461	1.0000	1.00000		0.98000	11
12	1.0000	14.8610	14.696	518.69	538.83	11.538	484.04	0.06434	1.0000	1.00000		0.98000	12

MASS AVERAGED VALUES

PT/PT1 1.0000 EFF PT 14.696 TT 518.69 TT/TT1 1.00000 CZ 625.97

CORR. FLOW 900.030 CORR. RPM 3792.8 CORR. U-TIP 1175.0

PT1 14.696
TT1 518.690
GAMMA 1.4000

Table II. Design Blade Element Parameters for QCSEE OTW Fan (Continued).

STATION 1.50000 Z 173.799999 ROTOR 1 EXIT ENGLISH UNITS

SL	PSI	RADIUS	% IMM	PHI	ALPHA	BETA	M-ABS	M-REL	C	W	CZ	U	CU	WU	SL
1	0.	35.5000	0.	0.	29.08	59.79	0.516	0.897	591.4	1027.1	516.9	1175.0	287.4	-887.6	1
2	0.1000	34.0513	8.1	0.61	29.13	57.30	0.534	0.863	610.1	986.5	532.9	1127.0	297.0	-830.1	2
3	0.2500	31.8175	20.6	1.49	29.28	53.87	0.549	0.812	625.6	925.3	545.5	1053.1	305.8	-747.3	3
4	0.4000	29.4646	33.7	2.62	29.96	49.54	0.567	0.757	644.1	859.4	557.4	975.2	321.6	-653.6	4
5	0.5400	27.1315	46.8	4.03	31.56	43.61	0.595	0.700	673.8	792.6	573.1	898.0	352.0	-546.0	5
6	0.6900	24.4581	61.7	6.18	34.61	33.47	0.648	0.639	730.8	721.2	599.2	809.5	413.4	-396.1	6
7	0.8000	22.3455	73.6	9.21	38.29	22.02	0.708	0.601	795.7	675.8	619.6	739.6	489.1	-250.5	7
8	0.8800	20.6714	82.9	13.34	44.29	8.37	0.769	0.564	863.7	632.8	609.5	684.2	594.5	-89.6	8
9	0.9420	19.1871	91.2	13.71	48.87	-4.44	0.819	0.549	916.0	614.2	595.0	635.1	681.2	46.1	9
10	0.9610	18.6945	94.0	14.07	49.66	-8.03	0.837	0.557	934.5	621.4	597.2	618.8	705.0	84.3	10
11	0.9810	18.1532	97.0	15.10	50.21	-11.77	0.863	0.575	960.2	639.8	605.5	600.8	727.0	126.2	11
12	1.0000	17.6150	100.0	16.96	50.63	-15.20	0.893	0.600	988.4	664.9	615.5	583.0	750.3	167.2	12

SL	PSI	RADIUS	PT	TT	TT-REL	PS	TS	RHO	PT/PTI	TT/TTI	EFF	BLKAGE	SL
1	0.	35.5000	19.707	574.90	633.59	16.430	545.79	0.08125	1.3410	1.10837	0.8069	0.96000	1
2	0.1000	34.0513	19.869	574.40	624.41	16.364	543.42	0.08129	1.3520	1.10741	0.8378	0.96000	2
3	0.2500	31.8175	19.942	572.30	610.99	16.245	539.73	0.08124	1.3570	1.10336	0.8817	0.96000	3
4	0.4000	29.4646	20.016	570.90	597.84	16.090	536.38	0.08097	1.3620	1.10066	0.9168	0.96000	4
5	0.5400	27.1315	20.178	571.30	585.81	15.881	533.52	0.08034	1.3730	1.10143	0.9347	0.96000	5
6	0.6900	24.4581	20.604	574.40	573.23	15.542	529.95	0.07916	1.4020	1.10741	0.9437	0.96000	6
7	0.8000	22.3455	21.162	578.90	564.22	15.152	525.20	0.07772	1.4400	1.11608	0.9459	0.96000	7
8	0.8800	20.6714	22.029	586.40	557.65	14.891	524.32	0.07665	1.4990	1.13054	0.9392	0.96000	8
9	0.9420	19.1871	22.257	590.70	552.26	14.329	520.86	0.07425	1.5145	1.13883	0.9070	0.96000	9
10	0.9610	18.6945	22.110	591.10	550.55	13.969	518.42	0.07273	1.5045	1.13960	0.8867	0.96000	10
11	0.9810	18.1532	21.934	591.40	548.74	13.486	514.67	0.07073	1.4925	1.14018	0.8647	0.96000	11
12	1.0000	17.6150	21.691	591.50	546.98	12.927	510.19	0.06839	1.4760	[illegible]	0.8382	0.96000	12

SL	PSI	TPLC	PR-ROW	DEL-T	D	DP/Q	CZ/CZ	SOLDTY	R-AVG	F-TAN	F-AXL	F-COEF	T-COEF	SL
1	0.	0.10798	1.3410	56.21	0.306	0.255	0.858	1.3000	35.5000	547.84	844.92	0.513	0.459	1
2	0.1000	0.09393	1.3520	55.71	0.315	0.277	0.88[illegible]	1.3340	34.0123	551.69	823.41	0.538	0.527	2
3	0.2500	0.07096	1.3570	53.61	0.326	0.316	0.887	1.3941	31.6895	538.57	764.06	0.589	0.581	3
4	0.4000	0.05247	1.3620	52.21	0.348	0.365	0.885	1.4672	29.2260	531.14	695.40	0.656	0.660	4
5	0.5400	0.04486	1.3730	52.61	0.376	0.414	0.895	1.5533	26.7633	540.35	627.54	0.733	0.784	5
6	0.6900	0.04512	1.4020	55.71	0.412	0.466	0.924	1.6754	23.8885	575.86	551.47	0.835	1.021	6
7	0.8000	0.05110	1.4400	60.21	0.437	0.493	0.966	1.7995	21.5564	617.68	479.11	0.933	1.323	7
8	0.8800	0.06958	1.4990	67.71	0.477	0.516	0.969	1.9203	19.6704	668.94	402.43	1.018	1.738	8
9	0.9420	0.12229	1.5145	72.01	0.486	0.472	0.972	2.0461	18.0068	674.27	296.83	1.099	2.145	9
10	0.9610	0.15387	1.5045	72.41	0.471	0.423	0.984	2.0911	17.4526	666.44	251.30	1.131	2.272	10
11	0.9810	0.18928	1.4925	72.71	0.441	0.349	1.001	2.1490	16.8429	659.44	199.73	1.177	2.420	11
12	1.0000	0.22906	1.4760	72.81	0.405	0.264	1.005	2.2310	16.2380	652.79	144.54	1.245	2.574	12

MASS AVERAGED VALUES

PT/PTI 1.3948 EFF 0.9040 PT 29.498 TT 575.91 TT/TTI 1.11032 CZ 571.73 ROW PT2/PT1 1.3948

CORR. FLOW 679.931 CORR. RPM 3599.5

Table II. Design Blade Element Parameters for QCSEE OTW Fan (Continued).

STATION 1.60000 Z 1~8.625000 CORE OGV INLET ENGLISH UNITS

SL	PSI	RADIUS	% IMM	PHI	ALPHA	BETA	M-ABS	M-REL	C	W	CZ	U	CU	WU	SL
1	0.9082	20.4450	0.	-2.03	46.70	5.70	0.755	0.520	850.1	586.2	582.9	676.7	618.5	-58.2	1
2	0.9420	19.6432	34.2	-0.68	47.93	-1.45	0.799	0.535	896.3	600.7	600.5	650.2	665.4	15.2	2
3	0.9610	19.1741	54.2	1.13	48.95	-4.87	0.811	0.535	909.0	599.2	596.9	634.6	685.5	50.8	3
4	0.9810	18.6489	76.6	2.94	51.01	-8.97	0.813	0.518	911.0	580.8	573.0	617.3	707.7	90.4	4
5	1.0000	18.1000	100.0	3.30	53.84	-13.80	0.807	0.491	904.9	550.4	553.7	599.1	730.2	131.1	5

SL	PSI	RADIUS	PT	TT	TT-REL	PS	TS	RHO	PT/PTI	TT/TTI	EFF	BLKAGE	SL
1	0.9082	20.4450	22.133	588.36	556.80	15.175	528.21	0.07754	1.5061	1.13431	0.9241	0.96000	1
2	0.9420	19.6432	22.257	590.70	553.87	14.617	523.83	0.07532	1.5145	1.13883	0.9070	0.96000	2
3	0.9610	19.1741	22.110	591.10	552.21	.4.341	522.33	0.07411	1.5045	1.13960	0.8867	0.96000	3
4	0.9810	18.6489	21.934	591.40	550.40	14.201	522.32	0.07338	1.4925	1.14018	0.6647	0.96000	4
5	1.0000	18.1000	21.691	591.50	548.56	14.132	523.35	0.07288	1.4760	1.14037	0.8382	0.96000	5

MASS AVERAGED VALUES

PT/PTI 1.5021 EFF 0.8894 PT 22.075 TT 590.58 TT/TTI 1.13861 CZ 584.27

CORR. FLOW 58.690 CORR. RPM 3554.5

Table II. Design Blade Element Parameters for QCSEE OTW Fan (Continued).

STATION 1.90000 Z 180.174999 CORE OGV EXIT

ENGLISH UNITS

SL	PSI	RADIUS	% IMM	PHI	ALPHA	BETA	M-ABS	M-REL	C	W	CZ	U	CU	WU	SL
1	0.9082	20.5080	0.	-2.03	6.00	45.17	0.526	0.742	608.7	858.4	605.0	672.2	63.6	-608.6	1
2	0.9420	19.5944	35.2	-2.36	6.00	42.57	0.551	0.744	637.5	860.6	633.5	648.5	66.6	-582.0	2
3	0.9610	19.1888	55.2	-1.21	6.00	42.25	0.544	0.731	630.4	846.8	626.8	635.1	65.9	-569.2	3
4	0.9810	18.7387	77.4	0.33	6.00	41.84	0.536	0.718	623.4	832.1	619.9	620.2	65.2	-555.1	4
5	1.0000	18.2800	100.0	3.30	6.00	42.40	0.514	0.692	596.9	804.4	592.7	605.0	62.5	-542.7	5

SL	PSI	RADIUS	PT	TT	TT-REL	PS	TS	RHO	PT/PT1	TT/TT1	EFF	BLKAGE	SL
1	0.9082	20.5080	21.040	588.36	618.84	17.427	557.52	0.08437	1.4317	1.13431	0.8059	0.94000	1
2	0.9420	19.5944	21.507	590.70	618.52	17.496	556.87	0.08480	1.4634	1.13683	0.8279	0.94000	2
3	0.9610	19.1888	21.191	591.10	617.71	17.323	558.03	0.08379	1.4420	1.13960	0.7857	0.94000	3
4	0.9810	18.7387	20.604	591.40	616.69	16.922	559.06	0.08170	1.4020	1.14018	0.7230	0.94000	4
5	1.0000	18.2800	19.841	591.50	615.69	16.572	561.84	0.07961	1.3501	1.14037	0.6379	0.94000	5

SL	PSI	TPLC	PR-ROW	DEL-T	D	DP/Q	C7/CZ	SOLDTY	R-AVG	F-TAN	F-AXL	F-COEF	T-COEF	SL
1	0.9082	0.15705	0.9506		0.447	0.324	1.038	2.0054	20.5765	700.54	317.00			1
2	0.9420	0.09821	0.9663		0.450	0.377	1.055	2.0778	19.6188	748.17	398.12			2
3	0.9610	0.11828	0.9564		0.467	0.384	1.050	2.1220	19.1814	740.07	397.17			3
4	0.9810	0.17204	0.9393		0.478	0.352	1.082	2.1725	18.6938	716.54	374.20			4
5	1.0000	0.24077	0.9147		0.505	0.323	1.111	2.2279	18.1900	672.98	340.39			5

MASS AVERAGED VALUES

PT/PT1 1.4280 EFF 0.7730 PT 20.985 TT 590.58 TT/TT1 1.13861 CZ 618.83 ROW PT2/PT1 0.9506

CORR. FLOW 61.739 CORR. RPM 3554.5

Table II. Design Blade Element Parameters for QCSEE OTW Fan (Continued).

STATION 11.6000 Z 192.000000 BYPASS OGV INLET ENGLISH UNITS

SL	PSI	RADIUS	% IMM	PHI	ALPHA	BETA	M-ABS	M-REL	C	W	CZ	U	CU	WU	SL
1	0.	35.5000	0.	0.	27.51	58.13	0.545	0.915	622.2	1045.1	551.6	1175.0	287.4	-887.6	1
2	0.1000	34.1221	9.4	0.09	27.63	55.80	0.561	0.884	639.0	1007.2	566.1	1129.4	296.3	-833.0	2
3	0.2500	31.9919	24.0	0.11	27.86	52.68	0.573	0.835	650.9	949.1	575.4	1058.9	304.2	-754.7	3
4	0.4000	29.7442	39.3	-0.05	28.62	48.75	0.587	0.782	665.2	885.6	583.9	984.5	318.6	-665.9	4
5	0.5400	27.5140	54.6	-0.32	30.20	43.39	0.610	0.726	689.9	820.5	596.2	910.7	347.1	-563.6	5
6	0.6900	24.9634	72.0	-0.65	33.10	34.13	0.658	0.666	741.8	750.7	621.4	826.3	405.1	-421.2	6
7	0.8000	22.9700	85.6	-0.76	36.30	23.71	0.715	0.630	803.7	707.5	647.7	760.3	475.5	-284.5	7
8	0.8800	21.4343	96.1	-0.35	40.66	11.52	0.786	0.608	885.1	681.3	667.6	709.4	573.4	-136.1	8
9	0.9582	20.8630	100.0	0.	42.47	7.27	0.852	0.596	897.6	667.4	662.1	690.5	606.1	-84.4	9

SL	PSI	RADIUS	PT	TT	TT-REL	PS	TS	RHO	PT/PTI	TT/TTI	EFF	BLKAGE	SL
1	0.	35.5000	19.707	574.90	653.59	16.105	542.68	0.08010	1.3410	1.10837	0.8969	0.96000	1
2	0.1000	34.1221	19.869	574.40	624.85	16.050	540.42	0.08016	1.3520	1.10741	0.8378	0.96000	2
3	0.2500	31.9919	19.942	572.30	612.01	15.963	537.04	0.08023	1.3570	1.10336	0.8817	0.96000	3
4	0.4000	29.7442	20.016	570.90	599.35	15.850	534.08	0.08010	1.3620	1.10066	0.9166	0.96000	4
5	0.5400	27.5140	20.178	571.30	587.71	15.691	531.69	0.07966	1.3730	1.10143	0.9347	0.96000	5
6	0.6900	24.9634	20.604	574.40	575.51	15.405	528.60	0.07866	1.4020	1.10741	0.9437	0.96000	6
7	0.8000	22.9700	21.162	578.90	566.80	15.045	525.14	0.07733	1.4400	1.11608	0.9459	0.96000	7
8	0.8800	21.4343	22.029	586.40	560.58	14.655	521.94	0.07579	1.4990	1.13054	0.9392	0.96000	8
9	0.9582	20.8630	22.133	586.36	558.38	14.491	521.30	0.07563	1.5061	1.13451	0.9241	0.96000	9

MASS AVERAGED VALUES

PT/PTI 1.3842 EFF 0.9059 PT 20.343 TT 574.43 TT/TTI 1.10746 CZ 598.57

CORR. FLOW 621.412 CORR. RPM 3604.1

ORIGINAL PAGE IS OF POOR QUALITY

Table II. Design Blade Element Parameters for QCSEE OTW Fan (Concluded).

STATION 11.90000 Z 200.000000 BYPASS OGV EXIT ENGLISH UNITS

SL	PSI	RADIUS	% IMM	PHI	ALPHA	BETA	M-ABS	M-REL	C	W	CZ	U	CU	WU	SL
1	0.	35.5000*	0.	0.	0.	56.04	0.453	1.116	522.0	1285.8	522.0	1175.0	0.	-1175.0	1
2	0.1000	34.0881	9.6	-0.61	0.	64.00	0.479	1.093	550.4	1255.4	550.4	1128.3	0.	-1128.3	2
3	0.2500	31.9368	24.3	-0.84	0.	62.29	0.484	1.042	555.2	1194.0	555.1	1057.1	0.	-1057.1	3
4	0.4000	29.6596	39.9	-0.99	0.	60.44	0.487	0.986	556.9	1126.6	556.8	981.7	0.	-981.7	4
5	0.5400	27.3949	55.4	-1.06	0.	58.11	0.493	0.935	564.3	1068.0	564.2	906.7	0.	-906.7	5
6	0.6900	24.8271	72.9	-0.84	0.	54.34	0.515	0.883	589.7	1011.4	589.7	821.7	0.	-821.7	6
7	0.8000	22.8609	86.4	-0.34	0.	50.68	0.541	0.853	619.7	978.0	619.7	756.7	0.	-756.7	7
8	0.8800	21.3945	96.4	0.00	0.	47.24	0.569	0.838	654.8	964.5	654.8	708.1	0.	-708.1	8
9	0.9082	20.8630*	100.0	0.	0.	46.68	0.565	0.823	651.1	949.1	651.1	690.5	0.	-690.5	9

SL	PSI	RADIUS	PT	TT	TT-REL	PS	TS	RHO	PT/PT1	TT/TT1	EFF	BLKAGE	SL
1	0.	35.5000	19.347	574.90	669.80	16.805	552.22	0.08214	1.3165	1.10857	0.7542	0.95000	1
2	0.1000	34.0881	19.682	574.40	680.35	16.821	549.19	0.08267	1.3393	1.10741	0.8105	0.95000	2
3	0.2500	31.9368	19.805	572.50	665.30	16.869	546.65	0.08329	1.3477	1.10336	0.8610	0.95000	3
4	0.4000	29.6596	19.889	570.90	651.11	16.916	545.09	0.08376	1.3534	1.10066	0.8971	0.95000	4
5	0.5400	27.3949	20.040	571.30	639.73	16.970	544.80	0.08408	1.3636	1.10143	0.9136	0.95000	5
6	0.6900	24.8271	20.420	574.40	630.60	17.040	545.46	0.08432	1.3895	1.10741	0.9174	0.95000	6
7	0.8000	22.8609	20.827	578.90	626.55	17.073	546.94	0.08425	1.4172	1.11608	0.9024	0.95000	7
8	0.8800	21.3945	21.269	596.40	628.13	17.073	550.71	0.08368	1.4472	1.13054	0.8533	0.95000	8
9	0.9082	20.8630	21.195	580.36	628.04	17.071	553.08	0.08331	1.4423	1.13451	0.8212	0.95000	9

SL	PSI	TPLC	PR-ROW	DEL-T	D	DP/Q	CZ/CZ	SOLDTY	R-AVG	F-TAN	F-AXL	-COEF	T-COEF	SL
1	0.	0.09995	0.9817		0.348	0.194	0.946	1.2320	35.5000	575.38	96.52			1
2	0.1000	0.04891	0.9906		0.315	0.202	0.972	1.3144	34.1051	594.78	133.53			2
3	0.2500	0.03438	0.9931		0.308	0.228	0.965	1.4525	31.9644	581.73	142.98			3
4	0.4000	0.03046	0.9937		0.311	0.256	0.954	1.6215	29.7019	572.44	150.23			4
5	0.5400	0.03073	0.9932		0.321	0.285	0.946	1.8177	27.4545	585.78	166.69			5
6	0.6900	0.03546	0.9911		0.336	0.314	0.949	2.0828	24.8952	643.85	205.27			6
7	0.8000	0.05475	0.9842		0.356	0.331	0.957	2.3292	22.9154	722.18	249.44			7
8	0.8800	0.10312	0.9655		0.384	0.328	0.981	2.5456	21.4144	837.80	306.96			8
9	0.9082	0.12270	0.9576		0.403	0.338	0.983	2.6340	20.8630	850.75	323.17			9

MASS AVERAGED VALUES

PT/PT1 1.5687 EFF 0.8730 PT 20.114 TT 574.43 TT/TT1 1.10746 CZ 573.60 RU= PT2/PT1 0.9888

CURR. FLOW 628.475 CORR. RPM 3604.1

*Bypass OGV exit tip and hub radii listed in this table were changed to 35.5450 in. and 20.5900 in. respectively, after the aero design was completed in order to improve transition of the fan flowpath into the bypass exhaust duct contours. The impact of these changes on OGV blade element parameters was estimated to be small, and the design data were not recomputed.

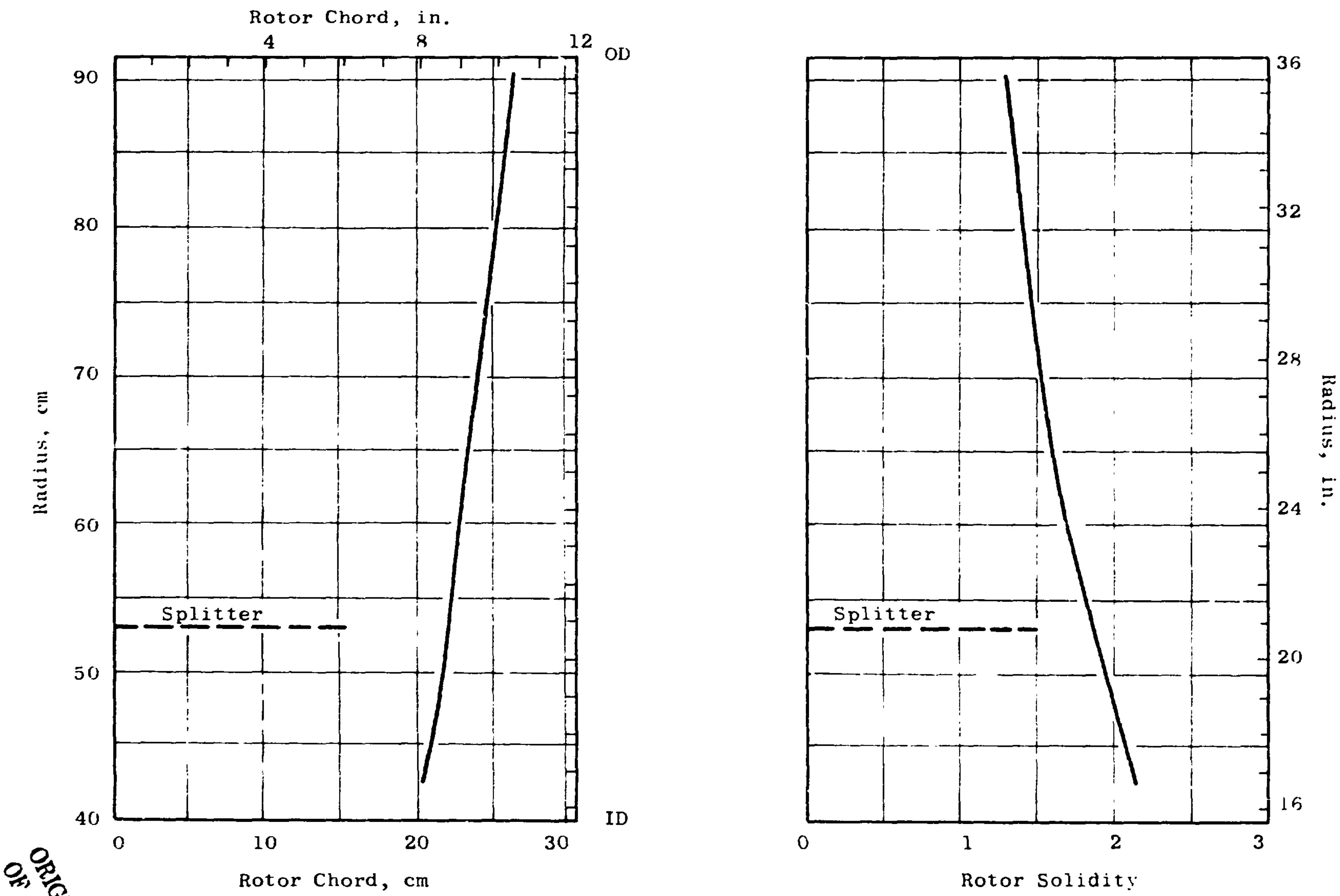

Figure 9. OTW Rotor Chord Distribution.

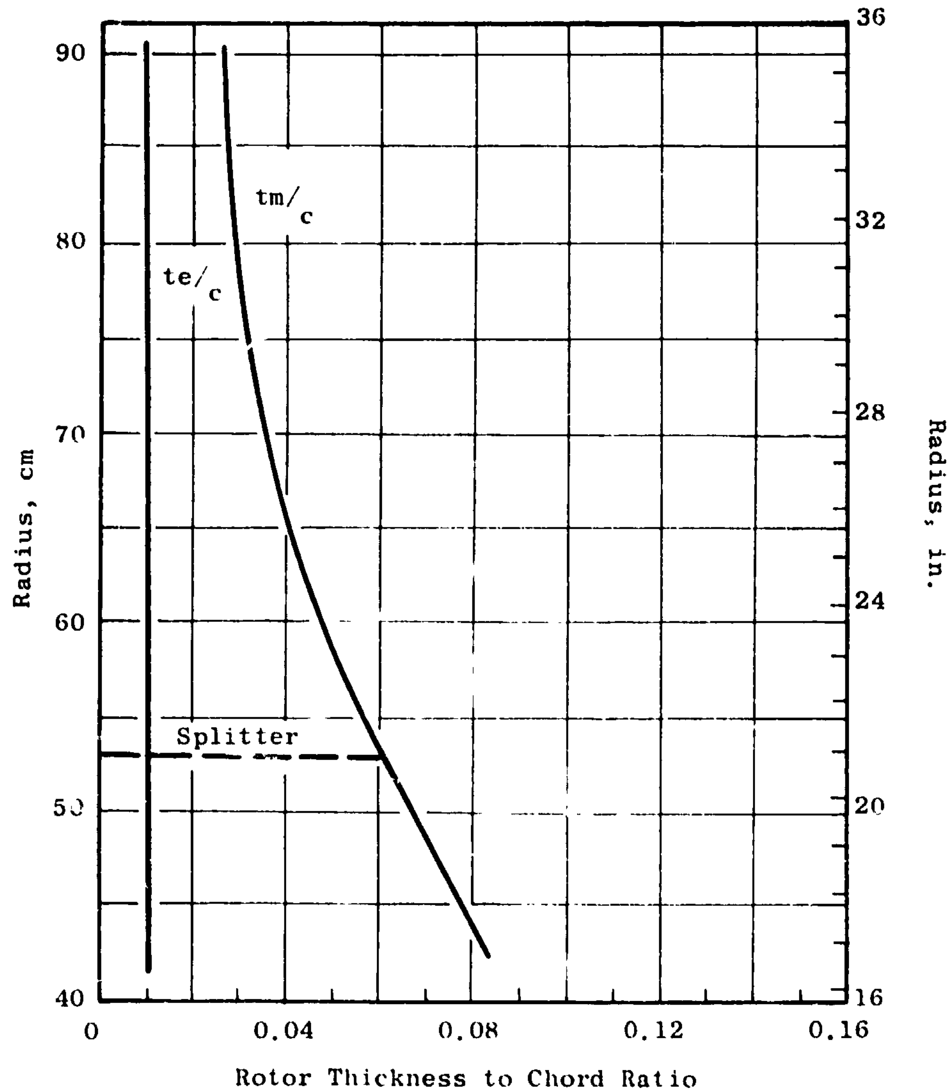

Figure 10. OTW Rotor Thickness Distribution.

yielded good overall performance for previous designs. In the hub region, where the inlet flow is subsonic, incidence angles were selected from NASA cascade data correlations with adjustments from past design experience. The blade trailing edge angle was established by the deviation angle which was obtained from Carter's Rule applied to the camber of an equivalent two-dimensional cascade with an additive empirical adjustment, X. This adjustment is derived from aerodynamic design and performance synthesis for this general type of rotor. However, in the rotor hub, the significant turning past axial results in profile shapes that resemble impulse turbine blades. Design practice in turbine blade layout suggested that blade sections using the full empirical adjustment would result in an overturning of the flow. This overturning by the rotor would aggravate a relatively high-Mach-number-high-loading condition on the core OGV. Consequently the empirical adjustment was reduced 2° in this region. The incidence and deviation angles and the empirical adjustment angle employed in the design are shown in Figure 11.

Over the entire blade span, the minimum passage area, or throat, must be sufficient to pass the design flow including allowances for boundary layer losses, and flow nonuniformities. In the transonic and supersonic region the smallest throat area, consistent with permitting the design flow to pass, is desirable since this minimizes overexpansions on the suction surface. A further consideration was to minimize disturbances to the flow along the forward portion of the suction surface to minimize forward propagating waves that might provide an additional noise source. Design experience guided the degree to which each of these desires was applied to individual section layouts. The percent throat margin, the percentage by which the ratio of the effective throat area to the capture area exceeds the critical area ratio, is shown in Figure 12. The values employed are generally consistent with past experience.

The resulting blade shapes have very little camber in the tip region. In the mid-span region, the shapes generally resemble multiple circular arc sections with the majority of the camber occurring in the aft portion. In the inner region, the shapes are similar to a double circular arc. Figure 13 shows plane sections through the blade at several radial locations. The resulting camber and stagger radial distributions are shown in Figure 14.

Table III gives the detailed coordinate data (in inches) for the blade sections shown in Figure 13. The coordinate center is at the stacking axis.

2.5 CORE OGV DESIGN

A moderately low aspect ratio of 1.3 was selected for the core portion OGV to provide a rugged mechanical system. This selection was in recognition of the potentially severe aeromechanical environment of the core OGV, i.e., large rotor blade wakes, because of its small size in relationship to that of the rotor blade. A solidity at the ID of 2.24 was selected to yield reasonable levels of diffusion factor, Figure 8. The number of OGV's which result is 1[illegible].

Profiles for the core OGV are multiple circular arcs. The incidence angle over the outer portion of the span was selected from a correlation of the NASA low-speed cascade data. Locally, in the ID region, the incidence angle was

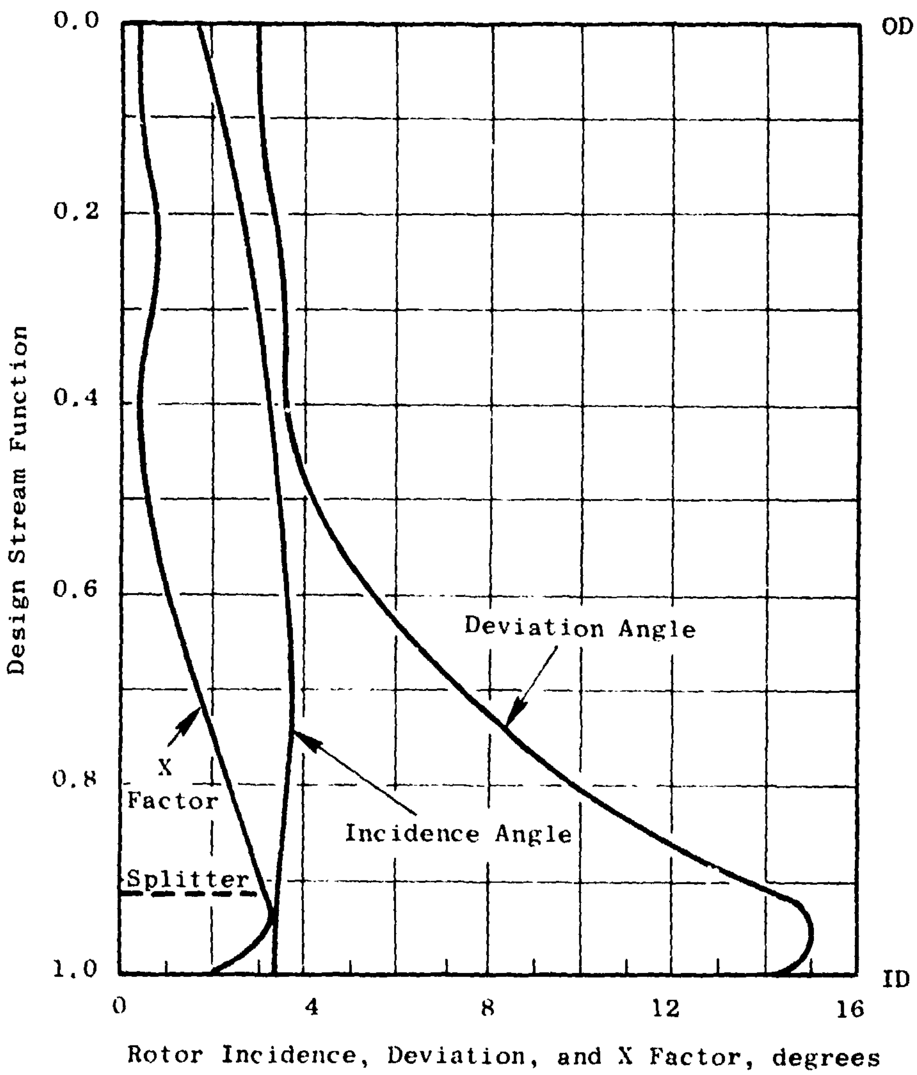

Figure 11. OTW Rotor Incidence, Deviation, and Empirical Adjustment Angles.

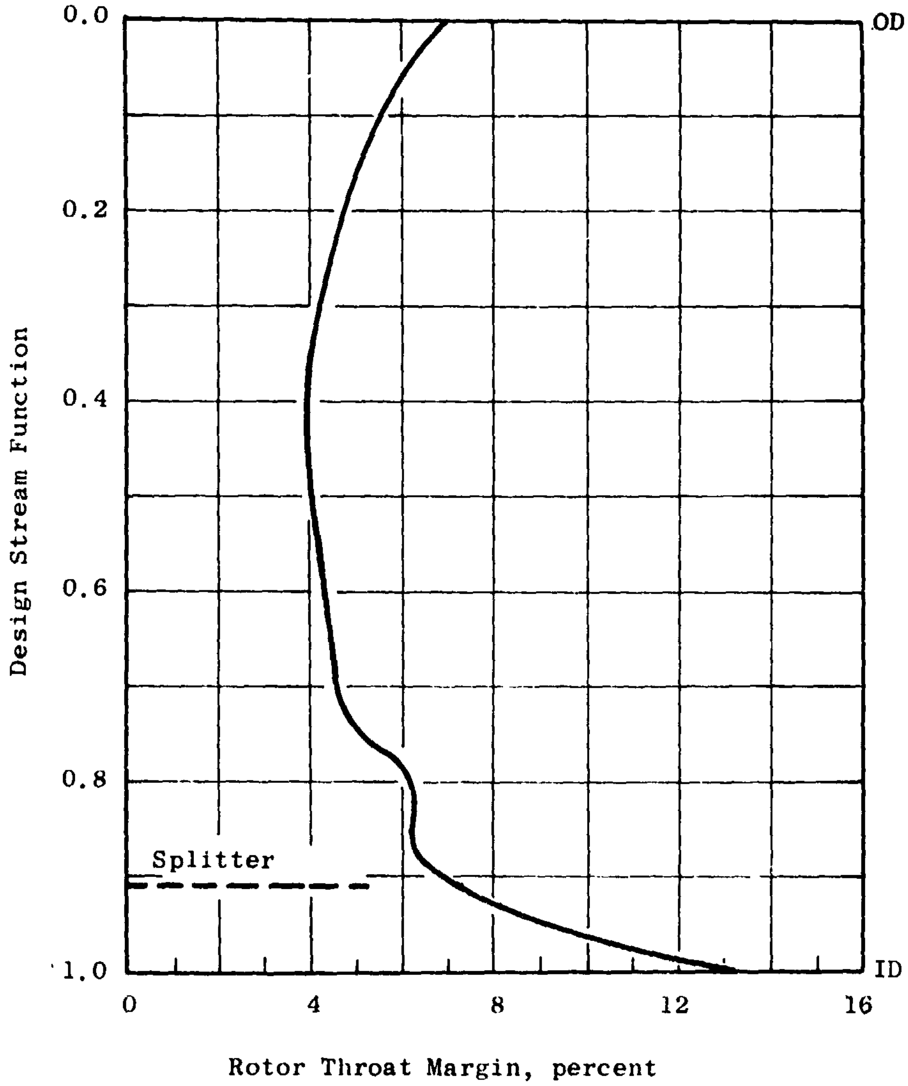

Figure 12. OTW Rotor, Percent Throat Margin.

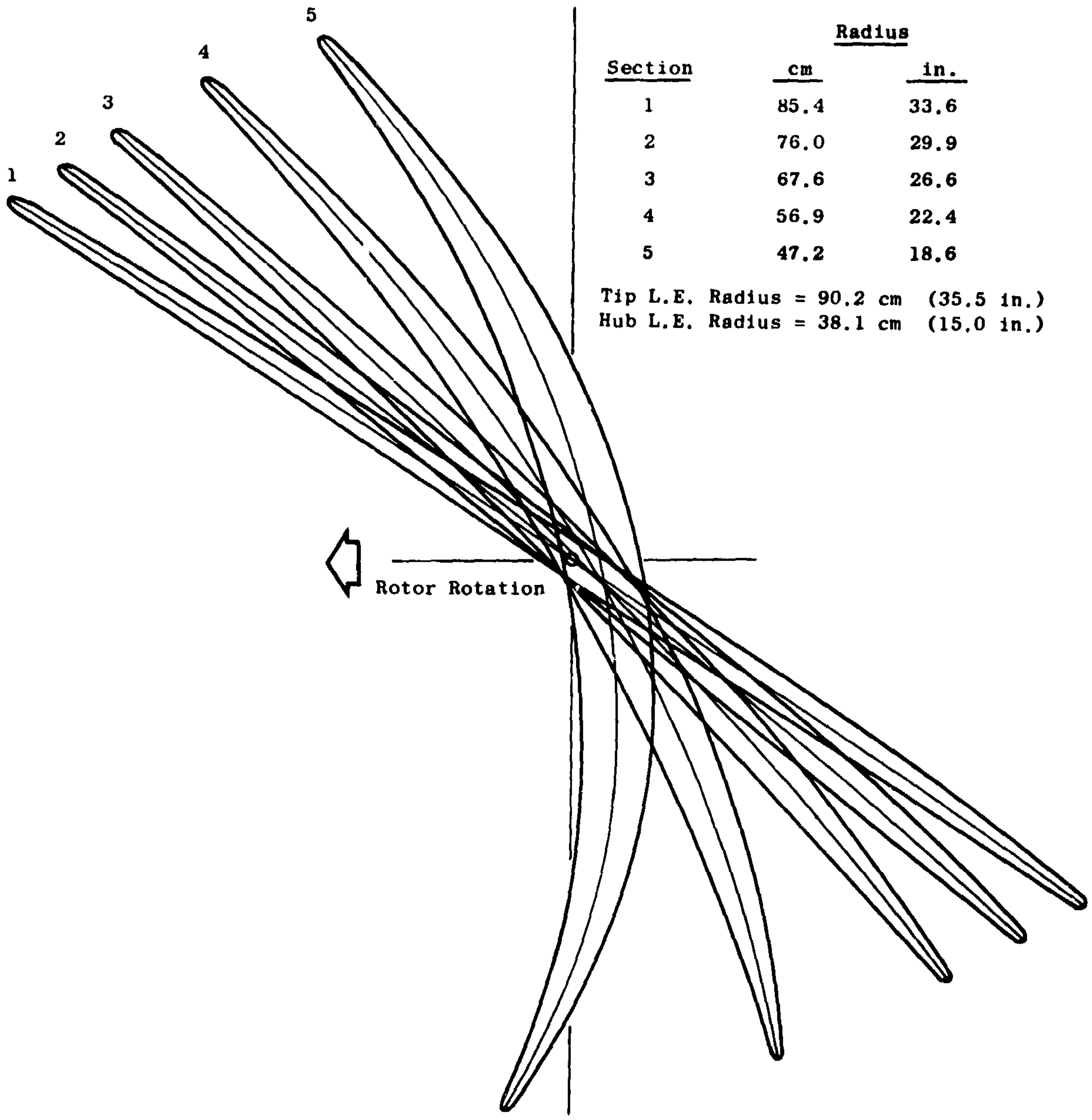

Section	Radius cm	Radius in.
1	85.4	33.6
2	76.0	29.9
3	67.6	26.6
4	56.9	22.4
5	47.2	18.6

Tip L.E. Radius = 90.2 cm (35.5 in.)
Hub L.E. Radius = 38.1 cm (15.0 in.)

Figure 13. OTW Fan Blade Plane Sections.

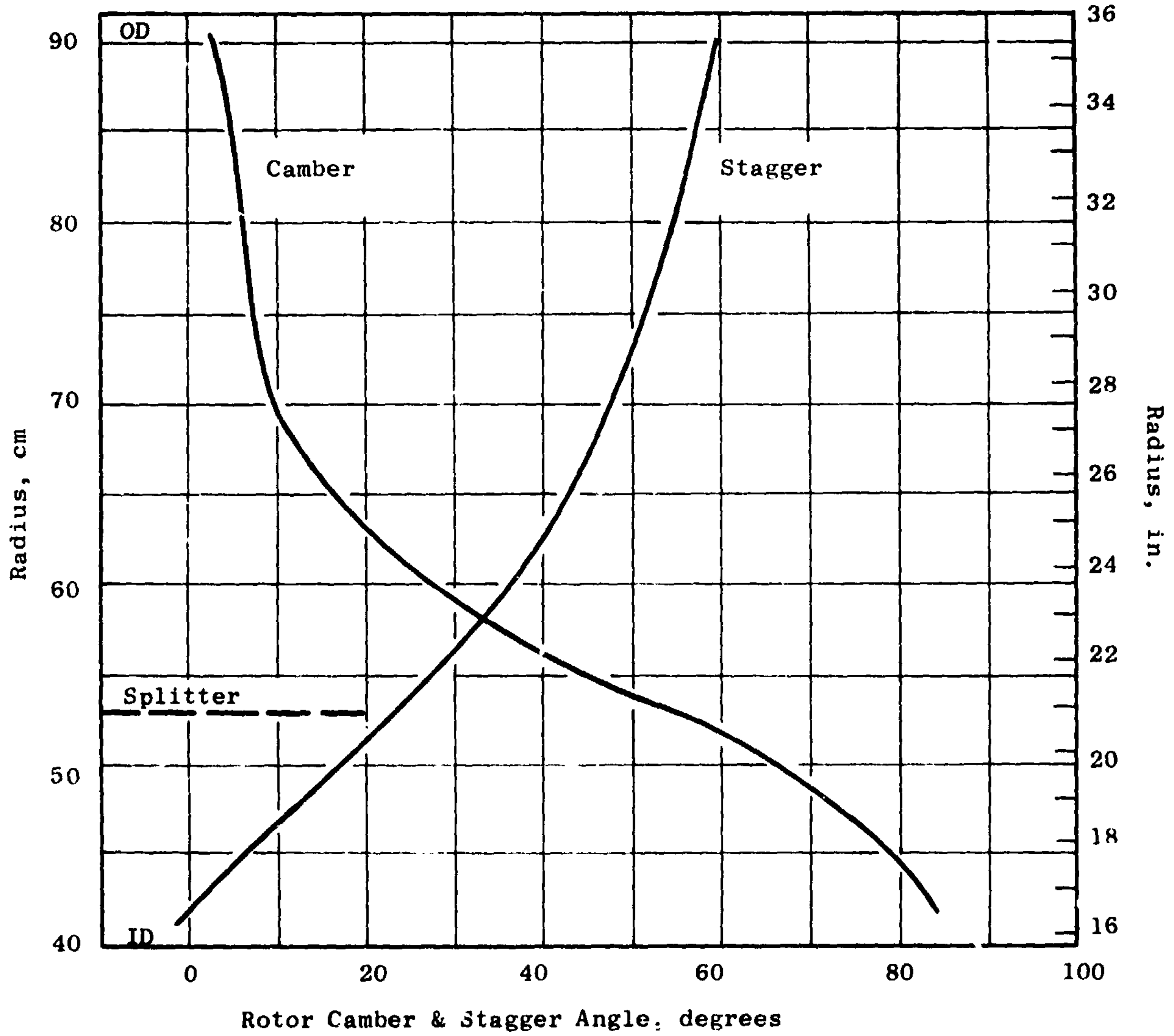

Figure 14. OTW Camber and Stagger Radial Distribution.

ORIGINAL PAGE IS
OF POOR QUALITY

Table III. OTW Rotor Blade Coordinates.

SECTION 1 RADIUS 85.4 cm (33.6 in.)

Convex		Concave	
X (Axial)	Y	X (Axial)	Y
-2,78178	-4,47491	-2,78178	-4,47491
-2,79734	-4,45788	-2,77430	-4,47669
-2,80533	-4,42957	-2,76476	-4,47444
-2,80416	-4,39092	-2,75367	-4,46786
-2,79192	-4,34304	-2,74166	-4,45656
-2,76740	-4,28666	-2,72913	-4,44034
-2,73155	-4,22121	-2,71574	-4,41937
-2,71888	-4,19897	-2,61686	-4,25975
-2,58580	-3,96699	-2,47536	-4,03354
-2,45267	-3,73754	-2,33392	-3,80988
-2,31947	-3,51046	-2,19255	-3,58855
-2,18619	-3,28551	-2,05125	-3,36926
-2,05284	-3,06239	-1,91003	-3,15167
-1,91940	-2,84078	-1,76890	-2,93541
-1,78587	-2,62035	-1,62786	-2,72013
-1,62549	-2,35700	-1,45875	-2,46267
-1,46493	-2,09456	-1,28982	-2,20577
-1,30418	-1,83272	-1,12109	-1,94912
-1,14319	-1,57124	-0,95258	-1,69248
-0,98196	-1,31000	-0,78432	-1,43570
-0,82047	-1,04887	-0,61633	-1,17865
-0,65868	-0,78782	-0,44863	-0,92127
-0,49658	-0,52680	-0,28124	-0,66355
-0,33416	-0,26586	-0,11417	-0,40551
-0,17141	-0,00506	0,05256	-0,14723
-0,00827	0,25547	0,21892	0,11116
0,15525	0,51555	0,38488	0,36950
0,31912	0,77501	0,55050	0,62749
0,48332	1,03358	0,71579	0,88485
0,64811	1,29083	0,88049	1,14148
0,81380	1,54626	1,04428	1,39730
0,98072	1,79942	1,20685	1,65230
1,14906	2,04991	1,36800	1,90641
1,31876	2,29756	1,52779	2,15941
1,48963	2,54228	1,68681	2,41109
1,66156	2,78404	1,84396	2,66132
1,83443	3,02285	2,00058	2,91007
2,00809	3,25888	2,15641	3,15734
2,18237	3,49236	2,31161	3,40316
2,35711	3,72353	2,46636	3,64755
2,50295	3,91458	2,59509	3,85012
2,62092	4,06810	2,69909	4,01315
2,64880	4,08567	2,70616	4,04554
2,68631	4,07802	2,68631	4,07802

Table III. OTW Rotor Blade Coordinates (Continued).

SECTION 2 RADIUS 76.0 cm (29.9 in.)

Convex		Concave	
X (Axial)	Y	X (Axial)	Y
-3.03623	-4.06821	-3.03623	-4.06821
-3.05028	-4.05023	-3.02900	-4.07056
-3.05600	-4.02175	-3.01942	-4.06910
-3.05196	-3.98360	-3.00798	-4.06351
-3.03635	-3.93762	-2.99527	-4.05337
-3.00805	-3.88401	-2.98164	-4.03844
-2.96796	-3.82234	-2.96678	-4.01892
-2.95669	-3.80562	-2.85970	-3.87436
-2.81140	-3.59153	-2.70310	-3.66771
-2.66608	-3.37962	-2.55054	-3.46322
-2.52070	-3.16957	-2.39603	-3.26051
-2.37525	-2.96112	-2.24159	-3.05929
-2.22971	-2.75404	-2.08724	-2.85931
-2.08407	-2.54818	-1.93300	-2.66041
-1.93831	-2.34344	-1.77887	-2.46247
-1.76321	-2.09914	-1.59411	-2.22608
-1.58788	-1.85627	-1.40958	-1.99079
-1.41231	-1.61472	-1.22529	-1.75646
-1.23647	-1.37440	-1.04126	-1.52297
-1.06034	-1.13525	-0.85752	-1.29019
-0.88391	-0.89717	-0.67409	-1.05802
-0.70715	-0.66013	-0.49099	-0.82638
-0.53005	-0.42410	-0.30823	-0.59522
-0.35256	-0.18906	-0.12585	-0.36453
-0.17474	0.04498	0.05619	-0.13432
0.00352	0.27793	0.23779	0.09536
0.18223	0.50968	0.41895	0.32440
0.36131	0.74013	0.59973	0.55254
0.54076	0.96910	0.78015	0.77959
0.72086	1.19614	0.95990	1.00560
0.90196	1.42080	1.13865	1.23069
1.08441	1.64265	1.31608	1.45502
1.26840	1.86136	1.49195	1.67871
1.45382	2.07691	1.66640	1.90163
1.64049	2.28932	1.83959	2.12360
1.82829	2.49865	2.01165	2.34456
2.01710	2.70494	2.18271	2.56440
2.20673	2.90831	2.35294	2.78300
2.39701	3.10888	2.52252	3.00022
2.58776	3.30674	2.69164	3.21586
2.74693	3.46962	2.83236	3.39420
2.87458	3.59893	2.94512	3.53619
2.90375	3.61272	2.95540	3.56710
2.93958	3.60096	2.93958	3.60096

ORIGINAL PAGE IS
OF POOR QUALITY

Table III. OTW Rotor Blade Coordinates (Continued).

SECTION 3 RADIUS 67.6 cm (26.6 in.)

Convex		Concave	
X (Axial)	Y	X (Axial)	Y
-3.30760	-3.65312	-3.30760	-3.65312
-3.32026	-3.63432	-3.30060	-3.65597
-3.32398	-3.60575	-3.29103	-3.65525
-3.31741	-3.56853	-3.27931	-3.65056
-3.29891	-3.52398	-3.26600	-3.64154
-3.26742	-3.47297	-3.25142	-3.62785
-3.22380	-3.41479	-3.23527	-3.60977
-3.21009	-3.39714	-3.11706	-3.47384
-3.05099	-3.19385	-2.94709	-3.28066
-2.89181	-2.99309	-2.77721	-3.09005
-2.73253	-2.79472	-2.60744	-2.90180
-2.57313	-2.59854	-2.43778	-2.71534
-2.41360	-2.40435	-2.26824	-2.53134
-2.25393	-2.21203	-2.09886	-2.34875
-2.09409	-2.02146	-1.92964	-2.16770
-1.90204	-1.79498	-1.72681	-1.95234
-1.70970	-1.57081	-1.52428	-1.73889
-1.51704	-1.34867	-1.32206	-1.52724
-1.32404	-1.12912	-1.12019	-1.31730
-1.13068	-0.91156	-0.91868	-1.10901
-0.93692	-0.69618	-0.71757	-0.90236
-0.74273	-0.48306	-0.51689	-0.69738
-0.54809	-0.27227	-0.31665	-0.49417
-0.35299	-0.06397	-0.11689	-0.29285
-0.15740	0.14169	0.08240	-0.09355
0.03870	0.34453	0.28118	0.10364
0.23529	0.54442	0.47945	0.29865
0.43229	0.74138	0.67733	0.49133
0.62968	0.93533	0.87481	0.68165
0.82779	1.12586	1.07157	0.86993
1.02699	1.31258	1.26724	1.05659
1.22762	1.49498	1.46148	1.24200
1.42989	1.67276	1.65409	1.42647
1.63363	1.84601	1.84522	1.60991
1.83864	2.01486	2.03508	1.79219
2.04479	2.17941	2.22380	1.97323
2.25192	2.33979	2.41155	2.15297
2.45984	2.49618	2.59850	2.33129
2.66836	2.64882	2.78485	2.50802
2.87729	2.79788	2.97079	2.68297
3.05154	2.91952	3.12561	2.82728
3.18938	3.01431	3.24809	2.94047
3.22012	3.02239	3.26295	2.96905
3.25310	3.00468	3.25310	3.00468

Table III. OTW Rotor Blade Coordinates (Continued).

SECTION 4 RADIUS 56.9 cm (22.4 in.)

Convex		Concave	
X (Axial)	Y	X (Axial)	Y
-3,70070	-2,94436	-3,70070	-2,94436
-3,71184	-2,92529	-3,69407	-2,94762
-3,71375	-2,89737	-3,68473	-2,9475[illegible]
-3,70520	-2,86173	-3,67305	-2,94391
-3,68470	-2,81977	-3,65952	-2,93615
-3,65130	-2,77257	-3,64441	-2,92403
-3,60574	-2,71883	-3,62746	-2,90783
-3,57466	-2,68367	-3,48527	-2,76947
-3,39242	-2,[illegible]3070	-3,28863	-2,58312
-3,20996	-2,28286	-3,09221	-2,40238
-3,02726	-2,09009	-2,89603	-2,22707
-2,84431	-1,90220	-2,70010	-2,05686
-2,66105	-1,71900	-2,50448	-1,89150
-2,47743	-1,54040	-2,30921	-1,73085
-2,29343	-1,36637	-2,11434	-1,57477
-2,07205	-1,16353	-1,88106	-1,39336
-1,84999	-0,96725	-1,64846	-1,21822
-1,62722	-0,77751	-1,41658	-1,04917
-1,40370	-0,59431	-1,18544	-0,88602
-1,17942	-0,41765	-0,95506	-0,72856
-0,95435	-0,24749	-0,72548	-0,57662
-0,72849	-0,08381	-0,49668	-0,43003
-0,50182	0,07338	-0,26869	-0,28863
-0,27432	0,22403	-0,04154	-0,15225
-0,04601	0,36813	0,18482	-0,02080
0,18299	0,50579	0,41048	0,10572
0,41270	0,63694	0,63542	0,22748
0,64329	0,76116	0,85949	0,34500
0,87489	0,87805	1,08255	0,45880
1,10755	0,98727	1,30454	0,56932
1,34126	1,08860	1,52549	0,67685
1,57587	1,18199	1,74553	0,78147
1,81125	1,26748	1,96481	0,88311
2,04717	1,34510	2,18355	0,98161
2,28342	1,41495	2,40196	1,07675
2,51976	1,47709	2,62027	1,16831
2,75600	1,53163	2,83869	1,25599
2,99191	1,57866	3,05744	1,33945
3,22717	1,61836	3,27684	1,41845
3,46159	1,65125	3,49708	1,49296
3,65635	1,67376	3,68119	1,55147
3,80694	1,68806	3,82437	1,59422
3,83712	1,68052	3,85068	1,61329
3,85821	1,64890	3,85821	1,64890

Table III. OTW Rotor Blade Coordinates (Concluded).

SECTION 5 RADIUS 47.2 cm (18.6 in.)

Convex		Concave	
X (Axial)	Y	X (Axial)	Y
-4.01950	-2.03176	-4.01950	-2.03176
-4.02898	-2.01315	-4.01344	-2.03528
-4.02944	-1.98693	-4.00466	-2.03594
-4.01988	-1.95415	-3.99347	-2.03339
-3.99904	-1.91614	-3.98027	-2.02721
-3.96615	-1.87371	-3.96527	-2.01717
-3.92184	-1.82620	-3.94822	-2.00355
-3.87249	-1.77546	-3.78535	-1.87231
-3.67613	-1.57936	-3.56818	-1.70557
-3.47906	-1.39170	-3.35172	-1.54845
-3.28116	-1.21231	-3.13608	-1.40053
-3.08235	-1.04104	-2.92135	-1.26146
-2.88252	-0.87775	-2.70765	-1.13090
-2.68156	-0.72245	-2.49507	-1.00864
-2.47939	-0.57518	-2.28371	-0.89447
-2.23508	-0.40916	-2.03177	-0.76780
-1.98887	-0.25492	-1.78173	-0.65197
-1.74074	-0.11256	-1.53363	-0.54648
-1.49077	0.01780	-1.28735	-0.45076
-1.23914	0.13620	-1.04274	-0.36410
-0.98592	0.24275	-0.79971	-0.28589
-0.73122	0.33748	-0.55817	-0.21563
-0.47499	0.42034	-0.31816	-0.15296
-0.21717	0.49101	-0.07974	-0.09781
0.04195	0.54901	0.15739	-0.05007
0.30202	0.59404	0.39356	-0.00965
0.56268	0.62589	0.62914	0.02352
0.82355	0.64443	0.86452	0.04945
1.08437	0.64960	1.09993	0.06805
1.34491	0.64119	1.33564	0.07905
1.60485	0.61896	1.57194	0.08206
1.86388	0.58258	1.80916	0.07650
2.12152	0.53172	2.04776	0.06166
2.37730	0.46628	2.28822	0.03678
2.63088	0.38623	2.53088	0.00103
2.88199	0.29165	2.77602	-0.04651
3.13032	0.18287	3.02394	-0.10670
3.37576	0.06074	3.27473	-0.17994
3.61867	-0.07388	3.52807	-0.26633
3.85941	-0.22028	3.78357	-0.36596
4.05[illegible]53	-0.35065	3.99799	-0.45899
4.22191	-0.46319	4.17587	-0.54185
4.23936	-0.48730	4.20729	-0.54982
4.23503	-0.52379	4.23503	-0.52379

reduced 4°. This local reduction in incidence was in recognition of traverse data results on other high bypass fan configurations which show core stator inlet air angles several degrees higher than the axisymmetric calculated values. The deviation angle was obtained from Carter's Rule as was described for the rotor blade, but no empirical adjustment was made. The resulting incidence and deviation angles are shown in Figure 15. An average throat area 5% greater than the critical contraction ratio was employed in the design. The throat area margin is shown in Figure 15. Locally, in the ID region, the margin is zero for the axisymmetric vector diagrams. However, as noted above, the anticipated inlet air angle in this region will be several degrees higher, and therefore the capture area will be several percent lower than the axisymmetric calculation. The effective throat-to-capture area ratio will therefore increase to provide adequate margin.

The multiple circular arc mean line consisted of a maximum radius arc forward of the throat, which occurs at the passage leading edge. This arc was determined by the incidence and throat area selection. A small blend region transitioned into a second arc prescribed by the overall camber requirement. The resulting radial distributions of camber, stagger, solidity, chord, and thickness-to-chord ratio are given in Figure 16. Figure 17 is a cylindrical section of the OGV at the pitch line radius. The coordinates for this section are given in Table IV. The coordinate data are in inches.

2.6 TRANSITION DUCT STRUT DESIGN

The transition duct flowpath is shown in Figure 18. It is common to both the UTW and OTW engines. The ratio of duct exit to duct inlet flow area is 1.02. There are six struts in the transition duct which are aerodynamically configured to remove the 0.105 radian (6°) of swirl left in the air by the core OGV's and to house the structural spokes of the composite wheels (see Figure 2). In addition, at engine station 196.5 (Figure 2), the 6 and 12 o'clock strut positions must house radial accessory drive shafts. The number of struts and axial position of the strut trailing edge were selected identical with the F101 engine to minimize unknowns in the operation of the core engine system. The axial positions and thickness requirements of the composite wheel spokes were dictated by mechanical considerations. The axial location of the strut leading edge at the OD was determined by its proximity to the splitter leading edge in the UTW engine configuration. At the OD flowpath, the strut leading edge is 17.8 mm (0.7 in.) forward of the wheel spoke. A relatively blunt strut leading edge results from the 26.7 mm (1.05 in.) wheel spoke thickness requirement. The wheel spoke is radial. The axial lean of the strut leading edge provides relief from the LE bluntness at lower radii and makes the LE approximately normal to the incoming flow. A NASA 65-series thickness distribution was selected for the basic profile thickness which was modified for the special considerations required in this design. The strut thickness is the same for all radii aft of the forward wheel spoke LE (Figure 18) to facilitate fabrication. A cylindrical cut cross section showing the nominal strut geometry at three radii is shown in Figure 19. The thickness distribution for the 6 and 12 o'clock struts was further modified for the

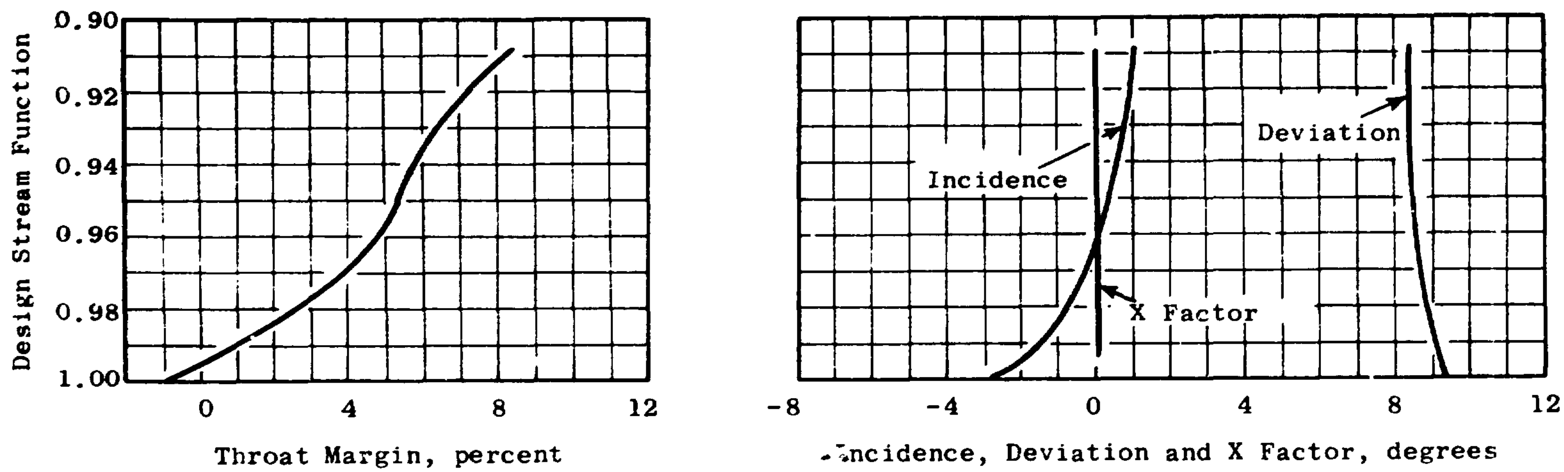

Figure 15. OTW Core OGV.

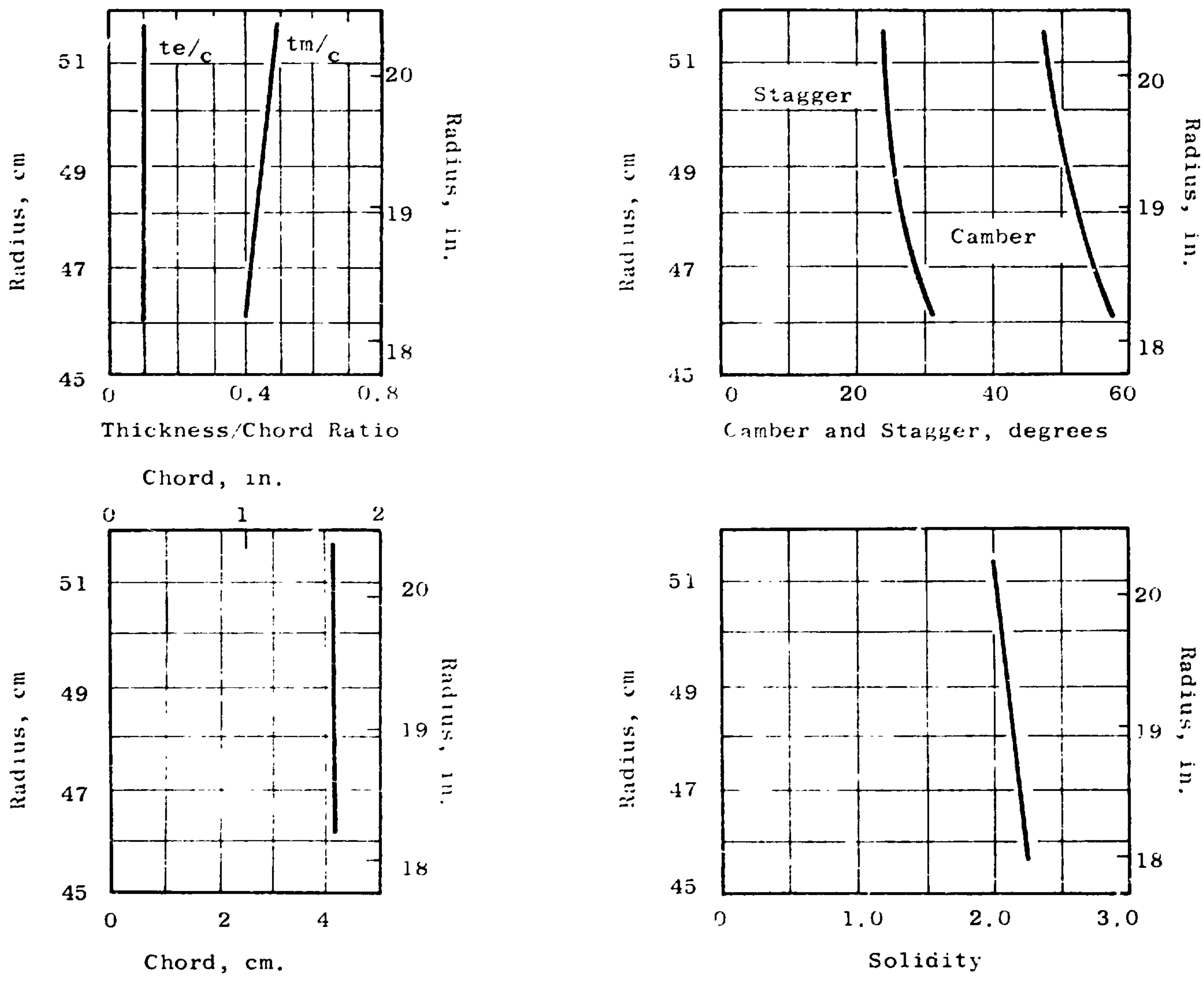

Figure 16. OTW Core OGV.

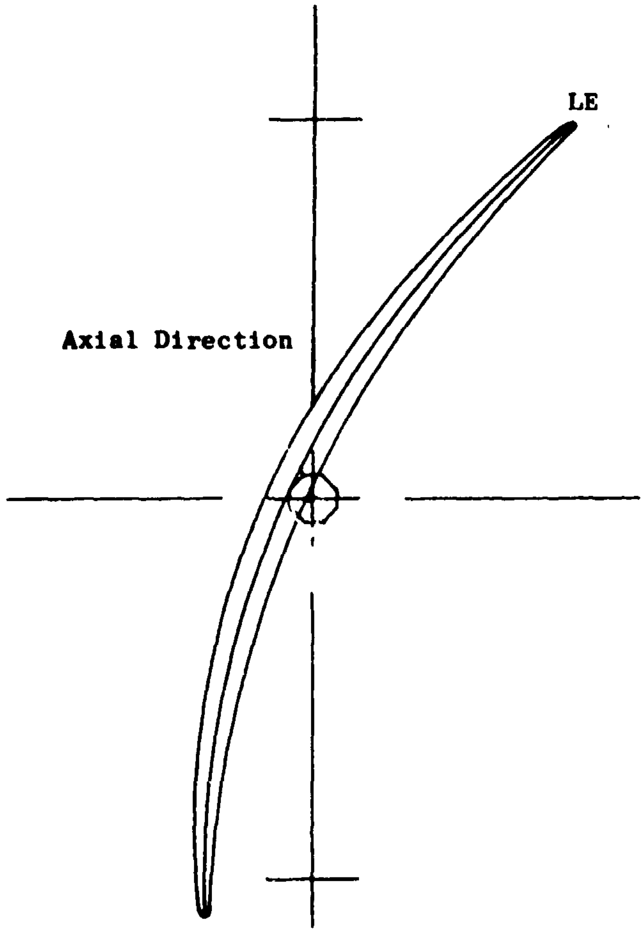

Figure 17. Cylindrical Section of OTW OGV at the Pitch Line Radius.

Table IV. OTW Core OGV Coordinates at the Pitch Line Radius.

Convex		Concave	
X (Axial)	Y	X (Axial)	Y
-0.69945	0.49823	-0.69945	0.49823
-0.70090	0.49528	-0.69819	0.49859
-0.70065	0.49048	-0.69620	0.49807
-0.69858	0.48394	-0.69354	0.49662
-0.69455	0.47578	-0.69027	0.49418
-0.68843	0.46613	-0.68644	0.49073
-0.68014	0.45503	-0.68199	0.48630
-0.66980	0.44240	-0.65740	0.46172
-0.63825	0.40533	-0.61859	0.42409
-0.60276	0.36534	-0.57997	0.38796
-0.56712	0.32684	-0.54151	0.35325
-0.53132	0.28973	-0.50320	0.31980
-0.49538	0.25390	-0.46503	0.28750
-0.45929	0.21930	-0.42701	0.25630
-0.42303	0.18591	-0.38917	0.22620
-0.37926	0.14753	-0.34401	0.19169
-0.33520	0.11117	-0.29914	0.15908
-0.29088	0.07695	-0.25454	0.12844
-0.24632	0.04494	-0.21017	0.09976
-0.20159	0.01510	-0.16597	0.07292
-0.15670	-0.01268	-0.12193	0.04776
-0.11167	-0.03852	-0.07803	0.02418
-0.06651	-0.06248	-0.03427	0.00209
-0.02121	-0.08461	0.00936	-0.01856
0.02419	-0.10493	0.05290	-0.03784
0.06964	-0.12351	0.09637	-0.05582
0.11516	-0.14043	0.13978	-0.07260
0.16075	-0.15571	0.18312	-0.08818
0.20637	-0.16936	0.22642	-0.10259
0.25198	-0.18148	0.26974	-0.11592
0.29759	-0.19198	0.31306	-0.12820
0.34319	-0.20104	0.35639	-0.13945
0.38876	-0.20861	0.39975	-0.14969
0.43428	-0.21472	0.44315	-0.15895
0.47973	-0.21938	0.48663	-0.16723
0.52510	-0.22263	0.53019	-0.17457
0.57036	-0.22449	0.57386	-0.18099
0.61552	-0.22499	0.61763	-0.18650
0.66056	-0.22414	0.66152	-0.19109
0.70546	-0.22190	0.70554	-0.19476
0.74277	-0.21894	0.74234	-0.19709
0.77178	-0.21597	0.77111	-0.19837
0.77702	-0.21344	0.77675	-0.20069
0.77961	-0.20683	0.77961	-0.20683

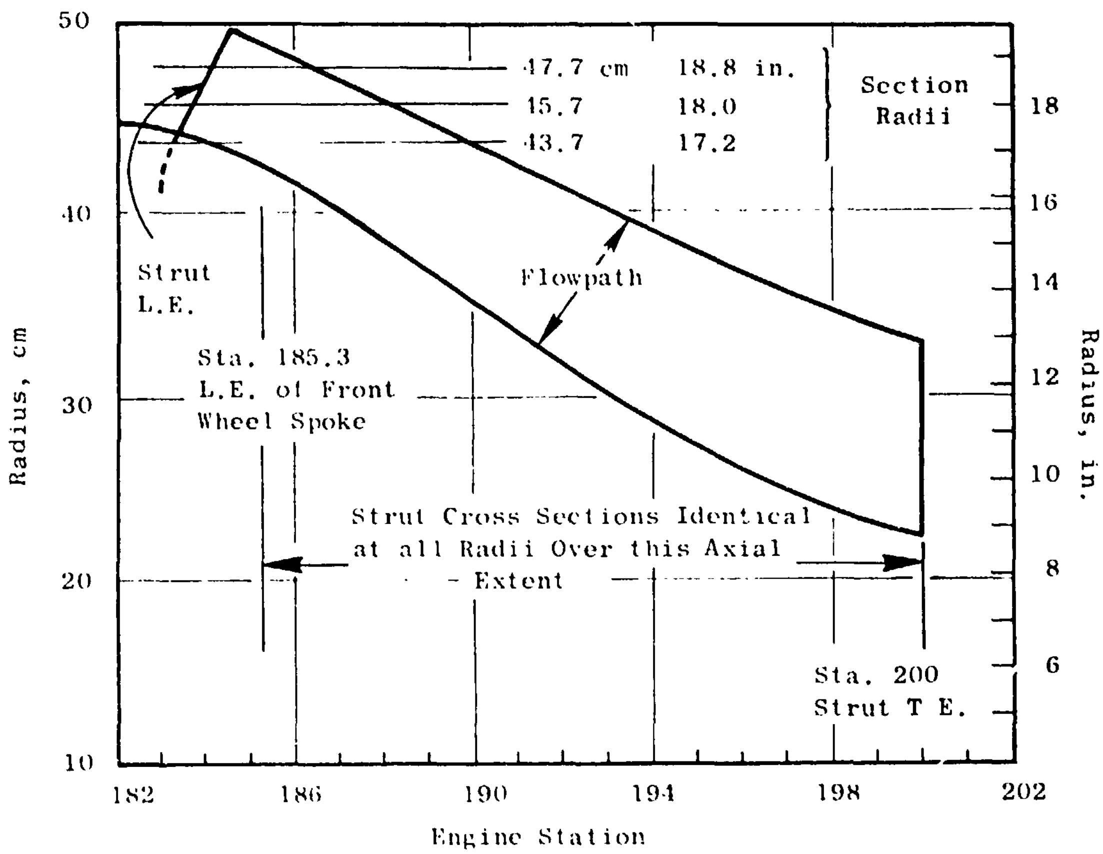

Figure 18. Transition Duct Flowpath.

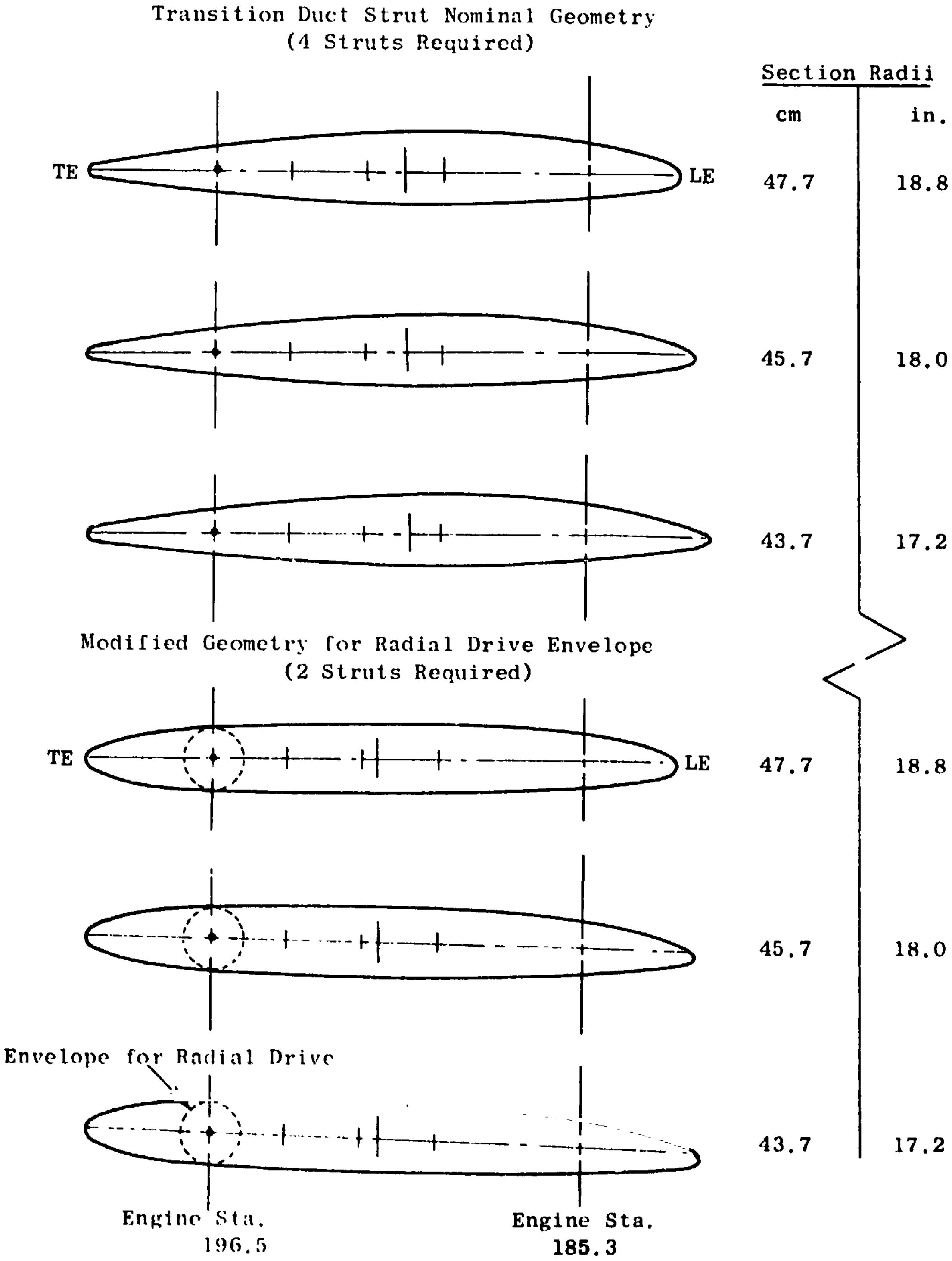

Figure 19. Transition Duct Strut.

envelope of the radial drive shaft. Cylindrical cut cross sections of these struts are also shown in Figure 19. The leading edge 40% chord of these further modified sections is identical to that of the nominal strut geometry, and aft of forward wheel spoke LE, the strut thickness is the same for all radii. The core engine has demonstrated operation in the presence of a similar thick strut in the F101 application without duress.

2.7 VANE-FRAME DESIGN

The vane-frame performs the dual function of an outlet guide vane for the bypass flow and a frame support for the engine components and nacelle. It is a common piece of hardware for both the UTW and OTW engine fans. It is integrated with the pylon which houses the radial drive shaft at engine station 196.50 (see Figure 2), houses the engine mount at approximately engine station 210, provides an interface between the propulsion system with the aircraft system, and houses the forward thrust links. The vane-frame furthermore acts as an inlet guide vane for the UTW fan when in the reverse mode of operation.

A conventional OGV system turns the incoming flow to axial. The housing requirements of the pylon dictate a geometry which requires the OGV's to underturn approximately 0.174 radian (10°) on one side and to overturn approximately 0.174 radian (10°) on the other side. The vanes must be tailored to downstream vector diagrams which conform to the natural flow field around the pylon to avoid creating velocity distortions in the upstream flow. Ideally, each vane would be individually tailored. However, to avoid excessive costs, five vane geometry groups were selected as adequate.

The Mach number and air angle at inlet to the vane-frame are shown in Figure 20 for both the UTW and OTW fans. In the outer portion of the bypass duct annulus, the larger air angle in the UTW environment results in a less negative incidence angle for it than for the OTW environment. The Mach number in the outer portion of the annulus is also higher in the UTW environment. When selecting incidence angles, a higher Mach number environment naturally leads to the desire to select a less negative incidence angle. The amount by which the incidence angle would naturally be increased due to the higher Mach number UTW environment is approximately equal to the increase in the inlet air angle of the UTW environment. In the inner portion of the annulus, the inlet Mach number and air angle are higher for the OTW environment. The natural increase in incidence angle desired because of the higher Mach number is approximately the same as the increase in the inlet air angle. As a result of these considerations, no significant aerodynamic performance penalty is assessed to using common hardware for both the UTW and OTW fans.

Locally, near the bypass duct ID, there is a discontinuity in the aerodynamic environment of the UTW configuration. This discontinuity represents that portion of the flow which passes under the island but bypasses the splitter. The calculation ignored mixing across the vortex sheet. In the design of the vane geometry no special considerations were incorporated because of this discontinuity since it is believed that in a real fluid the mixing process will greatly diminish the vortex strength.

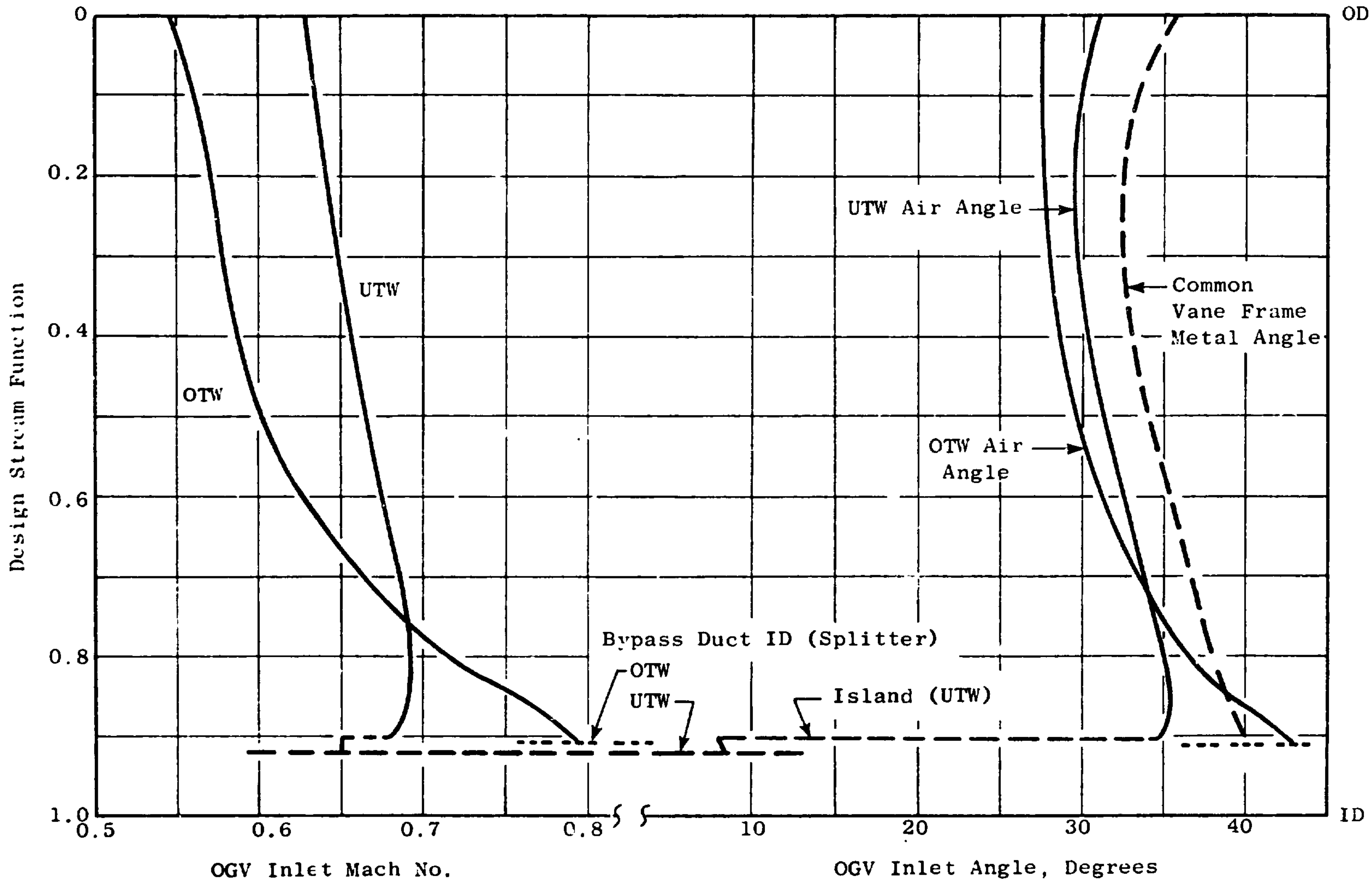

Figure 20. Vane Frame Aerodynamic Environment.

The vane chord at the OD was selected largely by the mechanical requirement of axial spacing between the composite frame spokes. At the ID the vane leading edge was lengthened primarily to obtain an aerodynamically reasonable leading edge fairing on the pylon compatible with the envelope requirements of the radial drive shaft. The ID region is significantly more restrictive in this regard because of choking considerations, particularly for the OTW environment, with the reduced circumferential spacing between vanes. The solidity resulting from 33 vanes, an acoustic requirement, was acceptable from an aerodynamic loading viewpoint as shown in Figure 21. The two diffusion factor curves are a result of the two aerodynamic environments, UTW and OTW, to which the common vane frame geometry is exposed. The thickness is a modified NASA 65-series distribution. Maximum-thickness- and trailing-edge-thickness-to-chord ratios of 0.08 and 0.02, respectively, were selected at the OD. The same maximum thickness and trailing edge thickness were used at all other radii which results in maximum-thickness- and trailing-edge-thickness-to-chord ratios of 0.064 and 0.016, respectively, at the ID.

As a guide in the selection of the overall vector diagram requirements of the vane frame, a circumferential analysis of an approximate vane geometry, including the pylon, was performed. This analysis indicated, for uniform flow at vane inlet, that the vane discharge Mach number was approximately constant circumferentially and that the discharge air angle was nearly linear circumferentially between the pylon wall angles. Figure 22, an unwrapped cross section at the ID, shows the flowfield calculated by this analysis. The specific design criteria selected for the layout of the five-vane geometry groups was to change the average discharge vector diagram with zero swirl to vector diagrams with $\pm$ 5° of swirl and $\pm$ 10° of swirl.

The meanline shapes for each of the five-vane groups vary. For the vane group which overturns the flow by +10° the meanline is approximately a circular arc. As a result of passage area distribution and choking consideratons, the meanline shape employed in the forward 25% chord region of this vane group was retained for the other four groups.

The incidence angle for all vane groups was the same and was selected for the group with the highest camber. A correlation of NASA low-speed cascade data was the starting point for the incidence selection. Over the outer portion of the vane, where the inlet Mach number is lower, the incidence angles were slanted to the low side of the correlation. This was done in consideration of the reverse thrust mode of operation for the UTW fan. In this mode, the OGV's impart a swirl counter to the direction of rotor rotation. Additional vane leading edge camber tends to increase the counterswirl and therefore the pumping capacity of the fan. In the inner portion of the vane the incidence angles are higher than suggested by the correlation because of the higher inlet Mach number. Also, in the reverse mode of operation, this reduction in vane leading edge camber in the ID region reduces the swirl for that portion of the fluid which enters the core engine and tends to reduce its pressure drop.

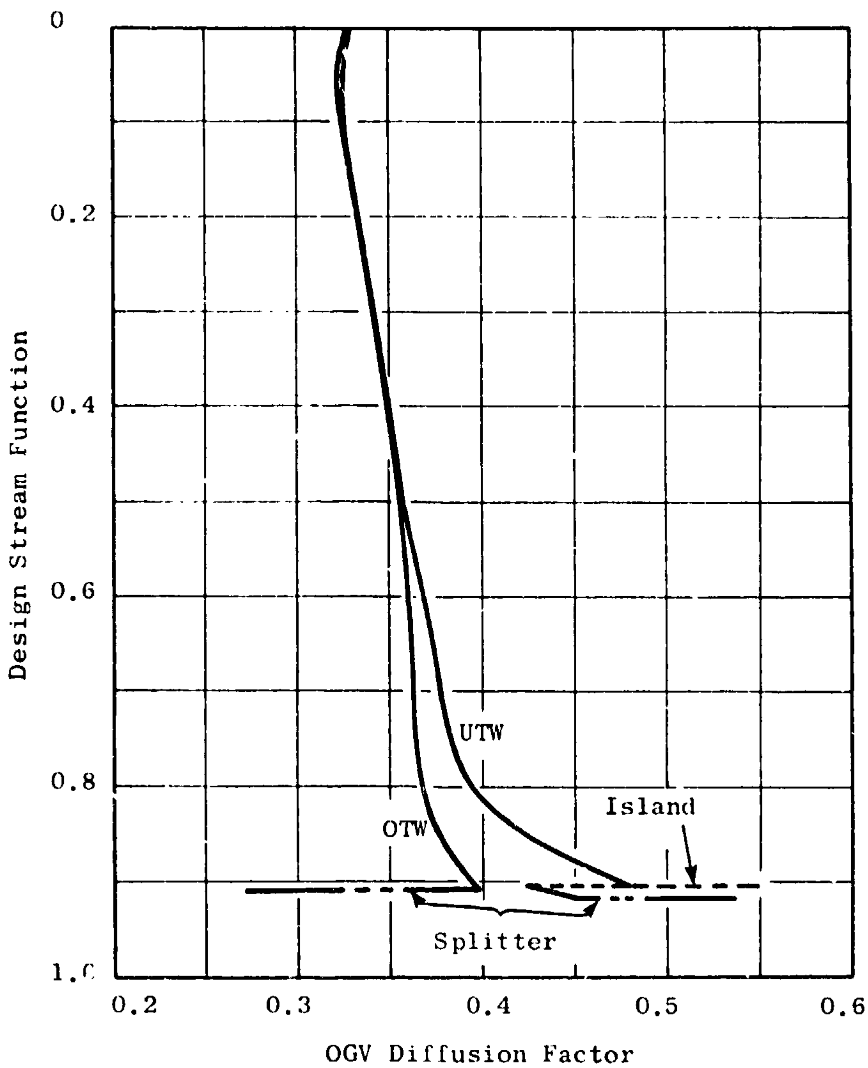

Figure 21. Vane-Frame Nominal Vane Configuration.

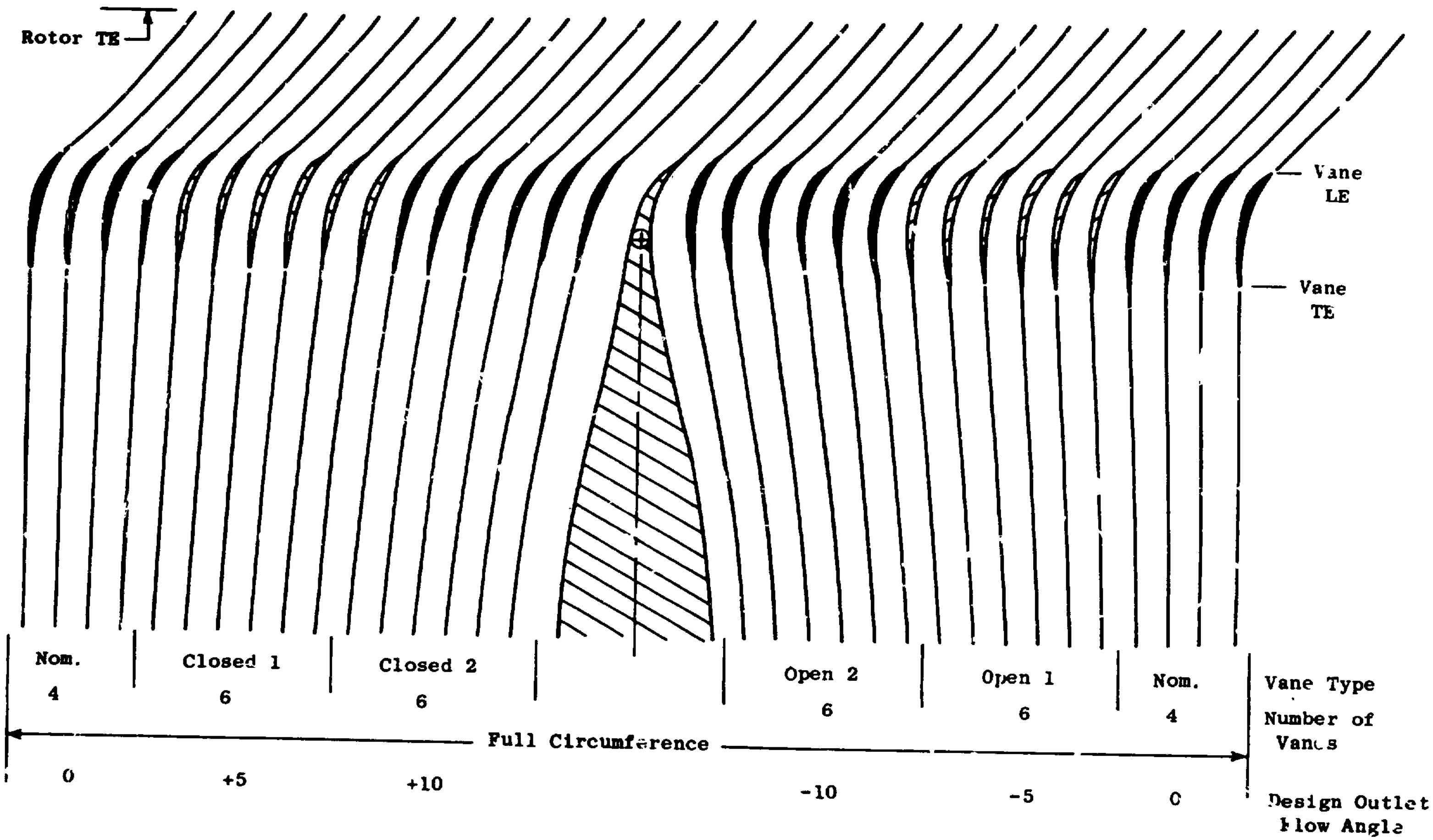

Figure 22. Vane Frame Unwrapped Section at I.D.

The deviation angle for each of the five vane groups was calculated from Carter's Rule as described for the rotor. The portion of the meanline aft of the 25% chord point approximates a circular arc blending between the front circular arc and the required trailing edge angle. For the vane group which underturns the flow by 10° the aft portion of the blade has little camber. Figure 23 shows an unwrapped cross section at the ID of two of the 10° over-cambered vanes and two of the 10° under-cambered vanes adjacent to the pylon. Note that the spacing between the pylon and the first under-cambered vane is 50% larger than average. This increased spacing was required to open the passage internal area, relative to the capture area, to retrieve the area blocked by the radial drive shaft envelope requirements.

Table V gives the detailed coordinate data for the two vane geometries and the pylon leading edge geometry shown in Figure 23. The coordinate data for the nominal vane geometry at three radial locations is also given in this table. The vane coordinates are in inches.

The radial distributions of camber and stagger for the nominal and two extreme vane geometries are shown in Figure 24. The radial distributions of chord and solidity for the nominal vane are shown in Figure 25. The design held the leading and trailing edge axial projection common for all five groups which results in slightly different chord lengths for the other four vane types.

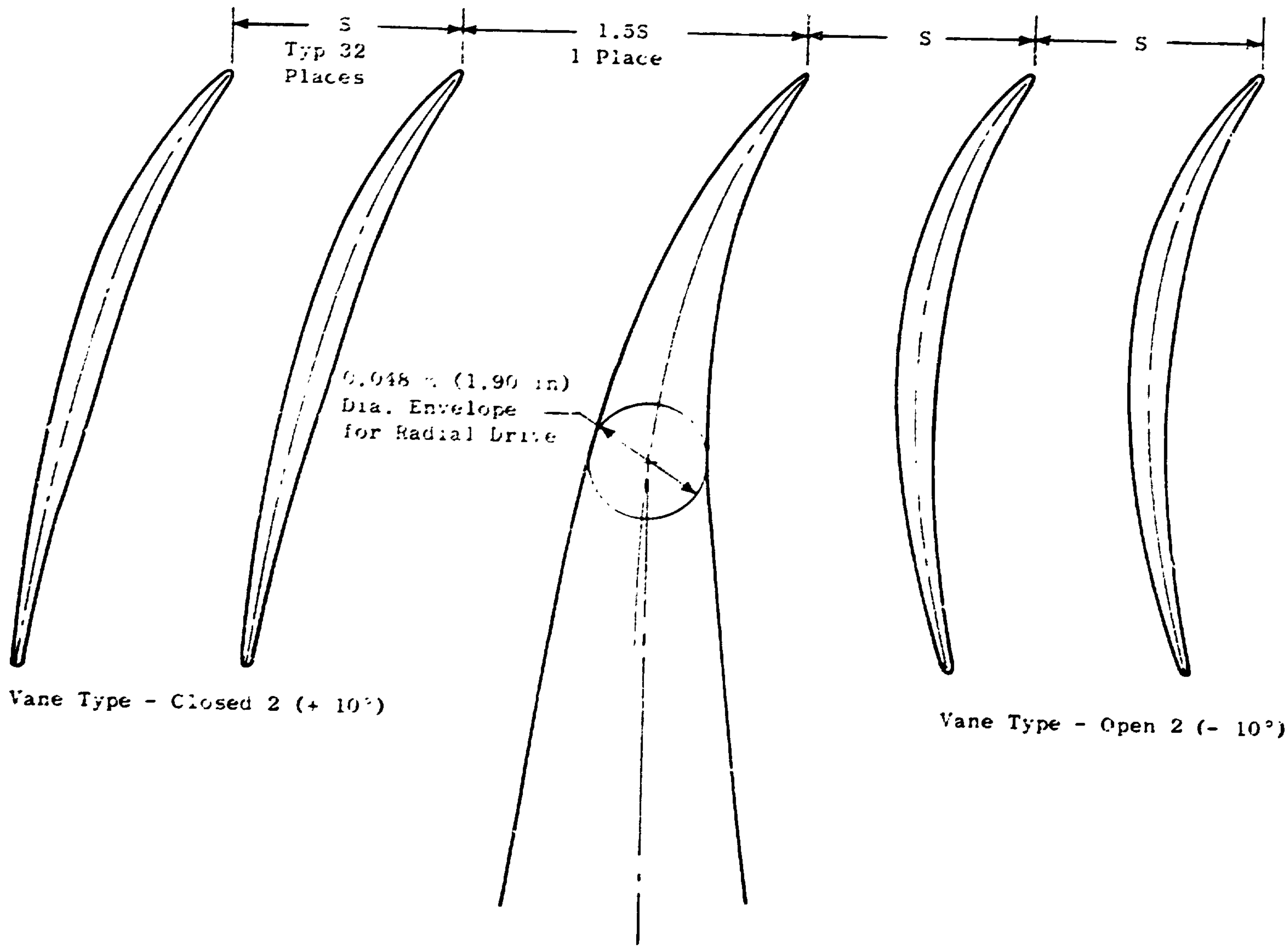

Figure 23. Vane-Frame Unwrapped Section at ID, 32 Vanes Plus Pylon LE Fairing.

Table V. Vane Frame Coordinates.

Vane Type: Closed 2
Radius 53.0 cm (20.86 in.)

Convex		Concave	
X (Axial)	Y	X (Axial)	Y
-6.48210	2.34116	-6.48210	2.34116
-6.48759	2.32790	-6.47014	2.34917
-6.48654	2.30949	-6.45181	2.35181
-6.47875	2.28616	-6.42730	2.34886
-6.46396	2.25823	-6.39677	2.34011
-6.44206	2.22584	-6.36025	2.32555
-6.41331	2.18867	-6.31735	2.30561
-6.29919	2.05618	-6.16591	2.22947
-6.07119	1.83449	-5.89480	2.07990
-5.83097	1.63835	-5.63592	1.92961
-5.58939	1.45347	-5.37839	1.79199
-5.34632	1.27982	-5.12236	1.66526
-5.10018	1.11977	-4.86939	1.54502
-4.85192	0.97171	-4.61855	1.43098
-4.60258	0.83339	-4.36878	1.32361
-4.30233	0.67897	-4.07011	1.20263
-4.00106	0.53619	-3.77245	1.08890
-3.69886	0.40428	-3.47572	0.98129
-3.39590	0.28251	-3.17976	0.87882
-3.09242	0.16986	-2.88431	0.78108
-2.78889	0.06546	-2.58892	0.68742
-2.48547	-0.03115	-2.29341	0.[illegible]9624
-2.18202	-0.12056	-1.99793	0.50613
-1.87857	-0.20389	-1.70246	0.41663
-1.57498	-0.28229	-1.40712	0.32765
-1.27110	-0.35637	-1.11208	0.23941
-0.96707	-0.42655	-0.81718	0.15212
-0.66307	-0.49346	-0.52225	0.06612
-0.35916	-0.55754	-0.22724	-0.01841
-0.05521	-0.61845	0.06774	-0.10206
0.24894	-0.67585	0.36251	-0.18531
0.55329	-0.73002	0.65709	-0.26774
0.85774	-0.78128	0.95157	-0.34873
1.16223	-0.82964	1.24600	-0.42780
1.46682	-0.87488	1.54034	-0.50454
1.77161	-0.91602	1.83448	-0.57877
2.07653	-0.95211	2.12848	-0.65013
2.38133	-0.98311	2.42260	-0.71727
2.68567	-1.00936	2.71719	-0.77845
2.98924	-1.03206	3.01255	-0.83131
3.24155	-1.04887	3.25934	-0.86832
3.41111	-1.05853	3.42574	-0.88974
3.46658	-1.04155	3.47884	-0.91753
3.50000	-0.98095	3.50000	-0.98095

ORIGINAL PAGE IS OF POOR QUALITY

Table V. Vane Frame Coordinates (Continued).

Vane Type: Pylon Leading Edge
Radius 53.0 cm (20.86 in.)

Convex		Concave	
X (Axial)	Y	X (Axial)	Y
-6.48132	2.39154	-6.48132	2.39154
-6.48473	2.38081	-6.47148	2.39700
-6.48161	2.36491	-6.45525	2.39712
-6.47179	2.34406	-6.43279	2.39173
-6.45509	2.31849	-6.40420	2.38068
-6.43144	2.28828	-6.36944	2.36404
-6.40114	2.25305	-6.32808	2.34232
-6.28510	2.12434	-6.17848	2.26374
-6.06174	1.89820	-5.90277	2.12120
-5.82801	1.69438	-5.63744	1.98182
-5.58938	1.50620	-5.37700	1.85097
-5.35069	1.32592	-5.11662	1.73488
-5.11131	1.15379	-4.85694	1.63146
-4.86999	0.99135	-4.59920	1.53737
-4.62695	0.83784	-4.34317	1.45194
-4.33354	0.66380	-4.03770	1.36062
-4.03838	0.49997	-3.73397	1.28070
-3.74142	0.34566	-3.43206	1.21133
-3.44249	0.20051	-3.13211	1.15184
-3.14194	0.06430	-2.83378	1.10152
-2.84029	-0.06372	-2.53655	1.05974
-2.53811	-0.18441	-2.23985	1.02584
-2.23601	-0.29875	-1.94307	0.99894
-1.93375	-0.40770	-1.64646	0.97830
-1.63088	-0.51145	-1.35045	0.96310
-1.32713	-0.60978	-1.05531	0.95241
-1.02219	-0.70205	-0.76138	0.94519
-0.71617	-0.78789	-0.46851	0.94075
-0.40945	-0.86865	-0.17635	0.94005
-0.10190	-0.94573	0.11497	0.94418
0.20685	-1.01906	0.40510	0.95304
0.51627	-1.08827	0.69456	0.96621
0.82574	-1.15361	0.98398	0.98345
1.13505	-1.21546	1.27354	1.00450
1.44405	-1.27381	1.56343	1.02871
1.73876	-1.32623	2.14355	1.08453
2.03355	-1.37574	2.44720	1.11734
3.50000	-1.64800	3.50000	1.20800

Table V. Vane Frame Coordinates (Continued).

Vane Type: Open 2
Radius 53.0 cm (20.86 in.)

Convex		Concave	
X (Axial)	Y	X (Axial)	Y
-6.48210	2.34116	-6.48210	2.34116
-6.48759	2.32791	-6.47013	2.34918
-6.48653	2.30950	-6.45180	2.35183
-6.47873	2.28619	-6.42726	2.34891
-6.46391	2.25830	-6.39669	2.34021
-6.44195	2.22597	-6.36008	2.32574
-6.41309	2.18893	-6.31705	2.30598
-6.29837	2.05743	-6.16673	2.23191
-6.06881	1.84013	-5.89719	2.08881
-5.82663	1.65165	-5.64026	1.94846
-5.58259	1.47746	-5.38519	1.82404
-5.33663	1.31730	-5.13205	1.71340
-5.08740	1.17343	-4.88217	1.61171
-4.83591	1.04408	-4.63456	1.51847
-4.58317	0.92682	-4.38819	1.43400
-4.27866	0.80069	-4.09378	1.34319
-3.97293	0.68941	-3.80058	1.26249
-3.66610	0.59230	-3.50849	1.19083
-3.35833	0.50871	-3.21733	1.12737
-3.04985	0.43788	-2.92688	1.07194
-2.74105	0.37917	-2.63676	1.02425
-2.43218	0.33258	-2.34670	0.98319
-2.12344	0.29797	-2.05652	0.94770
-1.81511	0.27447	-1.76592	0.91756
-1.50737	0.26103	-1.47473	0.89269
-1.20033	0.25681	-1.18284	0.87302
-0.89392	0.26100	-0.89033	0.85854
-0.58804	0.27293	-0.59728	0.84962
-0.28271	0.29217	-0.30369	0.84652
0.02205	0.31915	-0.00952	0.84873
0.32598	0.35420	0.28547	0.85578
0.62892	0.39664	0.58146	0.86776
0.93104	0.44568	0.87827	0.88487
1.23245	0.50099	1.17578	0.90731
1.53315	0.56243	1.47401	0.93516
1.83305	0.63035	1.77304	0.96799
2.13206	0.70496	2.07295	1.00552
2.43030	0.78549	2.37364	1.04842
2.72800	0.87086	2.67486	1.09772
3.02565	0.95941	2.97614	1.15510
3.27398	1.03479	3.22691	1.20994
3.44400	1.08772	3.39850	1.25063
3.49006	1.12317	3.45780	1.24339
3.50000	1.19138	3.50000	1.19138

Table V. Vane Frame Coordinates (Continued).

Vane Type: Nominal
Radius 53.0 cm (20.86 in.)

Convex		Concave	
X (Axial)	Y	X (Axial)	Y
-6.48210	2.34116	-6.48210	2.34116
-6.48759	2.32791	-6.47013	2.34918
-6.48654	2.30949	-6.45181	2.35182
-6.47874	2.28617	-6.42729	2.34888
-6.46394	2.25825	-6.39675	2.34014
-6.44203	2.22588	-6.36020	2.32561
-6.41324	2.18874	-6.31726	2.30572
-6.29896	2.05654	-6.16614	2.23018
-6.07054	1.83608	-5.89545	2.08244
-5.82980	1.64205	-5.63708	1.93498
-5.58753	1.46015	-5.38025	1.80119
-5.34355	1.29036	-5.12513	1.67933
-5.09631	1.13518	-4.87326	1.56502
-4.84677	0.99309	-4.62370	1.45801
-4.59597	0.86190	-4.37539	1.35882
-4.29378	0.71764	-4.07866	1.24915
-3.99047	0.58679	-3.78304	1.14834
-3.68627	0.46852	-3.48832	1.05511
-3.38139	0.36194	-3.19426	0.96836
-3.07616	0.26589	-2.90057	0.88755
-2.77084	0.17937	-2.60697	0.81205
-2.46549	0.10210	-2.31339	0.74054
-2.16009	0.03377	-2.01986	0.67182
-1.85478	-0.02657	-1.72625	0.60556
-1.54964	-0.07997	-1.43246	0.54168
-1.24470	-0.12720	-1.13847	0.48014
-0.93983	-0.16894	-0.84442	0.42105
-0.63494	-0.20568	-0.55038	0.36497
-0.33012	-0.23761	-0.25628	0.31230
-0.02535	-0.26417	0.03788	0.26268
0.27916	-0.28484	0.33230	0.21567
0.58316	-0.30022	0.62722	0.17134
0.88725	-0.31091	0.92205	0.13018
1.19188	-0.31606	1.21636	0.09358
1.49640	-0.31452	1.51076	0.06272
1.80035	-0.30547	1.80573	0.03755
2.10352	-0.28852	2.10149	0.01793
2.40575	-0.26457	2.39819	0.00441
2.70721	-0.23490	2.69565	-0.00204
3.00816	-0.20101	2.99363	0.00047
3.25869	-0.17029	3.24220	0.01049
3.42732	-0.14778	3.40980	0.02082
3.47856	-0.12068	3.46729	0.00351
3.50000	-0.05474	3.50000	-0.05474

Table V. Vane Frame Coordinates (Continued).

Vane Type: Nominal
Radius 69.8 cm (27.48 in.)

Convex		Concave	
X (Axial)	Y	X (Axial)	Y
-5,58734	1,85159	-5,58734	1,85159
-5,59204	1,83581	-5,57482	1,86239
-5,58888	1,81511	-5,55459	1,86805
-5,57767	1,78979	-5,52679	1,86834
-5,55820	1,76017	-5,49156	1,86305
-5,53036	1,72642	-5,44892	1,85215
-5,49435	1,68825	-5,39858	1,83610
-5,41795	1,61418	-5,30236	1,80216
-5,20924	1,44123	-5,05671	1,70308
-4,99074	1,28915	-4,82084	1,59775
-4,77087	1,14424	-4,58634	1,49967
-4,54950	1,00677	-4,35334	1,40820
-4,32535	0,87963	-4,12313	1,32006
-4,09911	0,76188	-3,89500	1,23567
-3,87166	0,65193	-3,66808	1,15607
-3,59755	0,52960	-3,39695	1,06657
-3,32237	0,41733	-3,12689	0,98287
-3,04629	0,31473	-2,85773	0,90412
-2,76943	0,22135	-2,58935	0,82965
-2,49196	0,13645	-2,32158	0,75933
-2,21403	0,05948	-2,05428	0,69304
-1,93557	-0,00932	-1,78749	0,62999
-1,65657	-0,06966	-1,52125	0,56948
-1,37718	-0,12194	-1,25540	0,51166
-1,09766	-0,16670	-0,98968	0,45683
-0,81820	-0,20440	-0,72390	0,40517
-0,53899	-0,23556	-0,45787	0,35687
-0,26019	-0,26089	-0,19143	0,31220
0,01826	-0,28092	0,07536	0,27132
0,29653	-0,29522	0,34234	0,23382
0,57458	-0,30326	0,60952	0,19928
0,85232	-0,30529	0,87702	0,16812
1,12961	-0,30174	1,14497	0,14089
1,40634	-0,29289	1,41349	0,11784
1,68247	-0,27890	1,68260	0,09902
1,95797	-0,25944	1,95234	0,08396
2,23282	-0,23433	2,22272	0,07231
2,50703	-0,20433	2,49376	0,06473
2,78065	-0,17056	2,76537	0,06229
3,05389	-0,13473	3,03738	0,06670
3,28146	-0,10422	3,26418	0,07653
3,42738	-0,08386	3,40977	0,08530
3,47882	-0,05633	3,46701	0,06804
3,50000	0,00941	3,50000	0,00941

Table V. Vane Frame Coordinates (Concluded).

Vane Type: Nominal
Radius 90.1 cm (35.5 in.)

Convex		Concave	
X (Axial)	Y	X (Axial)	Y
-4.49480	1.64519	-4.49480	1.64519
-4.50141	1.62777	-4.48003	1.65611
-4.49961	1.60423	-4.45704	1.66064
-4.48913	1.57488	-4.42603	1.65851
-4.46969	1.54012	-4.38719	1.64946
-4.44110	1.50020	-4.34056	1.63344
-4.40352	1.45490	-4.28574	1.61098
-4.36001	1.40641	-4.22984	1.58666
-4.17865	1.23208	-4.01147	1.48459
-3.98730	1.08043	-3.80307	1.38218
-3.79412	0.93890	-3.59652	1.26894
-3.59889	0.80698	-3.39201	1.20396
-3.40085	0.68675	-3.19030	1.12394
-3.20110	0.57636	-2.99032	1.04840
-3.00038	0.47518	-2.79129	0.97765
-2.75845	0.36283	-2.55353	0.89860
-2.51543	0.26034	-2.31686	0.82511
-2.27133	0.16734	-2.08128	0.75648
-2.02632	0.08355	-1.84660	0.69213
-1.78065	0.00833	-1.61258	0.63195
-1.53453	-0.05889	-1.37902	0.57580
-1.28796	-0.11786	-1.14590	0.52287
-1.04094	-0.16833	-0.91323	0.47240
-0.79365	-0.21078	-0.68083	0.42448
-0.54628	-0.24579	-0.44852	0.37939
-0.29894	-0.27378	-0.21617	0.33741
-0.05184	-0.29518	0.01642	0.29879
0.19482	-0.31062	0.24945	0.26389
0.44100	-0.32059	0.48296	0.23289
0.68673	-0.32477	0.71691	0.20524
0.93213	-0.32276	0.95120	0.18045
1.17721	-0.31479	1.18580	0.15901
1.42173	-0.30120	1.42078	0.14150
1.66547	-0.28239	1.65692	0.12812
1.90844	-0.25863	1.89364	0.11880
2.15059	-0.22976	2.13118	0.11295
2.39198	-0.19569	2.36947	0.11011
2.63272	-0.15716	2.60842	0.11097
2.87313	-0.11508	2.84770	0.11677
3.11356	-0.07029	3.08696	0.13000
3.31347	-0.03164	3.28679	0.14794
3.43200	-0.00838	3.40618	0.16054
3.48205	0.02185	3.46416	0.14584
3.50000	0.08854	3.50000	0.08854

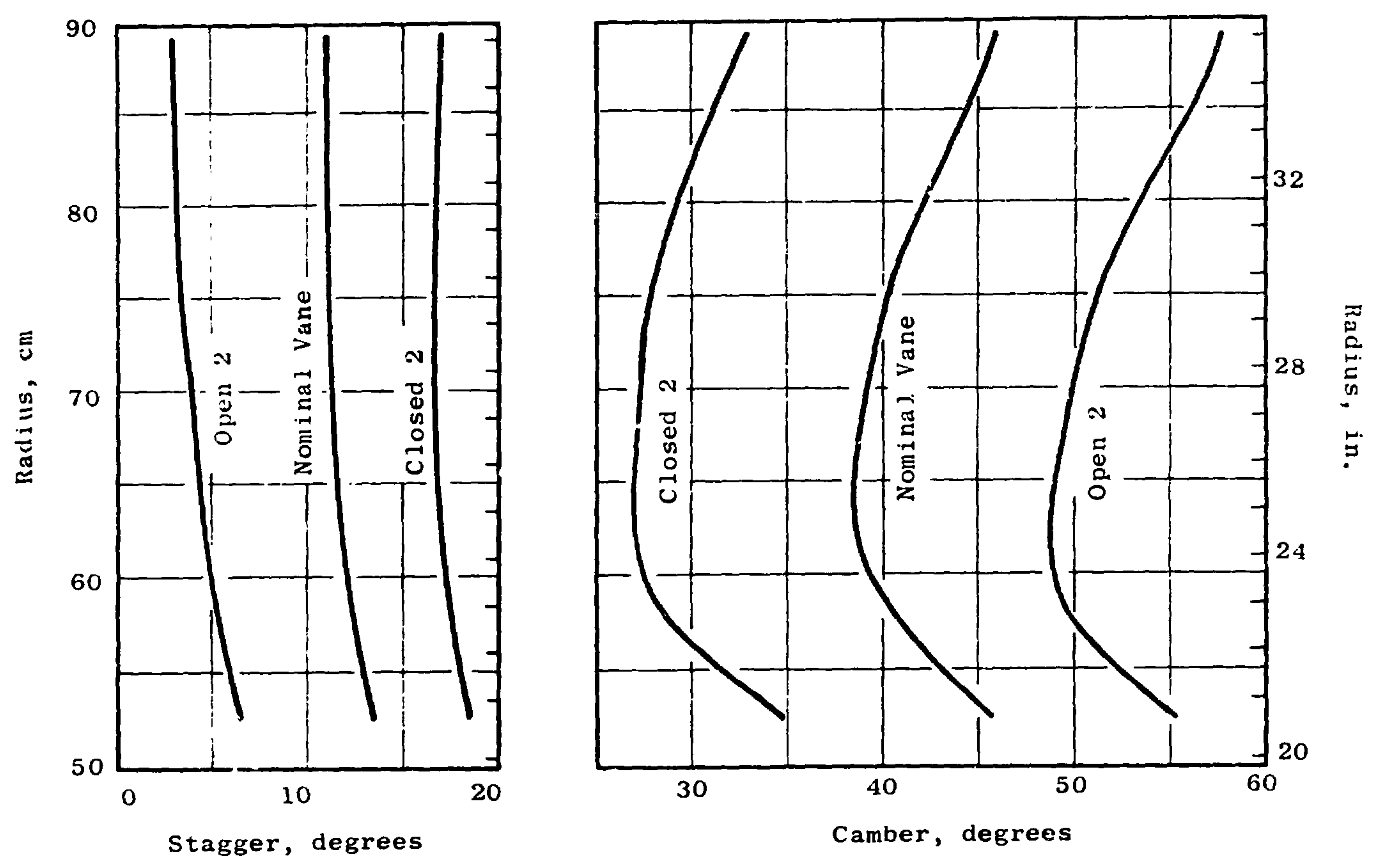

Figure 24. QCSEE Vane Frame.

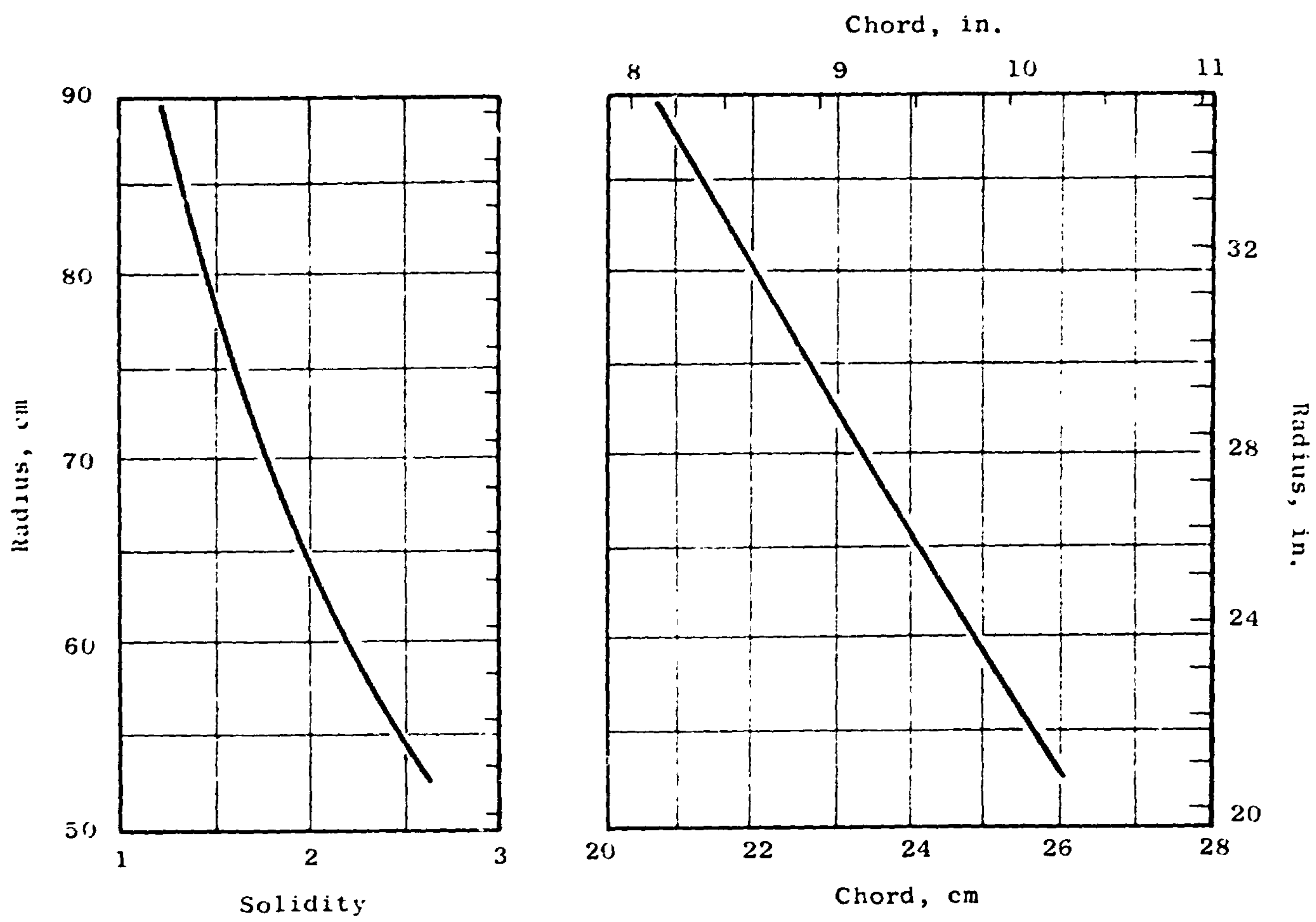

Figure 25. QCSEE Vane Frame.

SECTION 3.0

OTW FAN MECHANICAL DESIGN

3.1 FAN ROTOR SUMMARY

The OTW experimental fan has 28 fixed-pitch metal blades with a 180-cm (71-in.) fan tip diameter similar to that of the UTW fan. This rotor is shown in Figure 26. The conceptual design of this fan is based on using composite fan blades, but metal blades will be used for reasons of economy and low risk. The conceptual composite blade design dictates the absence of blade shrouds, determines the number of fan blades, and affects the sizing of such parameters as the blade solidity, reduced velocity, and leading edge thickness. In the flight engine, composite blades would be substituted for the metal blades without aerodynamic change or compromise in the composite blade mechanical design. While the demonstrator fan disk is heavier than the composite bladed flight weight disk, it reflects a flight configuration in both design criteria and material selection. A comparison between the experimental and flight OTW fan design criteria is given in Table VI.

The OTW fan has both a forward rotating spinner and aft flowpath adapter. The inner flowpath formed by these two parts and the blade platform is identical to the inner flowpath of the UTW fan from a point near the blade trailing edge aft. The tip speed of the OTW fan is about 17% higher than that of the UTW fan.

The fan blades and disk are fabricated of 6-4 titanium. 6-4 titanium couplings on the fore and aft sides of the disk isolate the relatively high stresses in the disk from the 6061 aluminum forward and aft spinners. Increased blade retention capability is provided to prevent axial movement of the blades (benefiting from General Electric experience in large fan design). Fan rotor materials and allowable stresses are shown in Figure 27.

Two-plane balance of the fan rotor will be provided at the forward and aft disk flanges. In addition, the forward spinner will be permanently balanced in two planes. Blade retainers will be pan weighted and blades will be moment weighed, all to be preprogrammed into the rotor. Final trim balancing or field balancing is accomplished through balance bolts mounted in the spinner.

3.2 DESIGN REQUIREMENTS

Design life of the fan rotor is 36,000 hours, including 48,000 flight cycles and 1000 full-power ground cycles. To match the rotor low cycle fatigue life to these design requirements, stress levels were kept to appropriate levels, and contouring and flange scalloping were used to minimize stress concentrations.

Fan blades can be individually replaced without removal of the fan rotor. Openings in the aft flowpath support permit access for the removal of the entire fan rotor package and gearbox.

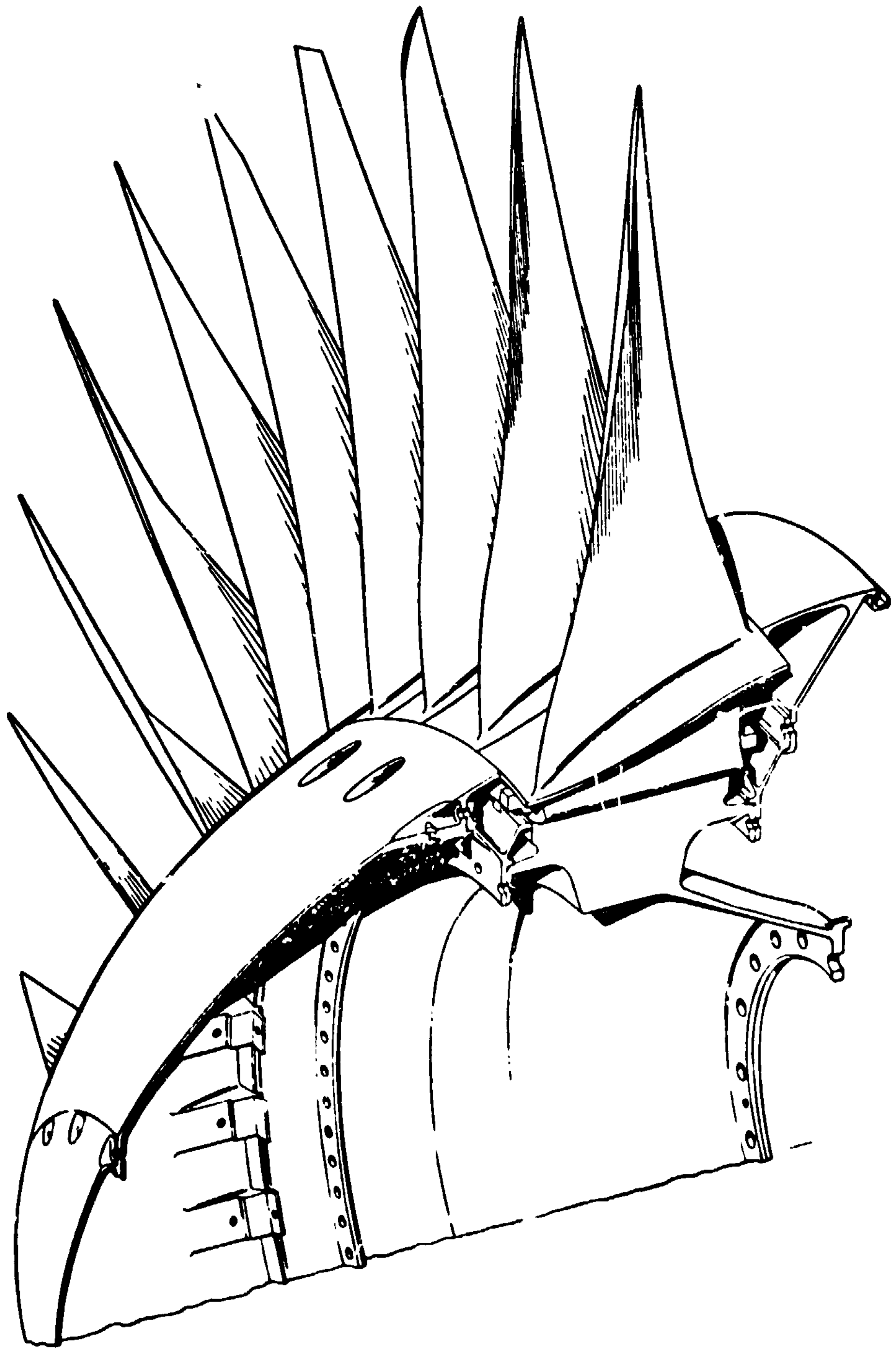

Figure 26. OTW Fan Rotor.

Table VI. QCSEE OTW Fan Design Criteria.

Component	Materials: Demonstrator	Materials: Flight
Disk	Titanium	Titanium
Blades	Titanium	Composite
Number of Blades	28	28
Per Blade Centrifugal Load, N (lb)	558,696 (125,600)	184,156 (41,400)
Design Point Speed, rpm	3792	3792
Design Burst Speed, rpm	5615	5615
Disk Low-Cycle Fatigue Life (Minimum)	>48,000 Flight Cycles	>48,000 Flight Cycles
Disk Low-Cycle Fatigue Life with Initial 0.025 × 0.076 cm (0.01 × 0.03 in.) Defect	>16,000 Flight Cycles	>16,000 Flight Cycles

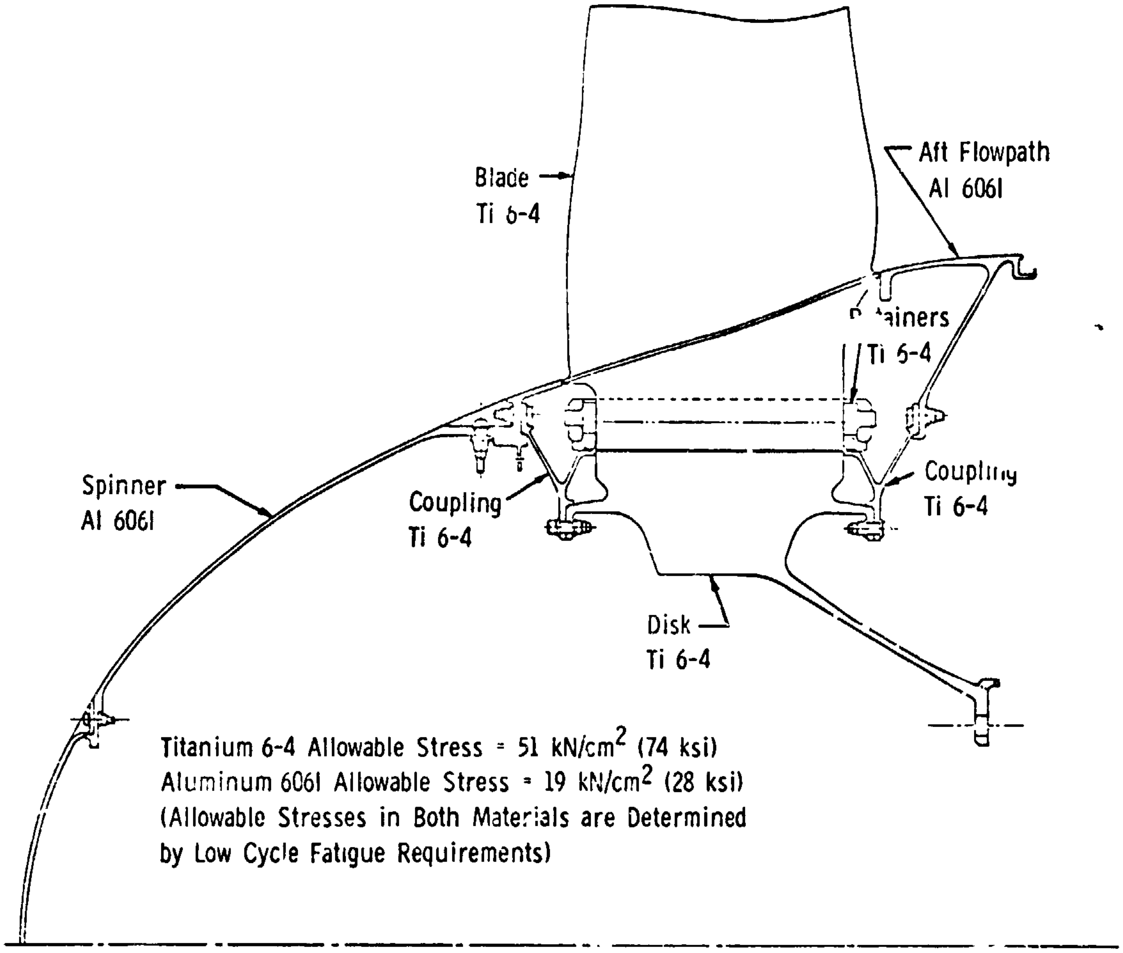

Figure 27. OTW Rotor Layout.

3.3 FAN BLADE DESIGN

The OTW fan blades (Figure 28) are machined from 6-Al-4V titanium forgings, a finished blade weighing 5.94 kg (13.1 lb). Blade geometry is summarized in Table VII and Figures 29 and 30. Operating steady-state stresses are summarized in Figure 31 and Table VIII. Blade airfoil stresses and vibratory frequencies were calculated by the use of standard General Electric mechanical design programs in the computer library. These include a twisted blade program for calculating airfoil stresses and frequencies and a shell program to determine blade root boundary conditions due to the flexibility of the disk and adjacent shells. Blade dovetail and disk post-stresses were calculated by a computer time sharing program based on the dovetail analysis of Dr. H.J. Macke (Report Nos. R59FPD611 and R63FPD?1).

The steady-state effective stress shown in Figure 31 is composed of the resultant of bending, induced tensile, and centrifugal stresses and permits a level of vibratory stress consistant with GE practice (minimum of 10 ksi vibratory stress capability) as shown in Figure 36 (35 ksi allowable). Since the blade leading and trailing edges are in compression except at the root, where the tensile stresses are very low, the blade is rather insensitive to foreign object damage on the edges. At the root, assuming damage that will produce a stress concentration of 3, the blade is still capable of tolerating a vibratory stress of 45 ksi single amplitude. The uncorrected gas bending stress is an indicator of stall stress levels. In the case of the OTW fan blade, the stall stress is projected to be less than the allowable vibratory stress.

The fan blades are a "low-flexed" design, i.e., the first flexural frequency of the blades crosses the two per rev line in the fan operating speed range. Without a thicker blade root, which would have been aerodynamically unsatisfactory, low-flexing was necessary because of the lack of blade shrouds. This approach, though not common, is used successfully on General Electric's TF34 fan and J79 stage 1 compressor blade and was successful on NASA's Quiet Engine "C" fan. The blade Campbell diagram is shown in Figure 32. The frequency of the disk-blade assembly (dashed lines) is somewhat lower than the fixed blade frequency (solid lines) due to the flexibility of the supporting fan disk. The frequency margin between the N=2 disk-blade mode and the two per rev resonance line is 19 percent at 100% fan speed. The two per rev resonance crossover occurs at about 66% speed which is in the flight idle range. However, in the experimental engine which is not a flight engine, there will be no reason to operate other than transiently in this speed range, so no problem is anticipated. In a flight engine utilizing composite blades, the resonant frequency of the blade is subject to some adjustment by a rearrangement and recomposition of the fabric plies; also, the flight idle speed of the engine can be varied somewhat. Experience with the 20 inch UTW simulator which had a similar low flex blade design, showed that the vibratory stresses at crossover were only 30% of scope limits.

The combined blade (second flex) disk (N=3) mode has a frequency margin of 14 percent from the 3 per rev line at 100% speed. In the absence of frame struts or inlet guide vanes ahead of the fan, higher order resonances have not been a problem on similar configuration engines such as the TF34 and CF6.

Figure 28. OTW Fan Blade.

Table VII. QCSEE OTW Fan Blade.

Number of Blades	28	
Fan Tip Diameter	180.3 cm (71 inches)	
Airfoil Length	52.1 cm (20.5 inches)	
Aspect Ratio	2.1	

	Blade Tip	Blade Root
Chord	26.31 cm (10.36 inches)	20.68 cm (8.14 inches)
Max. Thickness/ Chord	2.65 percent	8.6 percent
Solidity	1.3	2.34

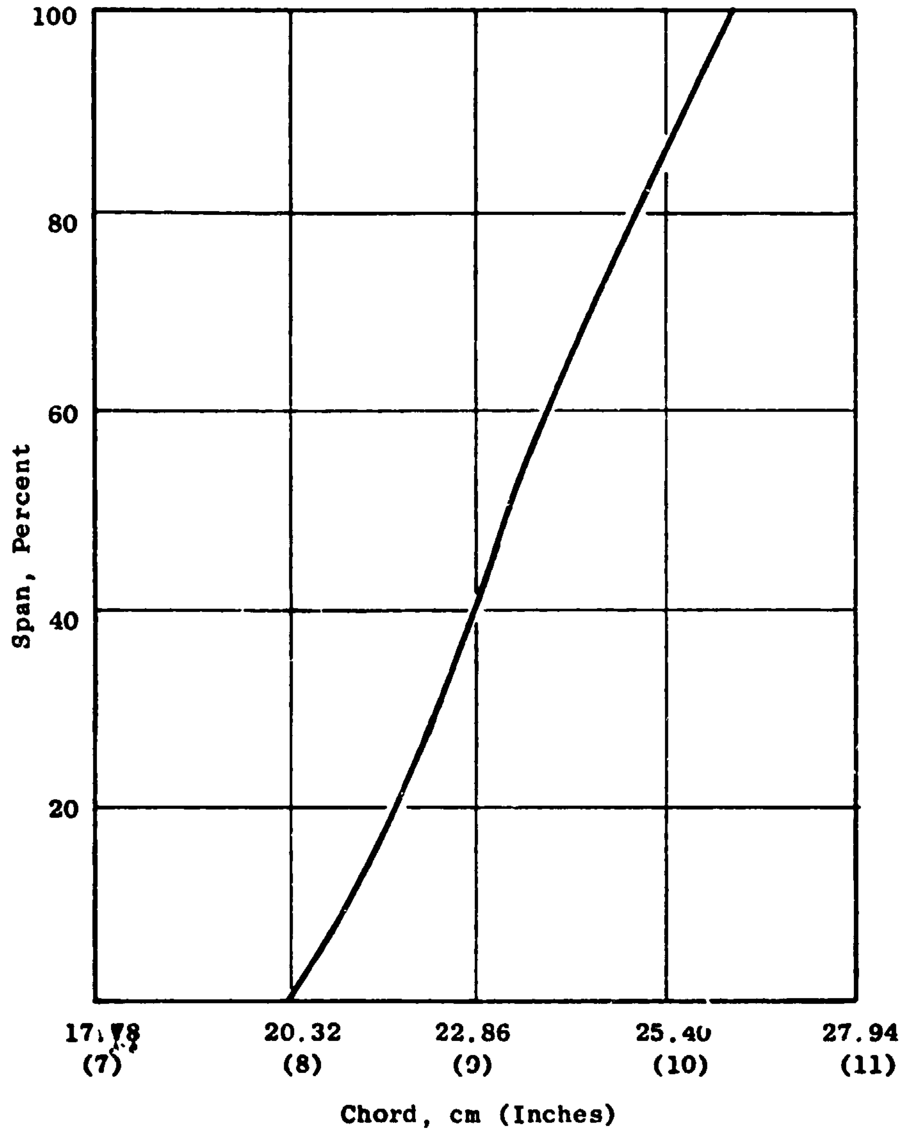

Figure 29. OTW Fan Blade Chord Vs. Span.

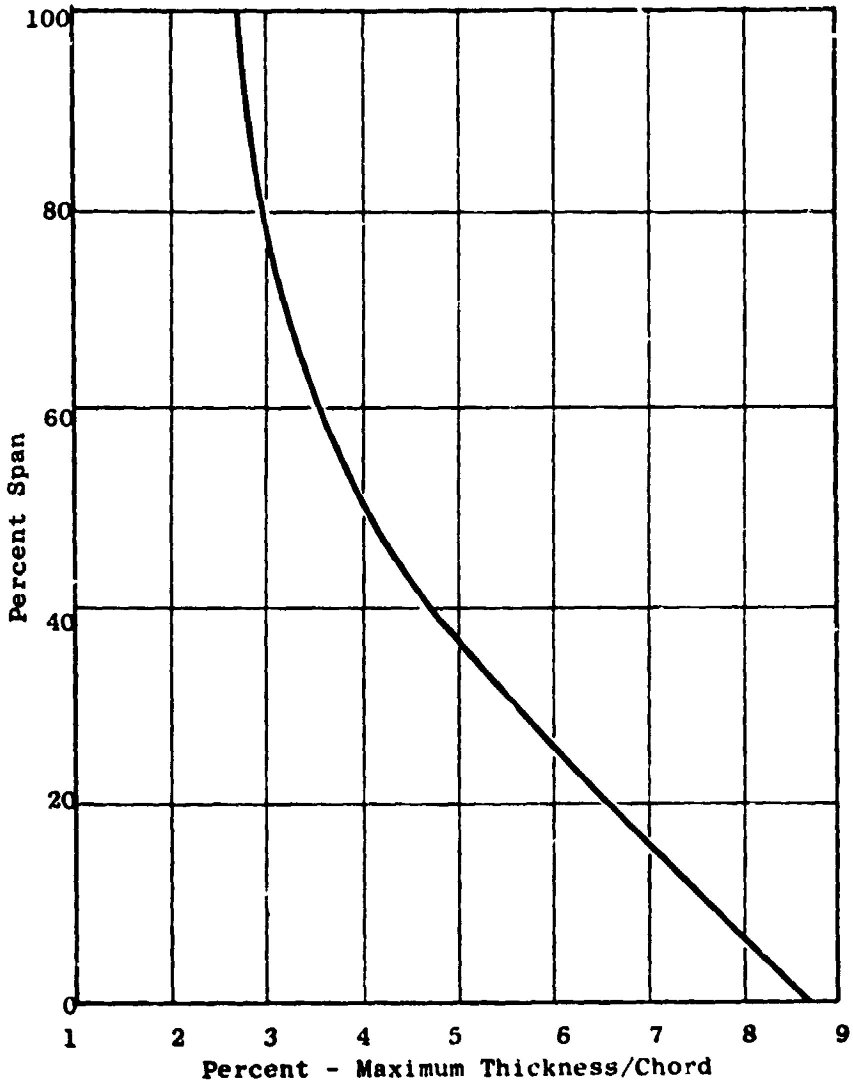

Figure 30. OTW Fan Blade Maximum Thickness Chord Vs. Span.

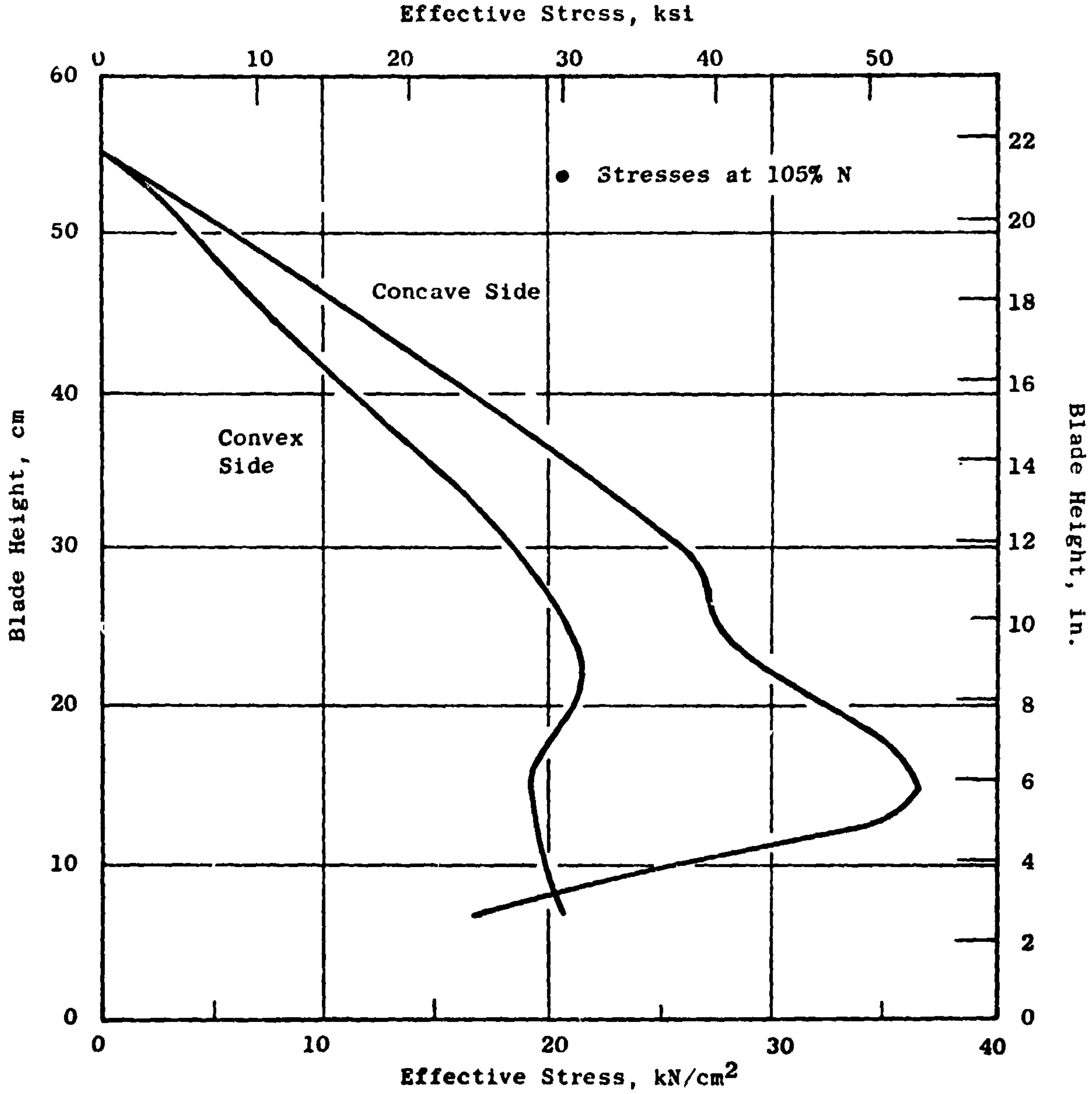

Figure 31. Blade Steady State Effective Stress.

Table VIII. Blade Stresses.

• Maximum Centrifugal	16.6 kN/cm^2 (24 ksi) @ 105% N 7.62 cm (3 in.) from root
• Maximum Effective (Steady State)	36.5 kN/cm^2 (53 ksi) @ 105% N 15.2 cm (6 in.) from root

- Leading and trailing edges in compression except at root - low tensile stresses permit an allowable vibratory stress of 31 kN/cm^2 (45 ksi SA) with a stress concentration of 3 (FOD)
- Anticipated vibratory stress at first flex - 2/rev crossing is approximately 30% of scope limits.
- Uncorrected gas bending stress = 12.4 kN/cm^2 (18 ksi).

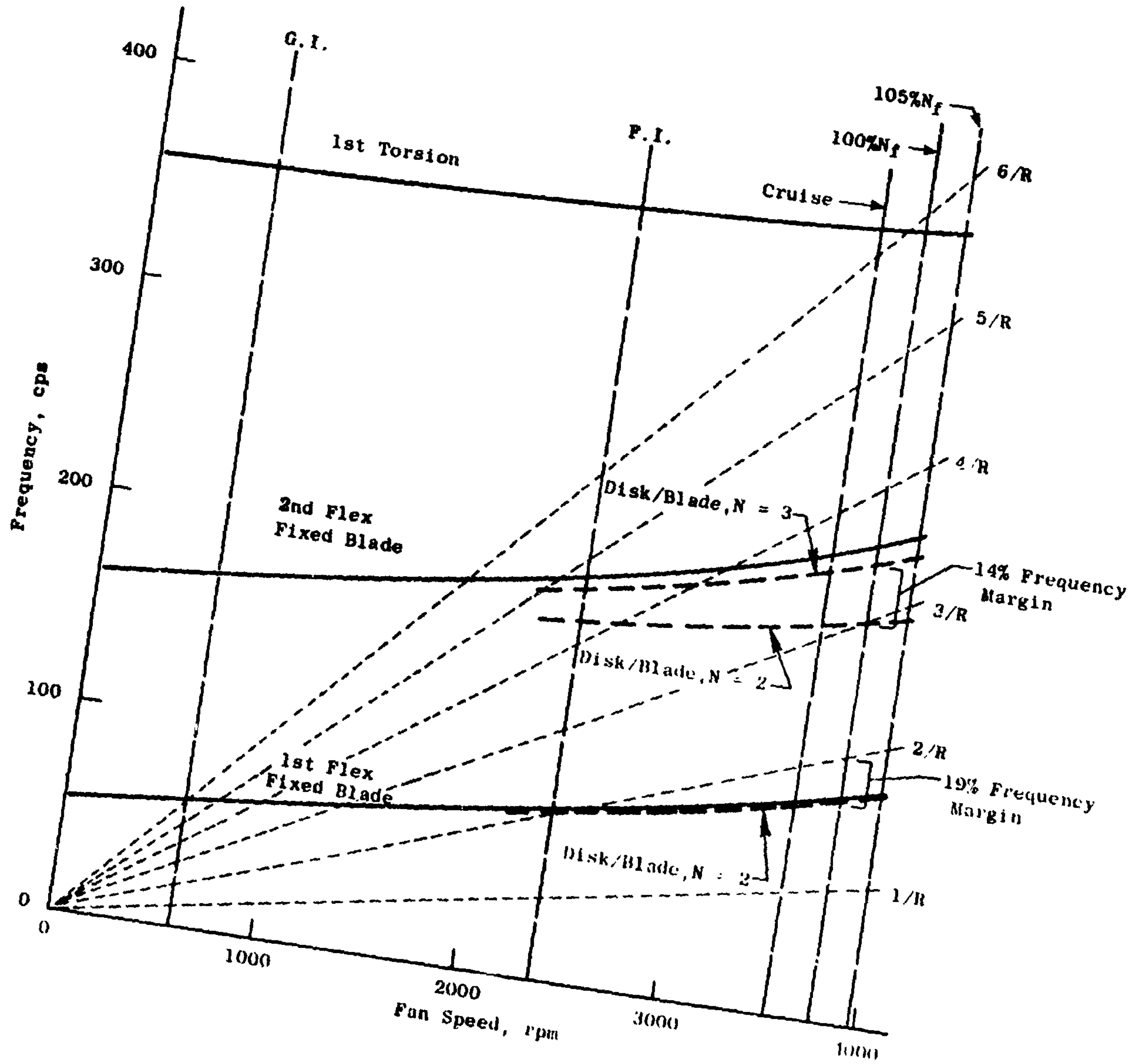

Figure 32. OTW Fan Blade Campbell Diagram.

It is desirable to have a minimum of 12% frequency margin from the combined blade-disk mode to a per rev stimulus at 100% speed. The present blade design, with a margin of 19% between the first flex N=2 blade-disk mode and the two per rev line, and a margin of 14% between the second flex N=3 blade-disk mode and the three per rev line (Reference Figure 32), is considered to have adequate margin in these two modes of greatest concern.

Blade "instability" or "limit cycle vibration" can be a problem on fans. It is characterized by a high amplitude vibration in a single mode (normally the first flexural or torsional mode) at a nonintegral per rev frequency. It is not one of the classical airfoil flutter cases and is apparently confined to cascades. Because of the nonlinearity in the aerodynamics involved, it has resisted practical solutions by solely theoretical means. Accordingly, General Electric has adopted a semiempirical "reduced velocity" approach for limit cycle avoidance. Reduced velocity gives a measure of a blade's stability against self-excited vibration. This parameter is defined as $V_R = W/bf_t$,

where: b = 1/2 chord at 5/6 span - (meters)

W = average air velocity relative to the blade over the outer third of the span - (meters/sec)

f_t = first torsional frequency at design rpm - (rad/sec)

The basic criterion used for setting the design of the OTW metal blade was the requirement of having a reduced velocity parameter no higher than 1.5. This allowable range is based on previous testing of a variety of fan configurations in combination with the specific aerodynamic design of the OTW blade.

Blade instability does not occur once the blades are stalled. The current design practice is to design blades such that when the fan is throttled, stall occurs before the empirically predicted blade instability is encountered. The blade stability is affected by varying the blade chord and thickness distribution which changes the reduced velocity parameter. The operating and stall characteristics of this blade are presented in Figure 33 in terms of reduced velocity versus incidence angle. This shows an acceptable blade design with the design point reduced velocity parameter at 1.3, and in which the throttled fan should stall before encountering the expected blade stability limit. The predicted blade stall line includes the effects of special casing treatment.

OTW composite flight blade would have additional stability margin due to the higher stiffness-to-weight ratio possible in composite designs.

The blade is attached to the disk by an axially oriented 55° flank angle dovetail (Figure 34). Maximum blade dovetail steady-state stress is 29.7 kN/cm^2 (43 ksi) in combined bending and tensile stress. Dovetail crush stress is 51 kN/cm^2 (74 ksi) and is life limiting by the mechanism of wear or fretting, not by low cycle fatigue, since neither a tensile stress nor a stress concentration is involved. Dovetail flanks are plasma sprayed with copper-nickel-indium and coated with Molydag to protect against fretting. In the event of loss of a blade airfoil, the resulting combination of tensile and bending stress

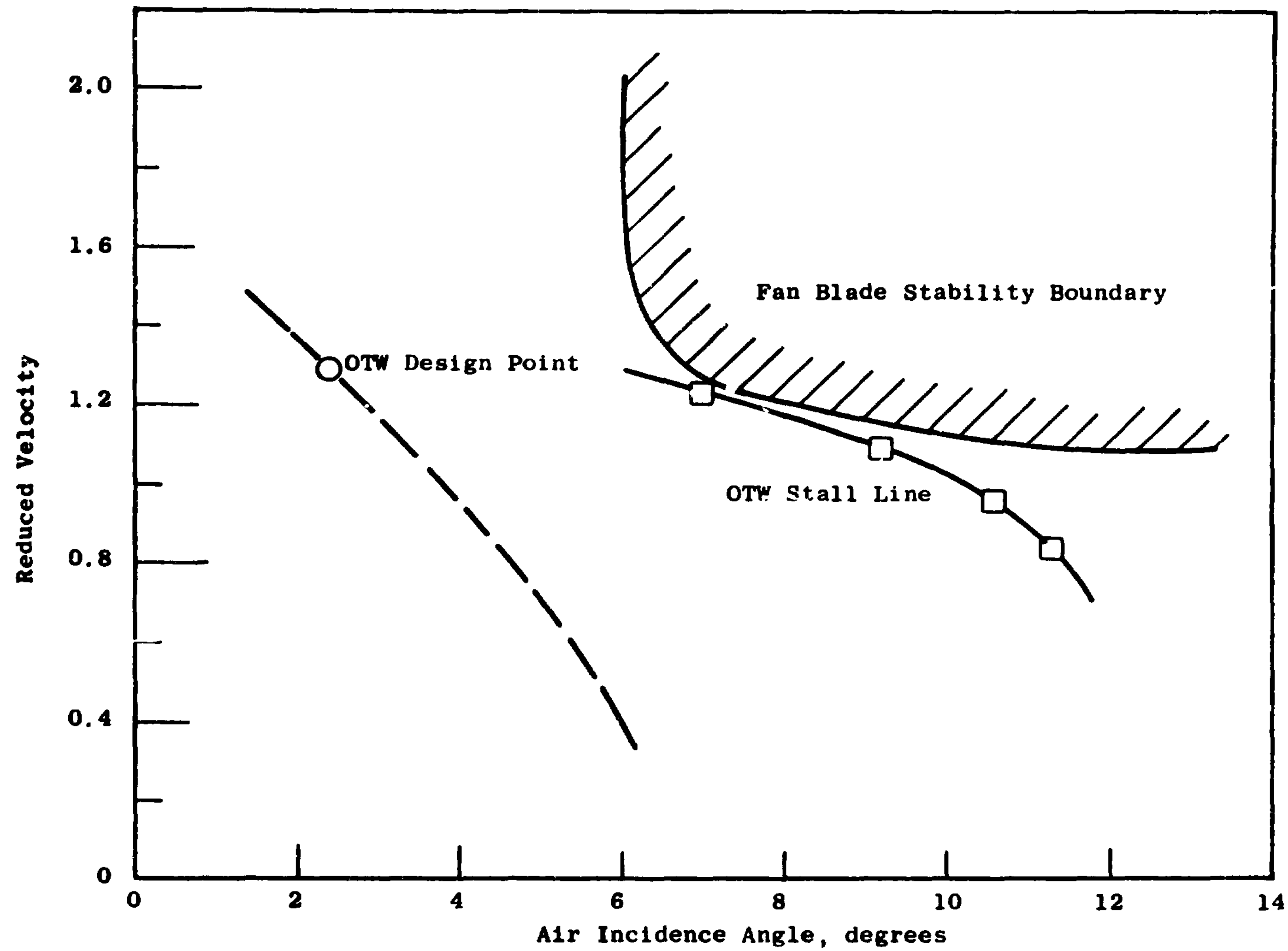

Figure 33. OTW Fan Limit Cycle Boundary.

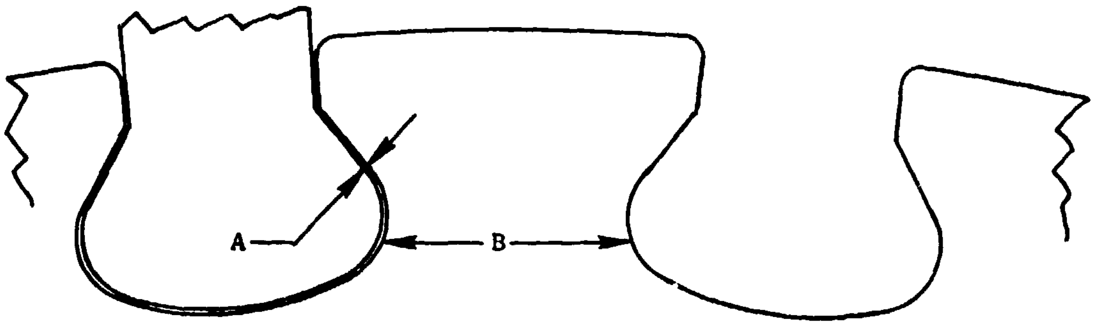

(A) Dovetail Crush Stress - 51 kN/cm^2 (74 ksi) at 105% Speed

(B) Maximum Stress on Disk Post Due to Blade Out - 44.1 kN/cm^2 (64 KSI)

Figure 34. OTW Fan Blade Dovetail.

on the disk post is 44 kN/cm^2 (64 ksi) within an allowable stress in this case of 85 kN/cm^2 (123 ksi). The loss of an airfoil will not cause the subsequent loss of adjacent blades through failure of the disk post.

The blade attachments were designed so that the blade airfoil is the weakest link in the airfoil, dovetail, and disk post system to minimize the size of the piece that will detach in event of a vibratory failure. The resulting design is such that when the airfoil is operating at its maximum allowable vibratory stress, the blade dovetail is at 98% of its maximum and the disk post is at 92% of its maximum. Figures 35 and 36 illustrate this design concept.

Figure 35 shows the points of maximum stress on the blade dovetail and the disk post for which stresses are calculated in the dovetail computer program. The ratio of the vibratory stresses at these points to the vibratory stress in the airfoil is shown in the fatigue limit diagram (Figure 36).

With the airfoil at its maximum allowable vibratory stress at 105% speed, all of the maximum stress points on both the blade and disk dovetails are at less than their allowable stresses.

3.4 FAN DISK DESIGN

The QTW fan disk is machined from a 6-Al-4V titanium forging. An integral cone attaches the ring disk to the main reduction gear shafting. Slots machined into the forward and aft ends of each disk post provide attachment for individual blade retainers. The rotor is required to have low-cycle fatigue (LCF) capability for 48,000 mission cycles and 1,000 ground cycles. To achieve this requirement, disk extensions were provided for the attachment of adjacent shell members. This, in addition to scalloping the flanges, lowered the stresses at the flanges sufficiently to meet the LCF requirements. Stresses in the disk and shells were calculated using a shell and ring program in the computer library. A finite element program was used to calculate stress in the disk dovetail post and in the bottom of the dovetail slot.

The total dead load supported by the disk is 18.5×10^6 N (4,150,000 lb). This includes the centrifugal weight of all nonself-supporting parts (blades, retainers, disk dovetail posts, etc.) as well as side loads imposed by adjacent members. Maximum permissible stress in the disk including stress concentrations was limited to 51 kN/cm^2 (74 ksi) to meet the LCF life requirements. Calculated stresses (105% N) including local stress concentrations are shown in Figure 37 for various parts of the disk and shaft. Crack propagation calculations indicate the LCF life in excess of 16,000 cycles with an initial 0.0254 - 0.0762 cm (0.01 × 0.03 inch) defect.

The disk is designed as a prime reliable component, capable of withstanding a stress twice that at the maximum cycle speed without bursting. This requires a special capability of 141% of the maximum cycle speed or 5615 rpm. The calculated burst speed of the disk as designed is 6260 rpm or 157% of maximum cycle speed.

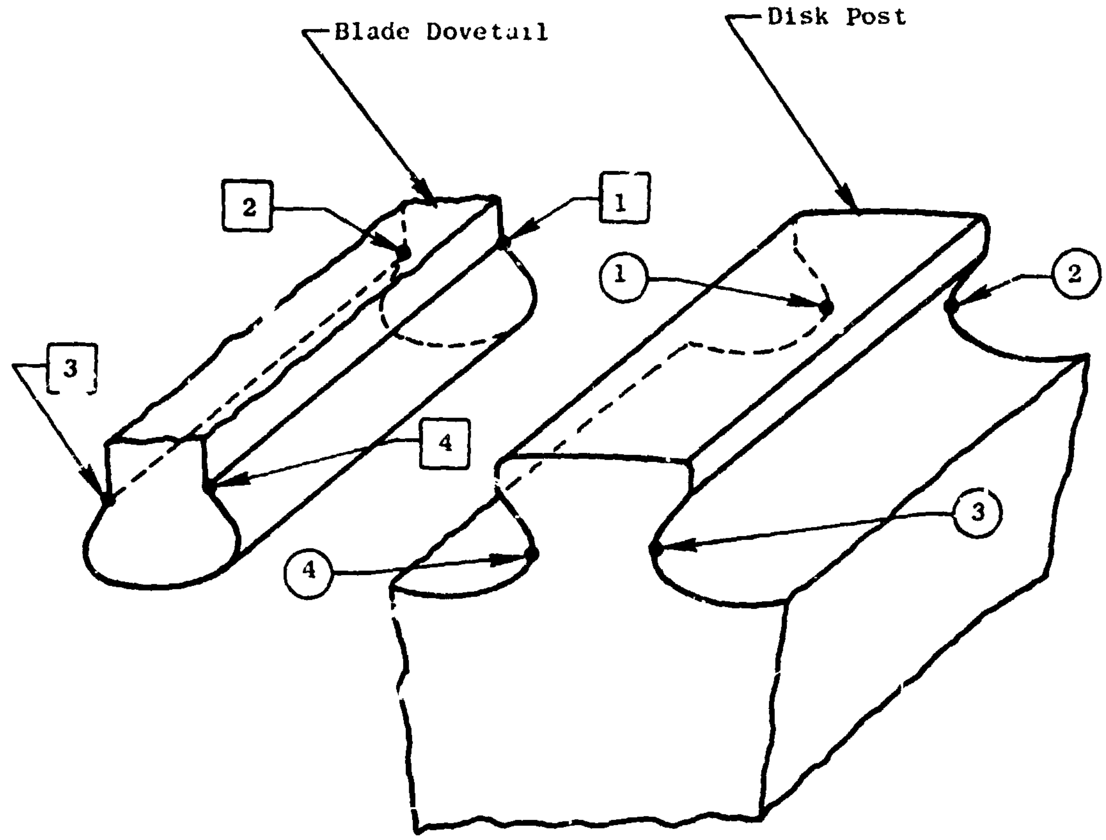

Figure 35. Stress Points on Blade and Disk Dovetails.

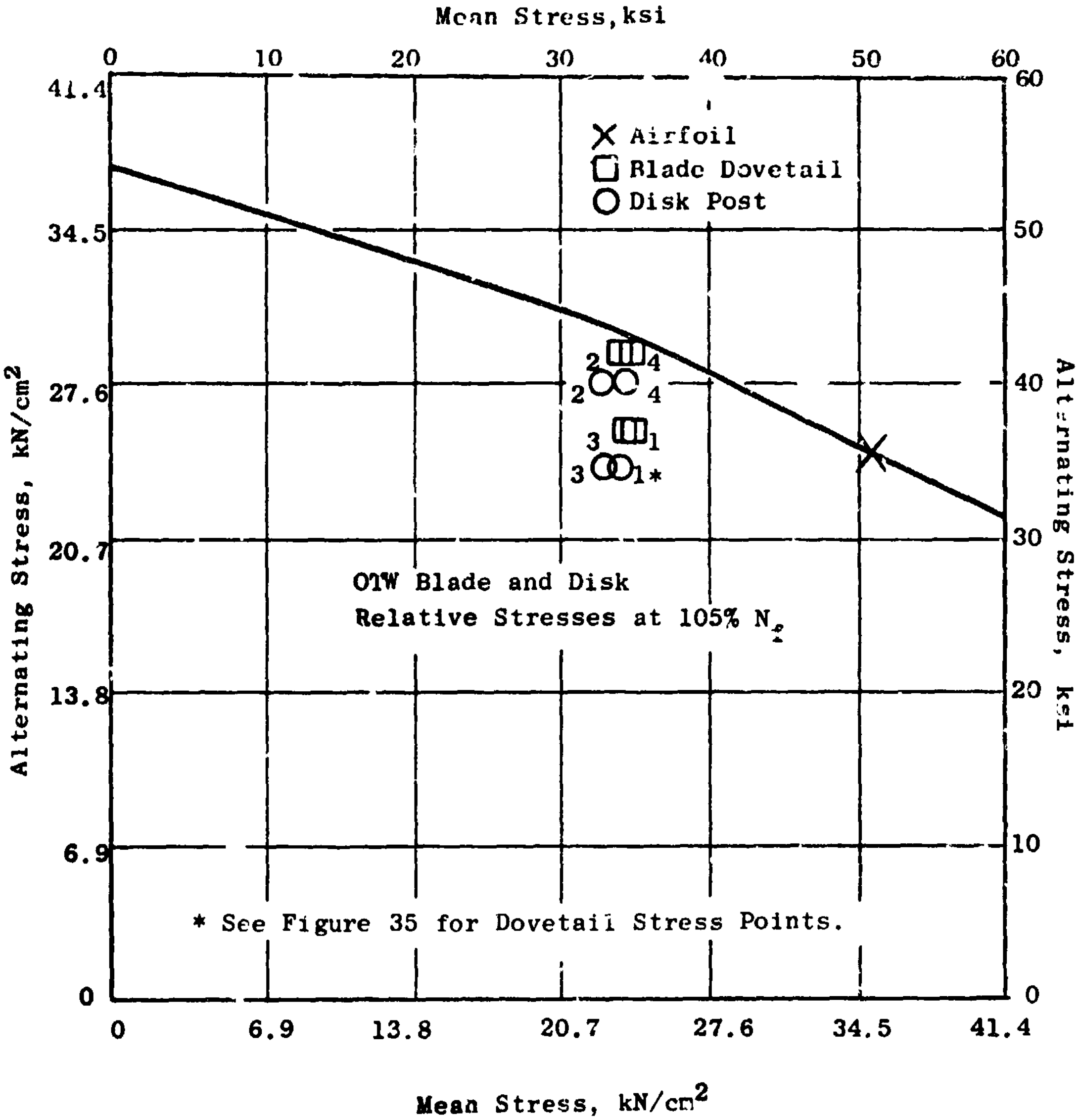

Figure 36. Room Temperature Fatigue Limit.

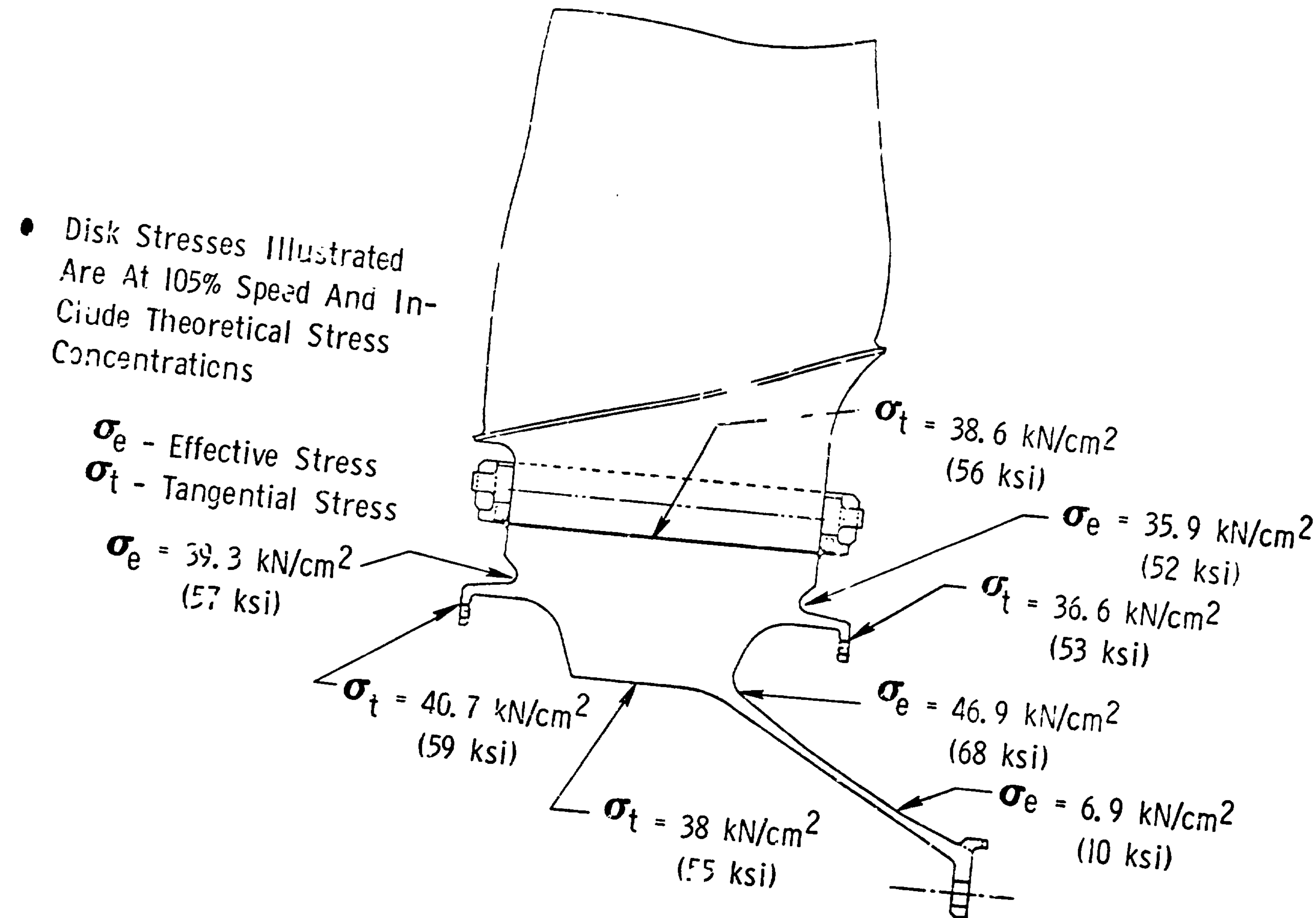

Figure 37. OTW Disk Stresses.

The additional burst margin is available because the disk was not sized solely on burst considerations, but also on the need to reduce dovetail stresses, meet low-cycle fatigue requirements, stiffen the disk to avoid blade frequency problems, and provide capability for reslotting for possible future testing of composite blades.

3.5 BLADE RETAINERS

The blade retainers are blocker plates at the ends of each dovetail slot held in place by slots at the ends of the dovetail post. Radial movement of the plates is restricted by tapering the slots and providing load points against the disk. Figure 38 illustrates the design. The plates are held in place during buildup by individual clips and are finally locked in place by installation of the coupling. This design permits individual blade change by removal of the spinner, coupling, and individual blocker plate.

To prevent the axial shifting of the blades under unusual load conditions, the retainers are designed to withstand thrust loads of up to 30% of the blade centrifugal force. This results in a possible axial load of 167 kN (37,500 lb) that must be restrained without failure of the retention system. At this maximum load condition, calculated stresses in the retainer are at or near the ultimate strength of the material. However, under normal operating conditions, stress in the retainer does not exceed 14 kN/cm^2 (20 ksi).

3.6 ROTOR SHELL MEMBERS

The forward spinner is machined from a 6061 Al forging and forms the forward inner flowpath of the fan. It is attached to the forward coupling which isolates it from the higher stresses of the disk. Scalloping between attachment bolt holes and contouring of the counterbore reduces stress concentrations such that the spinner meets life requirements.

On the experimental engine, the spinner will have a nose cap to provide access to the interior of the rotor. The opening is also available for instrumentation lead-in and slipring support.

Permanent two-plane balance of the spinner will be obtained by attachment of balance weights to the flange at the nose cap and a flange at the rear of the spinner. Rotor field balance capability is built into the spinner by the inclusion of a series of bolts of variable weight into the rear of the spinner.

The aft spinner is machined from a 6061 Al forging and continues the inner fan flowpath from the blade exit to the fan core OGV's. A flow discourager seal inhibits air recirculation at this point. Openings in the support member of the aft spinner provide access to fan frame bolts to allow removal of the fan package.

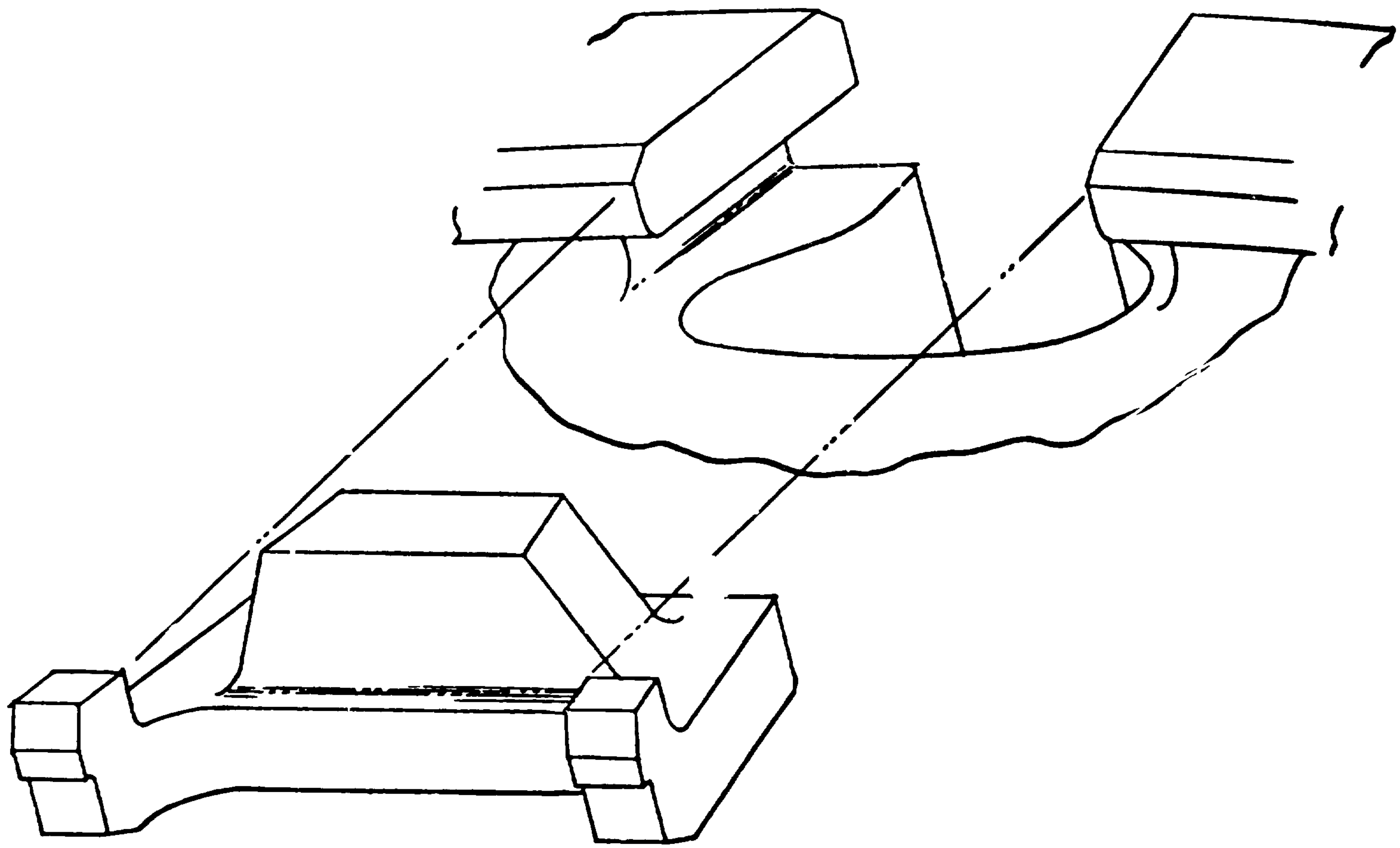

Figure 38. OTW Fan Blade Retainer.

Titanium couplings at the front and rear of the disk provide transition members from the disk to the aluminum spinners and isolate the aluminum parts from the relatively high stresses in the disk. The couplings also lock the blade retainers in place. The fore and aft coupling designs are interchangeable and may be used on either side of the disk. Jack points are provided at rabbeted joints to aid in separating the rotor parts.

Stresses in the rotor shells were calculated using a shell and ring program in the computer library. The stresses are shown in Figure 39 and include stress concentrations. Allowable stresses were determined by low cycle fatigue considerations and are limited to 51 kN/cm^2 (74 ksi) in the titanium parts and 17 kN/cm^2 (25 ksi) in the anodized aluminum parts.

Rotor deflections are given on Figure 40. Axial movements shown are relative to the shaft flange. The platform of the blade and the contours of the forward and aft spinners are dimensioned so that the operating deflections and dimensional stackups will not cause forward facing steps at the interfaces between these parts. The contours that form the flowpath are dimensioned to be on the aerodynamic flowpath at the fan design point.

3.7 FAN HARDWARE

All structural joints in the fan except the nose cap use 0.794 cm (5/16 in.) diameter Inco 718 bolts and Waspaloy nuts. The rotor joint at the fan stub shaft uses 18 1.27 cm (1/2 in.) diameter MP159 bolts and heavy walled Waspaloy nuts to permit higher loading of the bolts. The threads at all the joints are lubricated with MIL-T-5544 lubricant. A summary of design data on the stub shaft flange bolts is shown in Table IX.

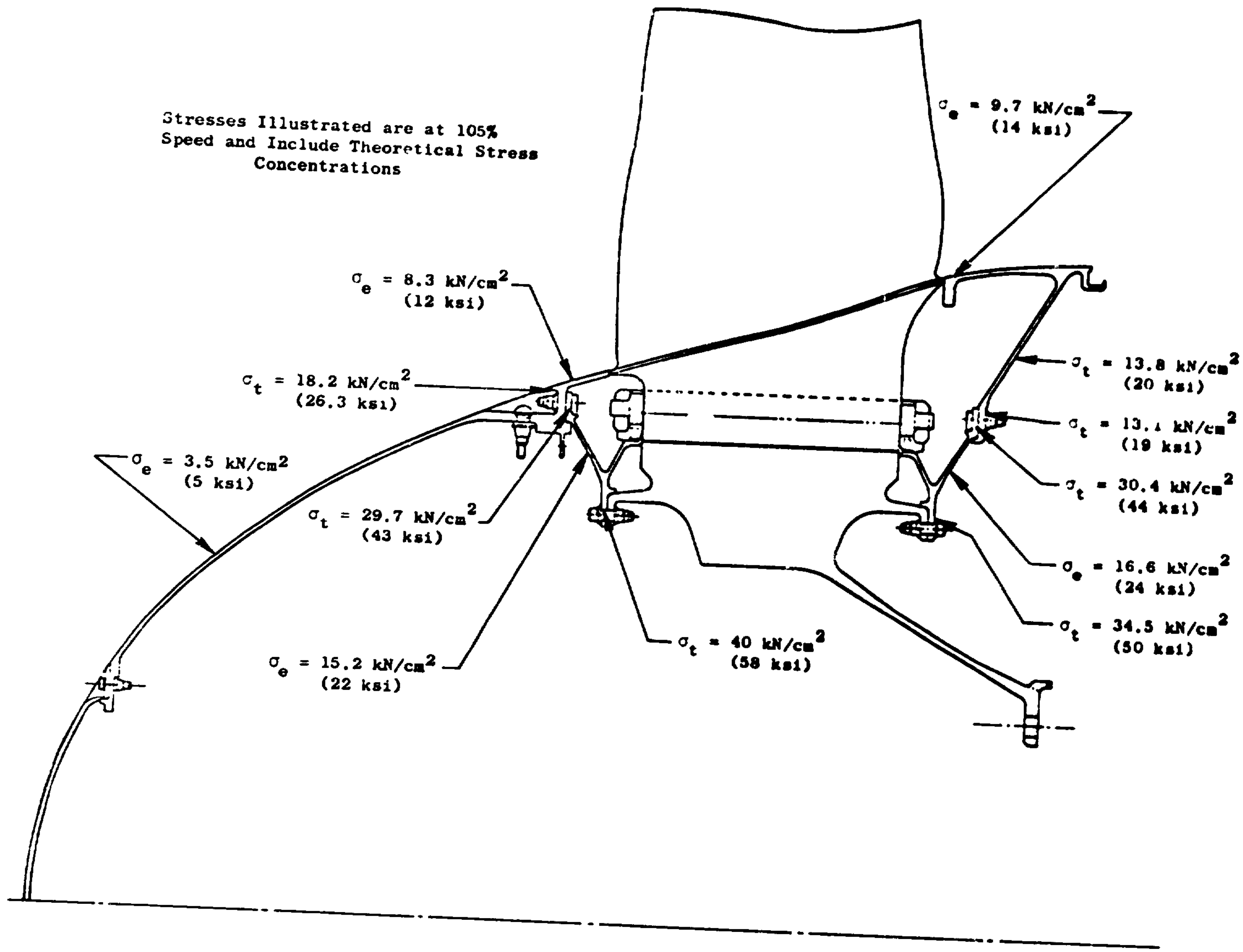

Figure 39. OTW Fan Rotor Shell Stresses.

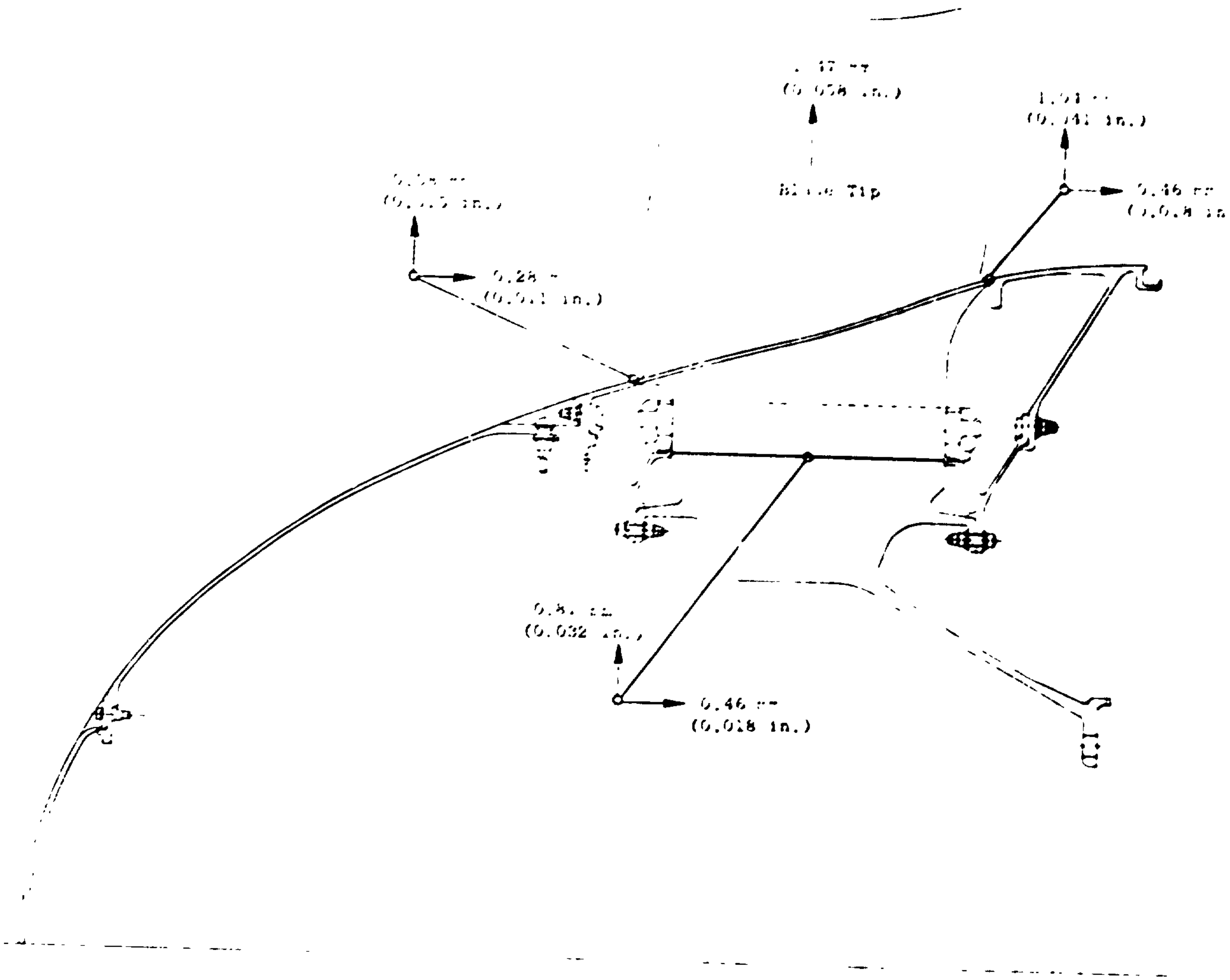

Figure 40. Rotor Deflections.

Table IX. Stub Shaft Flange Bolts.

- Number of bolts = 18
- Size = 1.27 cm - 7.87 thd/cm (1/2 in. - 20 thd/in.)
- Material = MP159
- Assembly torque = 176 N-m (130 ft-lb)
- Minimum preload = 95,230 N/Bolt (21,400 lb/bolt)
- Total preload = 1.714×10^6 N (385,000 lb)
- Minimum bolt preload stress = 92.3 kN/cm^2 (134 ksi)
- Percent fan torque carried by friction (for f = 0.15) = 105% capability
- Bolt tensile stress (1 metal airfoil out) = 25% of ultimate
- Bolt shear stress (1 metal airfoil out) = 31% of ultimate